Author:
Culleton, Naomi B

Title:
Corticothalamic interactions in associate recognition memory

Corticothalamic Interactions In Associative Recognition Memory

By

Naomi Bethan Culleton

Department of Physiology, Pharmacology and Neuroscience
University of Bristol

A dissertation submitted to the University of Bristol in accordance with the requirements of the degree of Doctor of Philosophy in the Faculty of Life Sciences.

December 2021

Word count: 35,039

Abstract

Associative recognition memory is the ability to make judgements about the prior occurrence of a stimulus within a spatial and temporal context. There is a critical role for the medial prefrontal cortex (mPFC) and the mediodorsal thalamus (MD) in supporting associative recognition memory in rodents. The MD is considered crucial for supporting associative recognition memory retrieval and requires incoming information from the mPFC during this time for successful retrieval to occur. Whilst cholinergic transmission has been studied in the mPFC during memory encoding and retrieval, its role in the MD during retrieval is unknown. There is also much to be understood regarding the properties of MD neurons, how they respond to incoming signals from the mPFC, and the properties of the mPFC - MD synapse. The projections from the mPFC to the MD are glutamatergic but it is not understood how N-methyl-D-aspartate receptors (NMDARs) are involved in this transmission or whether NMDARs are involved in plasticity mechanisms between the two brain regions during retrieval.

The experiments in this thesis used a combined *in vivo* and *in vitro* experimental approach to explore its objectives. These objectives were to investigate how the MD is modulated by acetylcholine in associative recognition memory retrieval, the properties of MD neurons and the mPFC-MD synapse, and the contribution of NMDARs to the transmission between the mPFC and MD.

This thesis provided the first evidence that $\alpha4\beta2$ nicotinic acetylcholine receptors and GluN2A and GluN2C/D containing NMDARs in the MD are required to support associative recognition memory retrieval. Data confirmed that MD neurons exhibit two different firing properties depending on their membrane potential and that the mPFC - MD synapse undergoes short term plasticity whereby the response facilitates in a frequency and NMDAR dependent manner.

Acknowledgements

Firstly, I would like to thank my supervisors Zaf and Clea, for their support and discussions throughout. Thank you to all the members of the Bashir and Warburton groups for many useful group meetings and discussions. Particular thanks to Clair, Gareth, Lisa and Paul for their time and help with training and troubleshooting - especially with the electrophysiology! Thank you also to Sam Southern who went above and beyond with providing support during the final stages of my PhD.

Next, I would like to acknowledge the support from the wonderful friends I have made throughout my PhD course. Thank you, Steph and Megan, for all the pep talks and enabling my caffeine addiction at the uni cafe. Huge thank you to Becks also for being an incredibly supportive friend and hilarious flatmate. Lastly, thank you to Emily who has made writing up the thesis bearable with frequent zoom writing sessions and daily updates. All of you have shared this journey every step of the way, we have celebrated the highs and cheered each other on during the lows.

Last of all I would like to thank all my other friends and especially my family for their continual love and support throughout. Thank you to my Mum and Dad for always encouraging and supporting my dreams, from helping me learn Pokemon names (you still don't know them all) to giving me life advice. Thank you to both Dad and Marketa for all your support and laughter, especially during lockdown. Lauren, Gina, Lindsay, Charlie, Ed, Emily, and Jacob, I cannot express how thankful I am to have such an amazing support network of close friends. From peaceful crochet dates to arguing on Overcooked (no Charlie, I've not forgotten) you have kept me smiling throughout stressful periods; thank you. Finally, thank you to Finn, for being the biggest cheerleader of them all and continuously going out of his way to help.

Declaration

I declare that the work in this dissertation was carried out in accordance with the requirements of the University's Regulations of Code of Practice for Research Degree Programmes and that it has not been submitted for any other academic award. Except where indicated by specific reference in the text, the work is the candidate's own work. Work done in collaboration with, or with the assistance of others, is indicated as such. Any views expressed in the dissertation are those of the author.

Signed: Naomi Bethan Culleton

Date: 17.12.2021

Table of Contents

List of Tables

Table **Page**

List of Figures

List of abbreviations

AC anterior cingulate cortex. 22

aCSF artificial cerebrospinal fluid. 50

AMPA α-amino-3-hydroxy-5-methyl-4-isoxazolepropionic acid receptor. 35

AP action potential. 30

BQCA benzyl quinolone carboxylic acid. 43

ChAT choline acetyltransferase. 33

CMD centromedial nucleus. 63

D3V dorsal third ventricle. 120

dlPFC dorosolateral prefrontal cortex. 25

DMSO dimethyl sulfoxide. 43

DNMS delayed non-matching to sample task. 82

EPSC excitatory postsynaptic current. 56

EPSP excitatory postsynaptic potential. 26

fMRI functional magnetic resonance imaging. 21

GPCR G protein coupled receptor. 31

HCN hyperpolarisation-activated cyclic nucleotide gated channel. 27

HPC hippocampus. 22

IL infralimbic cortex. 22

IMD intermedialdorsal nuclei. 63

LDDM laterodorsal thalamic nucleus. 120

lDMT lateral dorsomedial thalamus. 143

LDT lateral dorsal tegmentum. 33

LEC lateral entorhinal cortex. 22

LGN lateral geniculate nucleus. 27

LHbL lateral part of the lateral habenular nucleus. 120

LHbM medial part of the lateral habenular nucleus. 120

LTD long term depression. 116

LTP long term potentiaion. 116

LTS low threshold calcium spike. 27

mAChR muscarinic acetylcholine receptor. 31

MD mediodorsal thalamus. 3

MDC central mediodorsal thalamus. 25

MDL lateral mediodorsal thalamus. 25

MDM medial mediodorsal thalamus. 25

mDMT medial dorsomedial thalamus. 143

mGluR metabotropic glutamate receptor. 36

MLA methyllycaconitine citrate. 43

mPFC medial prefrontal cortex. 3

nAChR nicotinic acetylcholine receptor. 32

NMDAR N-methyl-D-aspartate receptor. 3

NRe nucleus reuniens. 22

OiP object in place task. 21

OR novel object recognition task. 60

PAM positive allosteric modulator. 34

PBS phosphate buffered saline. 49

PC paracentral thalamic nucleus. 120

PFA paraformaldehyde. 49

PL prelimbic cortex. 22

PPT pedunculopontine tegmentum. 33

PRH perirhinal cortex. 22

PV paraventricular nucleus. 63

rdTRN rostro dorsal thalamic reticular nucleus. 143

RiExt extrapolated input resistance. 54

RiSS steady state input resistance. 54

RJR RJR oxalate. 84

RMP resting membrane potential. 30

Ro 25-6981 (αR βS)-α-(4-hydroxyphenyl)-β-methyl-4-(phenylmethyl)-1-piperidinepropanol maleate. 43

rvTRN rostroventral thalamic reticular nucleus. 143

sm stria medullaris of the thalamus. 120

TRN thalamic reticular nucleus. 26

WGA wheat germ agglutinin. 33

Chapter 1

General Introduction

1.1 Associative recognition memory

Recognition memory is our ability to judge whether a stimulus encountered is novel or familiar. Associative recognition memory is the ability to make these judgements using spatial and temporal contexts [1, 2]. These processes contribute to our declarative memories that shape our interactions within the world, allowing us to adapt and plan our actions based on prior experiences [3]. Loss of this ability is detrimental to the sufferer and typically seen in pathological conditions like dementia, Korsakoff syndrome, and diencephalic amnesia to name a few [1, 4]. Investigations into the neural network supporting recognition memories are crucial to aid in understanding pathological states.

Recognition memory is considered to consist of familiarity and recollection components and there have been extensive debates within the literature as to whether they underlie a singular process or two distinct processes [5–8]. A common anecdote is the 'butcher on the bus' phenomenon where you encounter a person whom you may deem familiar, yet you are uncertain why [9]. In comparison, recollection involves the retrieval of other stimuli, such as spatiotemporal aspects of where the person was encountered [10]. It is mentally possible to experience these components separately, but there is much debate whether they are also separate mnemonic processes [5, 7].

Single process theorists view familiarity and recollection components as lying along the same continuum of memory strength and supported by the same neural substrates [5, 10]. Familiarity is considered to be a weak memory whereas stronger recognition

memory will result in recalling the experience [6]. In comparison, dual process theories suggest different brain regions have different functional contributions to either familiarity or recollection [10]. With an increase in data from functional magnetic resonance imaging (fMRI), behavioural and electrophysiology, there is now more evidence in favour for there being dual processes involved for familiarity and recollection [10, 11].

Associative recognition memory tasks require both familiarity and recollective processes as stimuli are deemed familiar but also qualitative information regarding when and where the stimuli was encountered must be recollected. Studies using fMRI have shown that associative recognition memory performance relies on increased activity within the medial temporal lobe, the mPFC and the thalamus [12, 13]. Alongside this, case studies in humans have demonstrated that damage to these regions will impair associative recognition memory [14, 15]. A major drawback of these data is that the lesions often affect surrounding regions, and thus differing effects on recognition memory can be observed. The use of non-human primates and rodent studies has proved essential for studying effects of site-specific lesions on several behavioural paradigms. Together, these studies have assimilated evidence for a neural network required for supporting associative recognition memories (see Figure 1.1).

Studies from rodents suggest that they are also capable of displaying associative recognition memory, and the ability to measure this has been developed over time using spontaneous exploration tasks [16–18]. These tasks exploit rodents' innate ability to explore novel over familiar stimuli. After the initial development of the non-associative object recognition task, there have been additions to this task to create the object-in-place (OiP) task and temporal order task which require rats to form spatial and temporal associations with stimuli to complete the task.

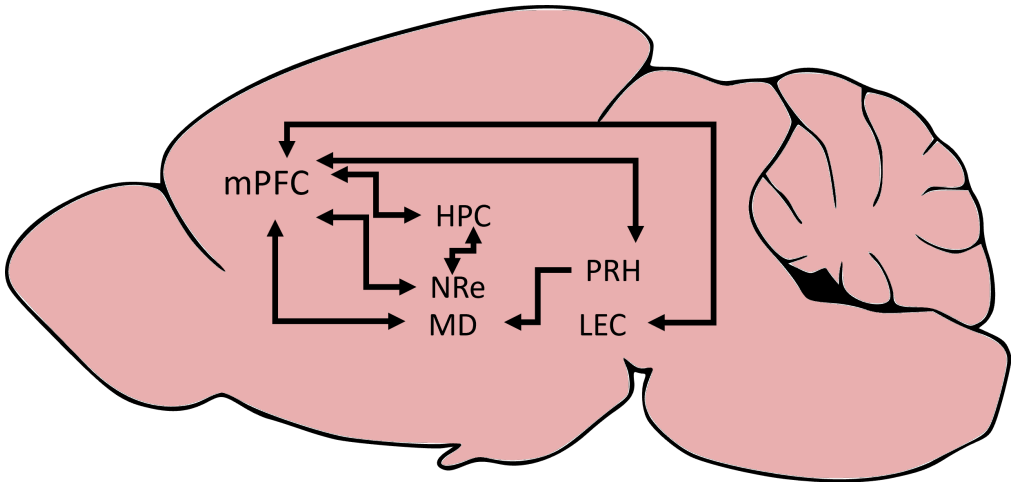

Figure 1.1: Associative recognition memory network

A diagram showing the brain regions considered essential for supporting associative recognition memory in rodents and their connections with one another. These are the mPFC, MD, hippocampus (HPC), nucleus reuniens (NRe), lateral entorhinal cortex (LEC), and the perirhinal cortex (PRH) [18].

1.1.1 Associative recognition memory network

As mentioned previously, there are several brain regions responsible for processing associative recognition memory, but for the purpose of this thesis, only the MD and mPFC will be discussed in detail, with a focus on rodent studies.

Medial prefrontal cortex

The prefrontal cortex, specifically the areas located in its medial division (mPFC), are required for associative recognition memory [19]. There are further subdivisions of the mPFC following a dorsoventral axis. These are: the anterior cingulate cortex (AC), prelimbic cortex (PL) and the infralimbic cortex (IL) [20, 21]. It is hypothesised that the mPFC is required for integrating contextual information and supporting memory retrieval via top-down control of memory processing whereby the mPFC favours the recollection of context appropriate memories and suppresses inappropriate memories [22]. In humans, damage to the prefrontal cortex does not affect their ability to recognise objects, it impairs their ability to form correct associations, especially when there are sources of interference [22]. For example, in one study patients with damage in the prefrontal cortex were asked to learn paired associates (e.g. orange - desk) then learn

new associations with the same items (e.g. orange - lamp) [22]. Patients exhibited difficulty in learning the new associations and would incorrectly recall the original associates [23]. Thus, the mPFC is critical for integrating information but is not vital for object recognition.

In rodents, lesions in the mPFC have no effect on performance in novel object recognition or object location tasks [17, 19, 24]. However, these lesions do impair rats' performance in the OiP task and temporal order tasks which involve associative recognition memory [19, 24]. Therefore, inactivation of the mPFC has no effect on familiarity or spatial discrimination but it does impair associative recognition memory.

Medial dorsal thalamus

Making up one of the nuclei of the thalamus, the MD is classified as a higher order nucleus and is essential for a variety of cognitive tasks, including recognition memory [25]. Thalamic nuclei relaying ascending sensory information to the cortex are classified as first order nuclei whereas higher order nuclei relay information between cortical regions [25–27]. The MD has dense reciprocal connections with the mPFC in both primates and rodents and is deemed crucial in supporting the mPFC during cognition [20, 25, 28–30].

Initial evidence of the MD in recognition memory arose from the observation that patients with Wernicke-Korsakoffs syndrome display deficits in recognition memory, however it is difficult to conclude firmly that the MD is the key site as in these cases there is widespread damage throughout the brain [1]. An fMRI study showed that upon successful recognition of an item together with the recall of associations produced stronger activation in the MD and the mPFC during encoding and retrieval compared to recognition without recall [12]. Whilst clinical studies can lack spatial and temporal resolution compared to animal studies, they have demonstrated that the MD and mPFC function together to support associative recognition memory.

In rats, lesions to the MD initially produced conflicting results on learning and memory tasks [31]. Lesions would often affect surrounding regions such as the anterior thalamic nuclei and the mammillothalamic tract, which also contribute to memory processes and contributed to contrasting results [31]. Using more specific lesion techniques, a later study found that MD lesions did not produce spatial deficits, and these deficits appeared only in animals that had also sustained damage to the anterior thalamic nuclei [32].

Impairments observed in spatial working memory tasks were later attributed to the MD damage affecting other aspects of the task that required rule learning and behavioural flexibility [32]. This was because whilst there were no impairments on the task itself, there were delays in the initial acquisition and learning of the task rules following MD lesions [32].

The MD was also hypothesised to be involved in familiarity judgements supporting recognition memory due to its strong connections with the PRH [31, 33]. However, unlike with PRH lesions, ablation of the MD has no effect on novel object recognition [4, 32]. A recent study targeting the MD showed that lesions to the MD in rodents produce effects similar to those observed when the mPFC is lesioned; rodents are unable to perform both the OiP and temporal order tasks [4]. Additionally, contralateral lesions to the MD and mPFC impaired rats' performance in the OiP and temporal order tasks whilst animals with ipsilateral lesions were unaffected [4]. Together these data demonstrate that a functional interaction between the MD and mPFC is crucial for associative recognition memory [4, 18].

Further work demonstrated that infusions of muscimol, a $GABA_A$ agonist, into the MD prior to the sample or test phase of the OiP task resulted in impairments in retrieval, but not encoding, thus suggesting the MD is crucial for the retrieval of associative recognition memories (unpublished work L. Cross, G. Barker). Contralateral infusions of NBQX, an AMPA receptor antagonist, in to the mPFC and MD prior to the sample or test phase of the OiP, produced impairments during memory retrieval but not encoding (unpublished work L. Cross, G. Barker). Together these data demonstrate that the MD is required for associative recognition memory retrieval, and not encoding, during the OiP task, and that it needs to be functionally connected during this period also (unpublished work L. Cross, G. Barker).

1.2 Reciprocal connections between mPFC and MD

1.2.1 mPFC anatomy

The medial prefrontal cortex (mPFC) is a section of frontal cortex located at the anterior section of the brain. Initially the mPFC was only distinguished in humans and non-human primates as having a granular layer IV [34]. The mPFC in rodents is considered

homologous to the dorsolateral PFC (dlPFC) in human and non-human primates, however it lacks a granular layer IV, and thus whether rodents possess a prefrontal cortex has been a topic of frequent debate within the literature [34]. Defining the dlPFC this way prevents comparisons between distantly related species, and many argue that it cannot be the only defining feature of the PFC. More recently, the dlPFC in humans and non-human primates has also been defined by its projections from the mediodorsal thalamus, a characteristic that it shares with the mPFC of rodents [34].

Within the neural circuit considered to be essential for associative recognition memory, two subdivisions of the mPFC, the PL and IL cortices, project to the PRH, LEC, NRe, and the MD [20, 30, 35–37]. Anatomical tracing studies show extensive projections arising from layers V and VI of the mPFC and projecting to the NRe and MD [20, 30]. A high density of projections from the PL cortex travel in a dorsal medial direction through the internal capsule and into the diencephalon [30]. Here, they terminate largely in the medial and lateral divisions of the MD, and the NRe [20, 30]. Unlike projections from the IL cortex, there is virtually no supply to the central division of the MD [30]. Projections from the IL cortex descend in a dorsal medial direction through the diencephalon where they supply the central and medial divisions of the MD, and the NRe [20, 30].

Within each of the cortical layers the neuronal population is comprised of roughly 80 % - 90 % excitatory pyramidal neurons and 20 % - 10 % inhibitory interneurons [38]. Both excitatory and inhibitory neuronal populations are made up of different subtypes of neurons that have distinct morphological and electrophysiological properties [39, 40]. Cortical interneurons can be identified by specific cell markers, the most heavily studied of which are parvalbumin and somatostatin expressing neurons [38].

1.2.2 MD anatomy

The MD of the rat is formed of three distinct regions based on their cytoarchitecture and chemoarchitecture [41]. These regions are the medial MD (MDM), central MD (MDC), and lateral MD (MDL) [25, 41]. Each segment of the MD receives diverse inputs from subcortical brain regions and relays this information across the mPFC [41]. The MDM receives afferents from the nucleus accumbens, ventral pallidum and amygdaloid nucleus and projects mostly to the IL, and sparsely to the PL; the MDC receives afferents from the endopirifrom nucleus and the olfactory tubercle and projects to the ventral part of

the agranular insular and orbital areas; the MDL receives input from the substantia nigra and brainstem whilst projecting to the AC and PL cortices. [34, 41–44]

The MD receives projections from layers V and VI of the mPFC, a projection pattern characteristic of higher order nuclei [26]. The MD receives "driver" inputs from layer V of the cortex, and "modulatory" inputs from layer VI. Approximately 20 % of the mPFC projections to the MD arise from layer V with the majority of inputs arising from layer VI. Projections defined as "drivers" are considered to transmit the main information from the cortex to the thalamus whereas modulators are capable of altering the driver input without changing the overall message [26]. Collins et al performed whole cell patch clamp recordings in MD neurons and optically stimulated mPFC fibres expressing channel rhodopsin [45]. They found that evoking trains of excitatory post synaptic potentials (EPSPs) from neurons in layer VI had a high probability of release which rapidly depressed, typical of "modulatory" inputs [45]. In comparison, when neurons from layer V were stimulated, the EPSPs recorded in the MD were small and rapidly increased in amplitude which are typical of "driver" inputs [45].

Projections back to the mPFC terminate in superficial layers II/III. Collins et al demonstrated that corticothalamic neurons synapse onto thalamocortical neurons that project back to the superficial cortical layers [45]. In these layers it was also shown that the thalamacortical neurons terminate on cortico-cortical interneurons that innervate corticothalamic neurons in layers V and VI [45]. This suggests there are complex reciprocal feedback loops between the mPFC and MD, but it is not yet understood how they may be signalling to each other to support associative recognition memory.

In contrast to the mPFC, there is limited information regarding cell subtypes and properties in the MD. Kuroda et al demonstrated that the cells located across the subdivisions of the MD are either stellate or fusiform in shape, and that these cells are all glutamatergic. Whilst they did not observe subregion specific neurons, they did observe that cells did not overlap between the subdivisions, with cells even shaping their dendrites to sit along the divisional borders [46]. They also found little evidence of GABAergic neurons in the MD; the population was <1 % [46].

Projections from the mPFC to the MD are considered to be solely glutamatergic [20, 42]. The MD receives the majority of its inhibitory input from the thalamic reticular nucleus (TRN) [47]. The TRN is a nucleus in the thalamus composed of inhibitory neurons and is

the largest inhibitory supply to the thalamus [48]. Interestingly, the mPFC sends direct projections to the TRN suggesting that anatomically it is capable of indirectly inhibiting the MD via the TRN [49]. Inhibitory drive to the MD would hyperpolarise neurons, and shift their firing pattern from 'tonic' to 'burst' firing. If the mPFC indirectly inhibits MD neurons via the TRN, it would allow the mPFC to fine tune responses from MD cells. This anatomical circuit has gained much attention, particularly in the context of working memory and there is growing interest in the TRN's role in the communication between the mPFC and MD [48, 50–53]. Currently it is unknown whether the TRN is required during associative recognition memory.

1.3 Properties of MD neurons

Understanding the properties of neurons is important for understanding how they respond to incoming signals. There are very few studies published regarding the electrophysiological properties of MD neurons, which vastly contrasts the amount of information regarding neuron types and properties within the mPFC [54–56]. General properties of thalamic relay neurons have been described from other areas of the thalamus, and a handful of studies have reported that MD neurons exhibit typical characteristics of thalamic relay neurons [45, 57, 58]. A study published this year appears to be the first to explicitly share these characteristics [59]. These characteristics being the cells display two types of firing modes, tonic and burst firing, depending on the cell's membrane potential [57].

In vitro recordings in the lateral geniculate nucleus (LGN) have shown that the burst firing mode is a result of low threshold calcium spikes mediated via T-type calcium channels, or also known as the current I_T [60]. These channels are termed low voltage activated calcium channels as they activate around -80 mV and are inactivated at membrane potentials higher than -60 mV [57, 60]. Depolarisation of the cell during the window where these channels are activated results in low threshold calcium spikes (LTS) that then activate voltage gated sodium and potassium channels resulting in a succession of fast action potentials riding on the LTS [60]. A more recent study has patched in the MDM and MDL and shown that neurons here exhibit the same switch between the two firing types [59].

Typically burst firing is a result of the I_T current working in concert with I_H, a current mediated by the hyperpolarisation-activated cyclic nucleotide gated channel (HCN). This

channel acts as a pacemaker between calcium spikes as upon membrane hyperpolarisation, it activates and allows cations in to the cell membrane causing a slow depolarisation. This inward current will then activate the next calcium spike, therefore the time course at which I_H activates can determine the time between calcium spikes [60].

In comparison, tonic firing occurs when the cell's resting membrane potential is above -60 mV as both I_T and I_H currents are inactive [57, 60]. In this form of firing, cells will fire single APs in succession in response to suprathreshold stimuli [60]. This firing relies on inward current through sodium channels to reach the action potential threshold, rather than a LTS [60].

1.3.1 Intrinsic properties

Intrinsic properties of neurons are determined by morphology and the passive and active membrane properties that arise from diverse ion channels across the cell membrane. One study characterised the morphology of MD neurons, as described earlier [46], but there is little published data regarding the passive membrane properties of MD neurons. Two studies, to my knowledge, have taken *in vitro* recordings from MD neurons using whole cell patch clamp [45, 59]. Only the study by Kloet et al included data regarding passive membrane properties of cells, but it was not extensive [59].

Studying the passive membrane properties of neurons is key to understanding how the neuron will respond to changes in voltage, and thus how it will respond to incoming stimuli. There are three passive membrane properties that can influence how neurons will respond to electrical signals [61]. Firstly, there is the membrane capacitance. As cell membranes are made of a lipid bilayer, it acts as an electrical insulator that can separate charges in the intracellular and extracellular solutions and so it can act as a capacitor which stores charge [61]. This property determines how quickly voltage will change across the cell membrane and can differ depending on the size of the cell. For example, a larger cell will have a larger membrane capacitance.

Next is the membrane resistance which determines how current will cross the membrane. For example, a low resistance means it is easy for current to cross the membrane [61]. As membranes are composed of a lipid bilayer, it is difficult for charged particles to cross the membrane. The presence of ion channels within the membrane allows ions to flow through the membrane and lowers the resistance. Thus, the amount of ion channels open is the

largest determinant of the membrane resistance of the cell [61].

Finally, there is the resistance along the dendrites and axons of the neuron termed the intracellular axial resistance [62]. This is a measure of the resistance of the cytoplasm and how well current can propagate along the neuron's processes [62]. A process with a larger diameter will have a lower axial resistance [62].

1.3.2 Measuring passive membrane properties

Passive membrane properties of neurons can be measured during whole cell patch clamp by applying current to the patched cell and recording the change in voltage resulting from the current injection. Typically, these measurements are made when applying hyperpolarising current steps to the cell, mainly because these measures are taken from when the change in voltage reaches a steady state, and depolarising current steps are more likely to result in the cell firing action potentials, and not allowing this measurement to be made.

As the cell membrane functions the same as a capacitor, changes in voltage in response to current will not be instantaneous, and instead will rise and decay on a slower time scale [61]. The resistive and capacitive properties of the cell membrane define the membrane charging time constant (τ_M) which describes the rate of change in membrane potential in response to a current injection/stimulus [61]. By applying hyperpolarising current injections, you can measure the input resistance, time constant, and capacitance.

Firstly, the input resistance can be calculated using Ohm's Law (Voltage = Current x Resistance). If two cells received the same current injection, the cell with a higher input resistance would display a greater change in membrane potential. The input resistance is determined by the number of ion channels on the cell membrane and the size of the cell [61].

To measure the charging time constant of the cell membrane, an exponential curve can be fitted to the voltage response prior to reaching steady state. The time constant is defined as the product of the membrane resistance and capacitance ($\tau_M = C_M * R_M$)

The capacitance (C_M) of the cell can be calculated by the equation ($C_M = \tau_M / R_M$) however this calculation assumes the cell is spherical as the input resistance is approximately equal to the membrane resistance (R_M) in a spherical cell [61]. Most published literature will report these measurements for membrane properties, but it is

still important to take into consideration that these measures are more accurate for a spherical cell. As neurons have many processes extending from the soma, the resistive properties of these will also affect the measurements [63].

Overall, the intrinsic properties of the cell shape how they respond to incoming signals and will shape the properties of the action potential. As these properties have not been investigated in the MD, it is unknown how these properties shape and determine the properties of action potentials.

Action potentials

Action potentials (APs) are how cells respond to incoming stimuli. Neurons can integrate information from synaptic inputs, and this is dependent on the underlying passive membrane properties and morphology. When synaptic inputs cause sufficient depolarisation of the cell membrane the threshold for the AP is overcome and the cell will fire an AP. The AP threshold varies between cells and is determined by the balance of sodium and potassium current.Once the threshold has been reached, the cell will rapidly depolarise and an AP will occur. This AP will then propagate along the neuronal processes. They are all or nothing events and the overall level of depolarisation from them will be the same regardless of the strength of the initial signal.

Inactivation of sodium channels occurs rapidly alongside opening of voltage-gated potassium channels that permit passive flow of potassium ion out of the cell. These mechanisms allow the cell to return to its resting membrane potential (RMP) promptly after AP initiation allowing the cell to recover and respond to further input.

There is a large variety of voltage gated ion channels that can be expressed within neurons, all shaping the AP in different ways, making neurons responses unique across brain regions and allowing variation in frequencies and patterns of APs. Thalamic neurons can fire APs tonically or in bursts depending on their membrane potential [57, 60, 64, 65]. It is likely MD neurons share this property also, but this remains to be tested.

Discussions in the literature proposed that thalamic neurons burst during slow wave sleep [57, 64, 66]. During sleep the thalamus receives inhibition from the thalamic reticular nucleus which results in hyperpolarised neurons and burst firing [48]. Generally burst firing is considered to occur during oscillatory activity during slow wave sleep, or it provides a

'wake-up' call to the cortex [48, 64, 66]. In comparison, tonic firing is thought to be responsible for encoding sensory stimuli and relaying this in a linear fashion. However, this idea has been rejected recently after findings of burst firing in awake animals [64, 66].

Whilst there is now evidence of burst firing occurring in awake animals, the question remains how this form of firing encodes sensory information. A computational study by Mease et al found that burst firing in the rodent thalamus is capable of encoding both low and high frequency stimuli [64]. They suggest information is encoded by the burst size, the onset time, and the timing between bursts. This allows thalamic cells to respond in hugely diverse ways to cortical input. Considering the transmission between the mPFC-MD, and the potential indirect inhibition from mPFC-TRN-MD, the mPFC is capable of fine tuning the resting potential of MD cells, and thus determining how they will encode incoming information and relay this back to the mPFC.

1.4 Cholinergic modulation of associative recognition memory

The neural network supporting associative recognition memory is under extensive regulation via the cholinergic system. Whilst acetylcholine acts as a primary neurotransmitter in some regions, its primary role is neuromodulation across the brain. Several cholinergic loci exist within the brain and cholinergic fibres arising from these loci supply diverse regions within the brain allowing it to support a variety of functions, not only memory [67–69].

Acetylcholine can act via muscarinic and nicotinic acetylcholine receptors at the synapse. Muscarinic acetylcholine receptors (mAChR) are G protein coupled receptors (GPCRs) that can be located pre- and postsynaptically [69, 70]. In contrast, nicotinic acetylcholine receptors are ligand gated ion channels permeable to cations Ca^{2+}, K^{+}, and Na^{+}. They are also located both pre- and postsynaptically. Both receptors exist as various subunit structures which are discussed in more detail below.

1.4.1 Nicotinic acetylcholine receptors

Nicotinic acetylcholine receptors (nAChRs) are part of a cys-loop receptor family; they are ligand gated ion channels assembled from five subunits [69, 71]. They can be activated by their endogenous ligand, acetylcholine, or exogenously by nicotine. Upon agonist binding, these receptors open quickly and are permeable to cations Na^+, K^+, and Ca^{2+} [69].

The relative properties of permeability, ion selectivity and channel gating are determined by the subunit arrangement forming the receptors [69]. Nicotinic acetlycholine receptors can be compromised of alpha (α1 - α10) and beta (β1 - β4) subunits. Receptors can exist either as a homopentameric structure or a heteropentameric structure. Alpha subunits can form homopentamers, such as α7 nAChRs, but beta subunits must pair with alpha subunits to form functional nAChRs. The most common type of heteropentamer is comprised of two α4, two β2 subunits and the fifth subunit is typically α4, β2 or α5. Both these types of nAChRs are widely expressed throughout the mammalian brain, with high levels in the cortex and $\alpha4\beta2$ found most abundantly in the thalamus [71].

Due to their different compositions, α7 and $\alpha4\beta2$ nAChRs have different sensitivities to acetylcholine. The α7 nAChRs rapidly desensitise in the presence of high concentrations of ACh whereas $\alpha4\beta2$ receptors desensitise much slower, but at lower concentrations of ACh [69, 72]. These properties are thought to allow ACh to elicit distinct effects at these receptors depending on its mode of release [73].

1.4.2 Muscarinic acetylcholine receptors

Muscarinic acetylcholine receptors (mAChRs) are part of the G protein coupled receptor family and activation of these receptors results in intracellular signalling cascades that can be excitatory or inhibitory [69, 74]. Five different subtypes have been identified M1-M5. M1, M3 and M5 are coupled to G_q protein and activate phospholipase C signalling cascade that results in increased calcium entry. M2 and M4 are coupled to $G_{i/o}$ which is an inhibitory G protein inhibiting adenylyl cyclase [69, 72].

M1 and M2 mAChRs are present within the MD, with M1 being the most abundantly expressed [75, 76]. Whilst these studies show that M1 and M2 receptors are present in the MD, they do not show where the receptors are expressed, whether they are found pre-

or postsynaptically. The role of these receptors in the MD during associative recognition memory is unknown.

1.4.3 Cholinergic input to the mPFC

Cholinergic fibres in the mPFC mostly arise from the basal forebrain [69, 77]. Within the basal forebrain, the nucleus basalis magnocellularis and the horizontal limb of the diagonal band send the most cholinergic projections to the mPFC [78]. The vertical diagonal band and medial septal area also supply cholinergic input to the mPFC, but it is much sparser [78]. A small number of projections are from the peduncolopontine nucleus (PPT) and lateral dorsal tegmentum (LDT) [69, 78, 79]. The mPFC is unique in that it is the only region of the cortex that has reciprocal projections with the basal forebrain and provides the largest cortical input to the basal forebrain [69].

1.4.4 Cholinergic input to the MD

The MD, similar to most thalamic nuclei, receives the majority of its cholinergic input from the PPT and the LDT [53, 79]. A unique feature of the MD compared to other thalamic nuclei is that it also receives cholinergic afferents from the basal forebrain, similar to the mPFC [53, 79].

An anterograde tracing study, with injections of wheat germ agglutinin (WGA) into the LDT, showed projections from the LDT supplying the MDL. Within the same study, a retrograde tracer injected into the MD showed projections arising from cell bodies in the LDT and also in the PPT, and that these cells stained positive for choline acetyltransferase (ChAT) indicating that the LDT and PPT supply cholinergic projections to the MD [79]. A more recent anatomical study showed that the LDT provides dense innervation to the MDL and MDC [80]. All subdivisions of the MD received cholinergic projections from the LDT and PPT, but the majority of these arise from the LDT [80].

1.4.5 Cholinergic modulation of object-in-place memory

Infusions of scopolamine, a mAChR antagonist, into the mPFC prior to encoding impaired performance in the OiP task at both short (5 minute) and longer (1 hour)

retention delays [81]. Additionally, infusions of subtype selective antagonists and allosteric modulators have been used to investigate the contributions of M1 and M2 mAChRs. Blocking M1 or M2 mAChRs blocked memory encoding in the mPFC, whilst effects on retrieval were specific to manipulating M1 mAChRs (unpublished work G Barker). Associative recognition memory retrieval was impaired when BQCA, a positive allosteric modulator (PAM) for M1 mAChRs was infused prior to the test phase of the OiP task (unpublished work G Barker). It is hypothesised that high levels of acetylcholine release favours memory encoding in the mPFC [73, 82], and infusions of a PAM mimicked these conditions but during the retrieval phase. Thus increasing the sensitivity of these receptors during memory retrieval results in an impairment and fits with the hypothesis of differential modes of acetylcholine release during encoding and retrieval [73, 82].

Nicotinic receptors in the mPFC have also been shown to be required for associative recognition memory. Infusions of specific $\alpha4\beta2$ and $\alpha7$ nAChRs antagonists had distinct effects in the mPFC during the OiP task [73]. Blocking $\alpha7$ nAChRs impaired memory encoding whilst blocking $\alpha4\beta2$ nAChRs impaired memory retrieval [73]. It is hypothesised that different modes of acetylcholine release occurs during encoding and retrieval and, as a result, activates either $\alpha4\beta2$ or $\alpha7$ nAChRs [73]. It is thought that the mPFC has different modes of acetylcholine release during encoding and retrieval, i.e high levels during encoding, then diffuse, phasic release during retrieval which favours the activation of $\alpha4\beta2$ [73, 83].

Whilst the cholinergic projections into the MD have been well characterised [27, 79, 84, 85], few studies have looked at the physiological effects of acetylcholine release during cognitive tasks in the MD, and there are certainly none in the context of associative recognition memory. One study infused DHβE and MLA during a working memory task and they found that blocking $\alpha4\beta2$ receptors improved working memory [86]. This improvement was attenuated by infusions of MLA, or systemic injection of nicotine, suggesting that both $\alpha4\beta2$ and $\alpha7$ nAChRs are present in the MD [86]. Another study also infused a general nicotinic antagonist prior to the serial arm maze, testing visual attention, and there were no effects [87]. Although each study has explored cholinergic contribution to different cognitive tasks, it is noteworthy that manipulating these receptors has task dependent effects, demonstrating that the roles of cholinergic receptors are extremely diverse.

Cholinergic release in the thalamus has been associated with awake and attentive states

[88, 89]. An *in vivo* microdialysis study, with probes located within the mid-line thalamic nuclei, showed that high levels of acetylcholine were maintained during awake states [88]. Although this was overall acetylcholine levels across several of the mid-line nuclei, not just the MD, so only a rough idea of acetylcholine release can be implied by this study. Whether similar release patterns of acetylcholine occur in the MD during retrieval as they do in the mPFC remains to be tested. The role of acetylcholine in the MD during OiP associative recognition memory is unknown. This will be explored within the chapters presented in this thesis.

1.5 Glutamatergic modulation of associative recognition memory

Glutamate is the primary, excitatory transmitter in the brain; it acts on both ionotropic and metabotropic receptors along the cell membrane [90–92]. Ionotropic receptors are ligand gated ion channels consisting of α-amino-3-hydroxy-5-methyl-4-isoxazoleproprionic acid (AMPA), NMDA, and kainate receptors [90]. AMPA and kainate receptors require glutamate to bind whereas NMDARs require both glutamate and glycine and are subject to a voltage dependent magnesium block at voltages lower than -40 mV [90, 92].

Site specific infusions of AP-5, an NMDAR antagonist, have caused impairments in the OiP task when infused into the PRH, NRe and HPC [93–95]. These impairments have been observed during memory encoding, and not retrieval. It has been speculated that their role in encoding could be related to NMDA dependent forms of synaptic plasticity [96, 97].

The MD receives glutamatergic projections from the cortex [53]. Of interest is the glutamatergic projections from the mPFC arising in layers V and VI. These inputs can then be modulated by other neurotransmitters such as acetylcholine, noradrenaline, dopamine, serotonin, and histamine [53]. It is currently unknown what the roles of these neurotransmitters are in modulating corticothalamic transmission between the mPFC and MD, especially in the context of associative recognition memory.

1.5.1 NMDARs

Whilst AMPA receptors support the majority of glutamatergic transmission in the brain, NMDA receptors are involved in the induction of synaptic plasticity and their role in learning and memory is well established [98–100]. Although the majority of studies have investigated the role of post synaptic NMDARs there is also evidence that they have roles presynaptically and extrasynaptically [91].

NMDA receptors are heterotetramers that are made up of GluN1 subunits, that can be from one of eight splice variants (1a - 4a, 1b - 4b) and GluN2A/B/C/D and/or GluN3A/B subunits [91]. For the receptor to function, at least one GluN1 subunit must be present in the receptor [90, 91]. This GluN1 subunit will then combine with at least one GluN2(A-D) subunit and less frequently will combine with a GluN3(A,B) subunit. The most commonly expressed receptor is made from two GluN1 subunits, a GluN2A subunit and a GluN2B subunits [90]. Different subunits form receptors allowing diverse receptor properties.

GluN2A/B containing NMDARs are the most abundant subtypes expressed in the adult brain whereas GluN2C/D NMDARs have expression restricted to specific regions, one of which is the thalamus [101]. A study by Ravikrishnan et al found GluN2C is abundantly expressed in the thalamus, including the MD [101]. There is also evidence of GluN2A containing NMDARs in the MD, and that they co-express with GluN2C. These data suggest that GluN2A and GluN2C subunits are present in the MD, and they may even form a triheteromeric receptor [102]. It is unknown which NMDAR subunits are specifically found in the MD, and whether they are involved in supporting associative recognition memory.

1.5.2 Metabotropic glutamate receptors

Metabotropic glutamate receptors (mGluRs) are G-protein coupled receptors [90]. These are membrane bound proteins that require activation by glutamate [90, 103]. Upon ligand binding, the associated G protein is activated and will activate intracellular signalling cascades [90, 103]. The effects of the mGluR can be inhibitory or excitatory depending on the type of G protein activated by the receptor [90, 103].

There are three groups of mGluRs which contain different receptor subtypes. Group 1 mGluRs consist of mGluR1 and mGluR5, group 2 contains mGluR2 and mGluR3, then

group 3 consists of mGluR4 and mGluR6-8 [90, 103]. Group 1 mGluRs couple to Gq/G11 and activate phospholipase C (PLC) leading to activation of protein kinase C (PKC) and calcium mobilisation. Group 2 and 3 mGluRs are mostly coupled to Gi/o proteins. These predominantly result in an inhibition of adenylyl cyclase [104]

A study using *in situ* hybridisation methods measured the expression levels of different mGLuR subtype mRNA throughout the rat thalamus, including the MD [105]. They found throughout the rostro-caudal length of the MD that there was mRNA expression for mGluR1, mGluR5, mGluR3, mGluR4 and mGluR7 [105]. Another study by Copeland et al made *in vivo* recordings in the MD whilst electrically stimulating the mPFC [58]. They found that infusing a general agonist for group 2 mGluRs resulted in a decrease in burst firing in MD neurons and thus indicated the presence of these receptors in the MD [58]. As a reduction in burst firing would mean a depolarisation of MD cells, the authors speculated that the group 2 mGluRs in the MD are expressed presynaptically on inhibitory fibres coming in to the MD [58].

1.6 Aims of thesis

As described in this introduction, there is little known about the MD and how it supports associative recognition memory retrieval. It is also unknown how incoming information from the mPFC during retrieval occurs on a synaptic level. The studies in this thesis aimed to explore the role of acetylcholine in the MD during associative recognition memory retrieval, characterise the properties of MD neurons, and characterise the properties of the mPFC - MD synapse using a combined experimental approach of *in vivo* and *in vitro* techniques.

1.7 Structure of thesis

This thesis is comprised of six main chapters, including this introduction. The second chapter provides a detailed explanation of all methods used for the experiments and data analysis throughout the project. A short recap of the main methods will be provided in each results chapter also. There are three main results chapters presenting data from experiments that addressed the aims of the project. These are: the role of acetylcholine in

the MD during associative memory retrieval; properties of MD neurons and the mPFC-MD synapse; the role of NMDARs and specific NMDAR subtypes in the MD during associative recognition memory retrieval and at the mPFC-MD synapse. Each of these chapters will contain their own discussion and then chapter 6 will provide a general discussion summarising the findings from all three results chapters.

Chapter 2

Methods and Materials

2.1 Animals

All procedures conducted on animals were in accordance with the University of Bristol guidelines and the UK Animals Scientific Procedures Act (1986). Male, Lister-Hooded rats (Harlan Laboratories) were used for all experiments. Experiments were conducted on rats weighing between 300 g - 500 g. Rats were housed under a twelve-hour light/dark cycle (light phase 20:00 - 08:00), with all procedures conducted during the dark phase of their cycle. Rats were housed in groups of four unless they underwent cannulation surgery, in which case they were pair housed. All cages were enriched with cardboard tubes. Water and food were available *ad libitum*.

2.2 Surgical procedures

Stereotaxic surgery was conducted for the implantation of cannulae and viral injections. Sterility was maintained throughout all surgeries. Anaesthesia was induced by isoflurane inside an induction box at 2 L/min. After the loss of hind leg reflex, the head was shaved, and the rat was placed and head-fixed in the stereotaxic frame (Kopf, USA). Anaesthesia was maintained with isoflurane via a stereotaxic gas mask at 1.5-2 L/min. A heat mat was placed underneath the rat to assist with body temperature regulation throughout the surgery. Prior to incision, the scalp was cleaned with 70% ethanol, numbed with topical lidocaine, and disinfected with chlorhexidine. During the surgery, rats were given

subcutaneous injections of sterile saline (sodium chloride 0.9 % w/v with glucose 5 % w/v) to a total volume of 5 ml. To manage post-surgery pain and infection risk, rats were given intramuscular injections of 0.05 ml vetergesic (0.3 mg/ml buprenorphine) and 0.1 ml antibiotic (150 mg/ml Clamoxyl). The suture wound was cleaned and covered generously with antiseptic powder (tosylchloramide sodium 2 w/w). Rats were then placed into a heated recovery box until fully aroused and stable. Diet gel and mashed food were provided in the animal's home cage for a minimum of 5 days post-surgery. Weights were also recorded over this 5-day period and then monitored once a week.

2.2.1 Cannulation

Twenty-nine animals received cannulation implants into the MD. Bilateral guide cannulae were implanted into the MD using the following co-ordinates from bregma (AP -2.9 mm, ML ± 0.75 mm, DV -4.9 mm from dura). After induction of anaesthesia and scalp preparation as described above, a flap of skin from the scalp was removed along with underlying connective tissue to expose the skull. Initial DV measurements of bregma and lambda were made and any adjustments to the frame were made to achieve a flat skull with less than 0.3 mm difference in the dorsoventral axis. Bilateral burr holes were drilled in the skull over the MD co-ordinates with an additional four holes (two anterior, two posterior) for the placement of stainless-steel screws (Plastics One, Semat, UK) to anchor the guide cannula. The guide cannulae were implanted after the stainless-steel screws, and dental cement was applied to secure the placement. The dummy cannula was inserted into the guide cannula to maintain patency and dust caps were screwed on top to reduce risk of infection. Animals were singly housed for seven days post-surgery before being paired.

Three cohorts of animals received these cannulations, cohort 1 consisted of 13 animals, cohort 2 consisted of 12 and cohort 3 consisted of 4. An additional animal received surgery in cohort one due to the loss of one animal after surgery. Both cohort 1 and 2 were used for behavioural experiments, and any losses within these cohorts were due to either animals being lost due to cannula blockages, or they were removed from the analysis if histology revealed cannulae were incorrectly placed. These losses are reflected in a change in the n number and degrees of freedom throughout the results sections. Cohort 3 were not subject to any behavioural tasks; they were used only to assess the spread of drug infusate as described in section 2.4.7.

2.2.2 Viral injections

For *in vitro* electrophysiology recordings of the mPFC-MD pathway, the adeno-associated virus, AAV9 : CaMKIIα : hChR2$_{(E123T/T159C)}$: mCherry (Addgene 35 512; 3.3 x 10^{13} genome copies/mL) was injected bilaterally into the mPFC (AP + 2.5mm, ML $\pm$ 0.8 mm, DV -4.5 mm) [106]. After the induction of stable anaesthesia and scalp preparation, the skull was exposed through a scalpel incision. Dorsoventral measurements were taken at lambda and bregma. Adjustments were made accordingly to ensure the skull was flat, with no greater differences than 0.3 mm. Bilateral burr holes were drilled and infusions of 300 nl of virus per hemisphere were administered at a rate of 200 nl/min. The needle was left *in situ* for a further ten minutes before withdrawal. The flow of virus was confirmed prior to, and after, each infusion. Ethanol was used to clean the needle between injections. Experiments were carried out at least two weeks after the surgery to allow for viral expression.

2.3 Behavioural experiments

2.3.1 Habituation

After recovering from surgery, the rats were habituated to daily handling, the behavioural arena and infusion procedure. Over four consecutive days in the behaviour room, the habituation sessions introduced increasing elements of the infusion process and arena to the animal. Animals received increasing duration of gentle restraint working up to a full five minutes on the experimenter's lap before being placed in the arena to explore freely for five minutes. Over the course of these sessions the animals were introduced to the sound of the infusion pump alongside removal and replacement of the dust cap and dummy cannula. Rats were re-habituated prior to starting the object-in-place task due to a change in arena configuration. Rats were also re-habituated to the arena following any breaks from testing that exceeded one week.

2.3.2 Arena

Tests were performed in an open field arena (length 100 cm x width 90 cm x height 50 cm). The arena floor was covered with sawdust that was unchanged throughout experiments. Two standing lamps situated outside the arena provided ambient lighting in the behaviour room. A webcam was mounted (approximately 1 m) above the arena so that live performance could be observed and recorded for subsequent analysis. Footage was recorded using OBS studio (v23.0.2, 64-bit), and DOSBox was used to record exploratory behaviour at each phase.

For the novel object recognition task, all four internal walls of the arena were black and black curtains were around all sides. The arena was adjusted for the object in place and object location tasks. For these tasks the left internal wall was grey to give a local spatial cue. The front and back edges remained covered by a black curtain, hiding the experimenter from view, but the curtains perpendicular to this were opened to provide the animal with global spatial cues.

2.3.3 Infusions and drugs list

Stock concentrations of each drug were made in sterile saline solution (sodium chloride 0.9 % w/v), aliquoted, and stored at -20 ℃. On the day of the experiment, aliquots were diluted in saline to give the required working concentration. Infusion lines were made with polyethylene tubing and connected the bilateral, 33-gauge infusion cannula to two, 25 µl Hamilton syringes (Hamilton, UK) filled with ddH_20. The lines were flushed clean with ddH_20 before filling with either saline or drug solution. Before inserting the cannula, the dust cap and dummy cannula were removed and stored in 70 % ethanol. An infusion pump (Harvard apparatus, UK) was used to deliver 1 µL of solution into each hemisphere at a rate of 0.5 μl/min. Flow of solution was confirmed prior to, and after each infusion. Infusions were administered 15 minutes prior to the sample or test phase to test memory encoding or retrieval, respectively. Due to the crossed study design, each animal acted as its own control, receiving both vehicle and drug conditions on separate trials (see figure 2.1). The experimenter was blinded to the animal's treatment groups until the experiment and analysis was completed.

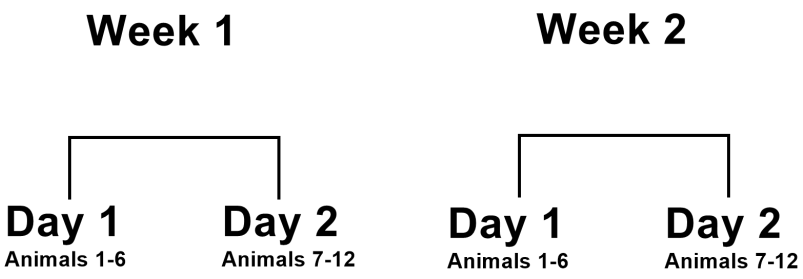

Figure 2.1: Timeline of behavioural experiments

As animals served as their own control, they were tested on two occasions for each behavioural task over a two week period. No more than six animals were tested per day due to three hour delay between sample and test phases making the timings impossible. In week 1 all 12 animals performed the same task using the same objects. In week 2 the same task was repeated but with new objects to remove the chance of animals recognising objects used in previous weeks. Animals that received 'Drug A' on Week 1 would receive 'Drug B' on Week 2 and vice versa.

The compounds D-(-)-2-Amino-5-phosphonopentanoic acid (AP5), DHβE, Ro 25-6981, NVP AAM077, and muscimol were purchased from Tocris, UK. UBP-791 was provided by Dr Mark Irvine, University of Bristol [91]. NVP AAM077, RO 25-6981 and UBP-791 were dissolved in 0.1 M NaOH before being diluted in sterile saline. For these infusions a 0.1 M NaOH concentration-matched saline solution was used for the control vehicle. Methyllycaconitine citrate (MLA), scopolamine, and benzyl quinolone carboxylic acid (BQCA) were purchased from Santa Cruz Biotechnology. BQCA was dissolved in sterile saline containing 0.1 % dimethyl sulfoxide (DMSO). For these infusions, a DMSO concentration-matched saline solution was used for the control vehicle.

Zeta inhibitory peptide (ZIP) and its scrambled counter part (Scr-ZIP) were purchased from Tocris, UK. TAT-GluR2$_3\gamma$ and its scrambled counter part, Scr-TAT-GluR2$_3\gamma$, were purchased from Eurogentec, Belgium. All were dissolved in sterile saline and the scrambled versions were used for the control vehicle infusions. A summary of drug concentrations and their mechanisms of action are displayed in table 2.1.

Table 2.1: Drugs used *in vivo*

Drug	**Function**	**Concentration**	**Solvent**
AP-5	NMDAR antagonist	25 mM	Saline
BQCA	M_1 mAChR PAM	100 nM	Saline and 0.1% DMSO
DHβE	$\alpha4\beta2$ nAChR antagonist	1 μM	Saline
MLA	$\alpha7$ nAChR antagonist	100 nM	Saline
Muscimol	$GABA_A$ agonist	2.4 mM	Saline
Muscimol BODIPY TMR-X	$GABA_A$ agonist	2.4 mM	25% DMSO, 75% PB
NVP AAM077	GluN2A NMDAR antagonist	10 μM	Saline and 0.1M NaOH
RO 25-6981	GluN2B NMDAR antagonist	30 μM	Saline and 0.1M NaOH
Scopolamine	mAChR antagonist	26 mM	Saline
Scrambled TAT-GluR$2_3\gamma$	GluA2 Subunits	30 μM	Saline
Scrambled ZIP	PKM,PKC	10 mM	Saline
TAT-GluR$2_3\gamma$	GluA2 Subunits	30 μM	Saline
UBP-791	GluN2C/D NMDAR antagonist	1 μM	Saline and 0.1M NaOH
ZIP	PKM,PKC	10 mM	Saline

2.4 Behavioural tests

To assess recognition memory and associative recognition memory, several spontaneous exploration tasks were utilised. All the tasks depend on the rats innate preference to explore novelty in its environment. All tests consist of a sample phase where novel stimuli are presented, a retention delay and then a final test phase where the animals' ability to remember stimuli, stimuli location or configurations are tested. These tests used rats that had received cannula implants into the MD, thus allowing for site specific infusions to be administered during the behavioural tasks.

2.4.1 Objects

All tests used objects made from Duplo® that varied in size range and colour. Objects were chosen that were known to be equally salient and used previously by other laboratory members. Objects were positioned in the corners of the arena, approximately 15 cm from the arena walls. Objects were cleaned with 100 % ethanol prior to every sample and test phase.

2.4.2 Novel object recognition

Two identical objects were placed in the back left and right corners of the arena. The sample phase terminated when the animals had explored for more than 40 seconds or was terminated after a duration of four minutes. After a three-hour delay, animals were returned to the arena for the test phase. For this phase, one of the two objects was replaced with a novel object. Animals were given 5 minutes to explore both objects during the test phase. The novel object was counterbalanced between animals, so some animals were presented object A as the novel object, and others were presented with object B (Figure 2.2). The position of the novel object was also switched, appearing either on the left or right. For testing the effects of drugs on memory retrieval, infusions were administered 15 minutes prior to the test phase (see Figure 2.2).

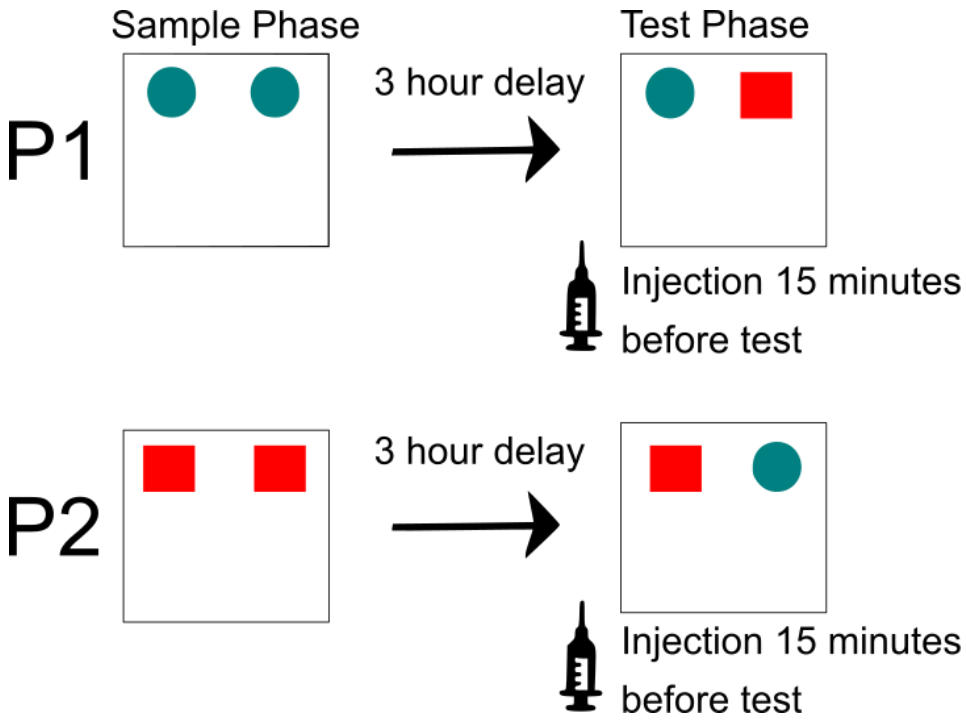

Figure 2.2: Novel object recognition task with pre-test infusions
A schematic overview of the OR task. Some animals encountered object A (blue circle) first and object B (red square) was the novel object. Others encountered object B first and then A was the novel object. Both examples show the novel object on the right, but some animals also encountered this on the left, so the trials were counterbalanced.

2.4.3 Object location

The object location task assesses spatial discrimination. This task is dependent on the HPC and not the MD, so was used as a control for any damage to the HPC during cannula implantation and/or the effects of drug spread dorsal from the cannula tip [4, 107]

Rats were placed in the front of the arena facing toward the experimenter and away from the objects. They were allowed four minutes of free exploration during the sample phase. Following a three-hour retention delay, rats were returned to the arena for a three-minute test phase. The two objects in the arena had been replaced by two identical replicas for the test phase. One object was replaced in the location previously occupied by the sample phase object, then the other object was placed in a new location in the arena (see Figure 2.3). The position of the moved object was counterbalanced across rats. For testing effects of drugs on memory retrieval, infusions were administered 15 minutes prior to the test phase (see Figure 2.3).

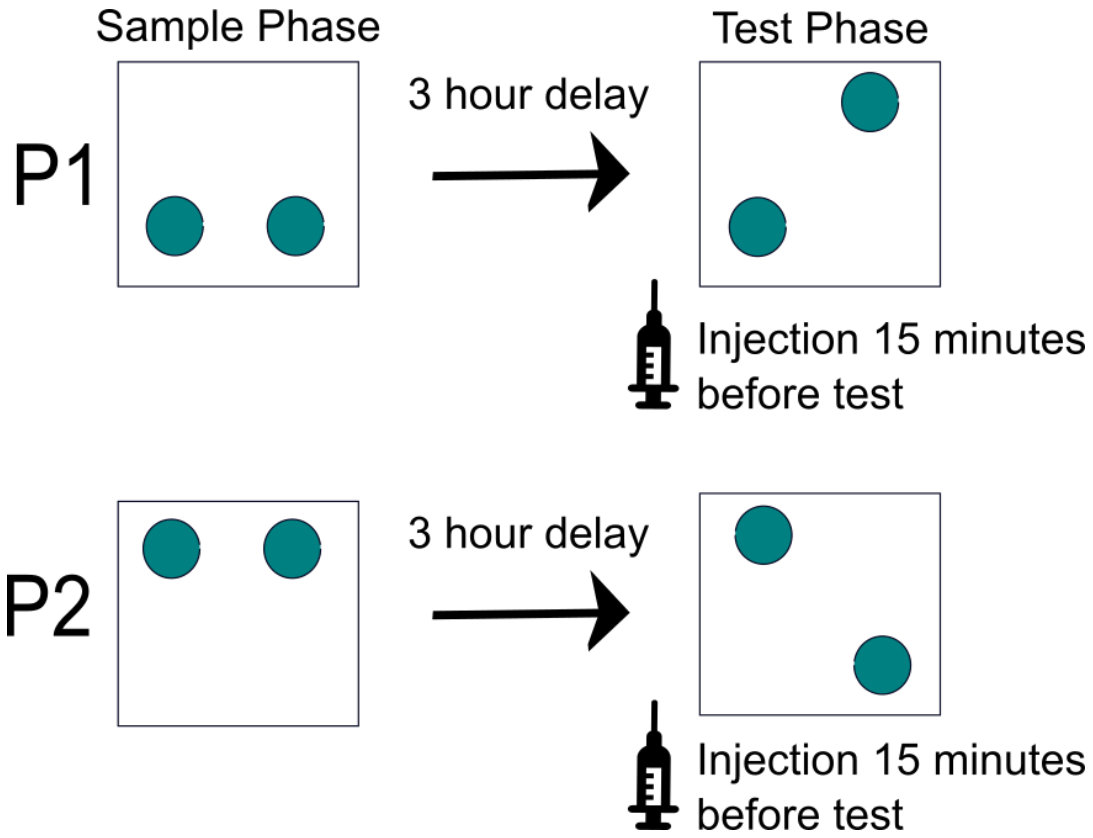

Figure 2.3: OL task with pre-test infusions

A diagram representing the object location task. Animals would encounter objects in the test phase in position one (P1) or position two (P2). The object in the novel location at test phase would then either be located on the left or the right. In this example the novel object location is on the right in P1 and on the left for P2.

2.4.4 Object in place

Animals were placed into the arena, facing the objects, for five minutes for the sample phase. Here they encountered four objects, all different in colour and shape, placed in each corner of the arena. After a three-hour delay, animals were returned to the arena for the three-minute test phase. In this phase, two of the original four objects switched places to give a novel object configuration (see Figure 2.4). Position of the objects was counterbalanced within trials whereby some animals encountered the novel objects on the left, and the others on the right. Drug infusions were given 15 minutes prior to the test phase to test effects on memory retrieval, as shown in Figure 2.4, or 15 minutes prior to the sample phase to test effects on memory encoding.

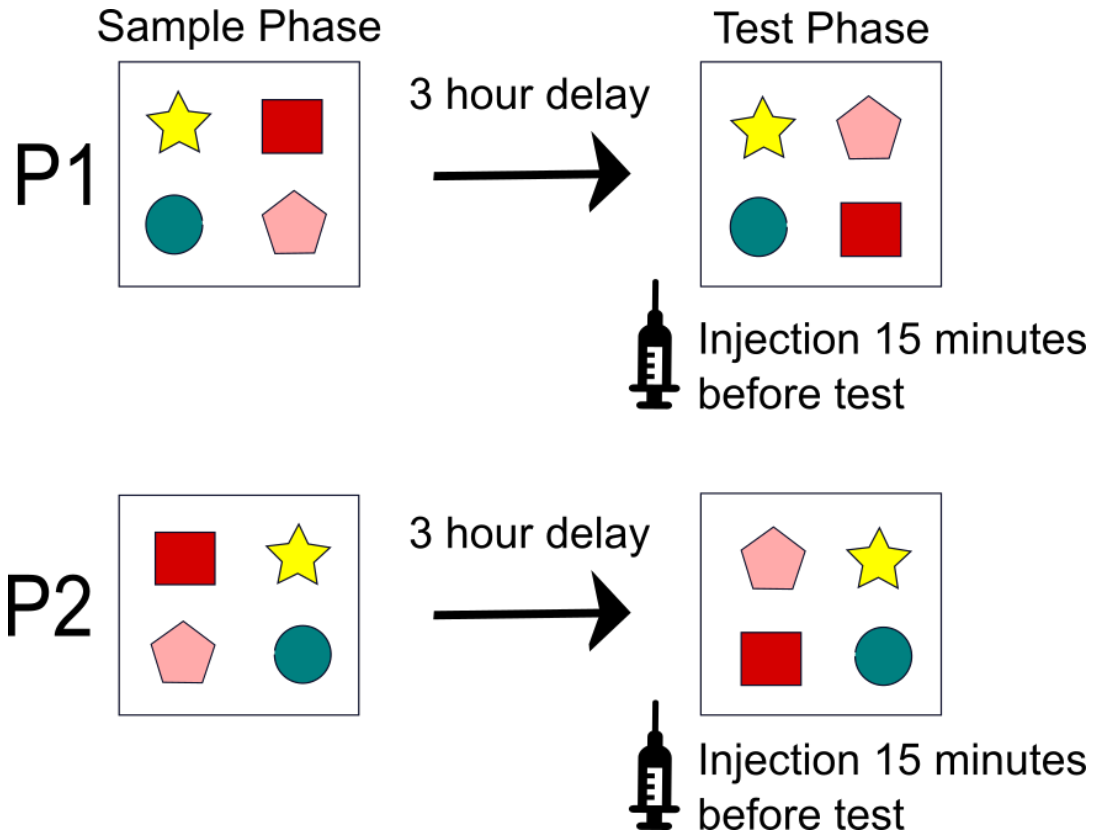

Figure 2.4: OiP task with pre-test infusions

A schematic overview of the OiP task. Animals would encounter objects in either position P1 or P2 and then the novel object configuration would be made by switching objects on either the left or right sides. This diagram shows only the novel object on the right-hand side for both P1 and P2, but some animals would encounter the novel configuration on the left hand side so overall the trials were counterbalanced.

2.4.5 Scoring of exploration

Object exploration was scored live throughout the experiment, but videos were saved for later analysis if required. Exploration times were recorded on Microsoft disk operating system (MS-DOS) designed by Professor Bussey (University of Cambridge). Exploration was defined as the animal pointing its nose toward an object with its nose being within 2 cm of the object. Digging, biting, and idly sitting on the object was not counted as exploration. An animal was omitted from analysis if their exploration score was below 15 seconds during the sample phase, and 10 seconds during the test phase.

2.4.6 Discrimination ratio

Using exploration times of novel and familiar objects, a discrimination ratio was calculated for each animal. The calculation is made by calculating the difference in exploration time at novel and familiar objects divided by the total exploration time at novel and familiar objects. This produces a value whereby a value of 1 would indicate the animal only spent time exploring the novel object, -1 the familiar object only, and 0 they spent equal amounts exploring novel and familiar objects.

2.4.7 Histology

After completion of the behavioural tasks, animals were sacrificed by transcardial perfusion. Rats were anaesthetised with pentobarbital (euthatal). Once breathing had ceased and the palpebral reflex was lost, animals were perfused with phosphate buffered saline (PBS) followed by 4 % paraformaldehyde (PFA). Brains were post-fixed in PFA for a minimum of two hours followed by 48 hours in 30 % sucrose in phosphate buffer. Coronal sections (40 μm) from the mediodorsal thalamus were taken on the cryostat and mounted on polylysine cover slips. Sections were stained with cresyl violet and coverslipped with DPX mounting medium. Slides were viewed under a light microscope to confirm correct cannula placement. Locations were confirmed against standardised coronal sections [108].

Drug spread

To calculate the area of MD targeted by intracortical infusions, four rats were infused with the GABAA receptor agonist conjugated to an orange fluorescent dye (Muscimol BODIPY TMR-X conjugate) at 0.5 μl/minute.

Sections were taken on the cryostat and mounted five at a time on polylysine cover slips with an approximate anterior-posterior distance of 200 μm between slides. Sections were DAPI-stained (VECTASHIELD® HardSet H-1500, Vector Laboratories, USA) and the spread was imaged by fluorescent microscopy (CTR500; Leica Biosystems, Germany). The area of visible fluorescence was measured using ImageJ (Wayne Rasband, 1.52g) and multiplied by the AP distance of spread to produce an approximate volume of drug spread for each hemisphere.

2.4.8 Statistical analysis: behaviour data

All statistical analysis was conducted using IBM® SPSS® Statistics (IBM Corp, Version 24). All data sets were tested for normality by assessing the results of the Shapiro-Wilk test along with the appearance of normality histograms and Q-Q plots. For ANOVA, these normality tests were conducted on the standardised residuals. Additionally, sphericity of the data for ANOVA was assessed using Mauchly's test of sphericity. Parametric or non-parametric tests were conducted depending on whether test assumptions were sufficiently met. Details of specific tests conducted are mentioned within the relevant results section. Data are all presented as mean ± the standard error of the mean (SEM) unless stated otherwise. Significance level was set at 0.05. Throughout the study, some animals were lost due to cannulae blockage, or incorrect cannula placement. This loss is represented by adjustments to the n number and degrees of freedom reported throughout the results section.

2.5 Electrophysiology

To investigate the properties of MD neurons and the mPFC-MD synapse, in vitro electrophysiological recordings were made in the MD.

2.5.1 Solutions

Several solutions were used during these experiments. There were two different external solutions used; a sucrose solution for the dissection and artificial cerebrospinal fluid (aCSF) which slices were bathed in. The internal solution also differed between a caesium-based solution and a potassium-based solution for voltage clamp and current clamp recordings, respectively. All internal solutions were adjusted to pH 7.3 with potassium hydroxide or caesium hydroxide depending on the base of the solution, and osmolarity was 290 $\mathrm{mOsm} \cdot \mathrm{L}^{-1}$. Details of these solutions can be found in table 2.2 and table 2.3.

Table 2.2: External solutions

Compound	**Sucrose aCSF (mM)**	**Normal aCSF (mM)**
Sucrose	189	-
D-Glucose	10	10
NaCl	-	124
$NaHCO_3$	26	26
KCl	3	3
NaH_2PO_4	1.25	1.25
$MgSO_4$	5	1
$CaCl_2$	0.1	2

Table 2.3: Internal solutions

Compound	**Potassium gluconate (mM)**	**Caesium methylsulfonate (mM)**
K Gluconate	120	-
$CsMeSO_4$	-	130
NaCl	2	-
KCl	-	4
HEPES	40	10
EGTA	0.2	0.5
GTP-Na salt	0.3	0.3
ATP-Mg salt	2	4
QX-314-Cl	-	2
Biocytin	13.4	2.69

2.5.2 Drugs

Stock solutions of drugs used *in vitro* were made in double distilled water and then stored at -20 °C. Drugs were then diluted to working concentration in aCSF and added to the bath perfusion system.

RJR-2403 oxalate, AP5, DHβE, RO 25-6981 and NVP AAM07 were purchased from Tocris, UK. Picrotoxin and NBQX were purchased from HelloBio, UK. UBP-791 was provided by Dr Mark Irvine, University of Bristol.

Table 2.4: Drugs used *in vitro*

Drug	**Function**	**Concentration**
AP-5	NMDAR antagonist	50 μM
DHβE	$\alpha 4\beta 2$ nAChR antagonist	1 μM
NBQX	AMPAR antagonist	5 μM
NVP AAM077	GluN2A NMDAR antagonist	1 μM
Picrotoxin	$GABA_A$ antagonist	50 μM
RJR-oxalate	$\alpha 4\beta 2$ nAChR agonist	3 μM
RO 25-6981	GluN2B NMDAR antagonist	1 μM
UBP-791	GluN2C/D NMDAR antagonist	1 μM

2.5.3 Slice preparation

Rats were anaesthetised using isoflurane and then killed by decapitation. The brain was removed and immediately submerged in chilled (2 - 5 °C) oxygenated (95 % O_2, 5 % CO_2) sucrose cutting solution. The frontal lobe and cerebellum were trimmed off before gluing the remaining brain (caudal side up) on to the stand and placing in the vibratome chamber. This was filled with oxygenated sucrose solution and the outside chamber filled with ice to minimise vibrations and reduce mechanical damage to the tissue. Coronal slices, 350 μm thick, were taken that contained the MD. These sections were trimmed and placed into oxygenated aCSF at room temperature. The slices were incubated for one hour at 32 °C and then kept at room temperature until recording. Stock concentrations of sucrose aCSF and aCSF were made at the beginning of each week. Working concentrations of aCSF were made in the morning of recordings by a 1 in 10 dilution.

2.5.4 Whole cell patch clamp

Slices were transferred to a recording chamber continuously perfused with aCSF at 2.5 ml/min and maintained at a temperature of 32 – 33 °C. Pharmacological agents were added to the aCSF to give working concentrations stated in table 4.1. Neuronal somas were visually identified using infra-red differential interference contrast immersion microscopy. Recording electrodes were pulled and polished from borosilicate glass capillaries to give resistances of 2 – 5 MΩ. These were back filled with the appropriate internal solution

for the recording mode. Data were amplified using an Axopatch 200B amplifier, digitised with Axon data acquisition board and acquired on the laboratory computer using WinLTP (WinLTP LTd. and The University of Bristol, version 2.30). Recordings were low pass filtered at 8 kHz and digitised at 40 kHz.

Recordings were not made from cells that had a RMP above -55 mV (with liquid junction potential error applied), cells broken into before making a gigaohm seal, or cells with a series resistance over 25 MΩ (20 MΩ for voltage clamp experiments).

Current Clamp

Whole cell current clamp recordings were made using a potassium gluconate based internal solution (table 2.3) with no correction applied for liquid junction potential. Current clamp protocols were used to assess the intrinsic properties of MD neurons and studying the mPFC – MD pathway. Current clamp recordings were acquired using the bridge-balance circuit of the amplifier to compensate access resistance. The bridge balance value was monitored throughout recording to ensure it was stable and remained below 20 MΩ.

Voltage clamp

Voltage clamp recordings were made using a caesium methylsulfonate based internal solution to have greater control over the cell's voltage. Pairing this internal solution with the aCSF produces a liquid junction potential error which was corrected for after breaking into the cell by adjusting the holding potential. The liquid junction potential was calculated using Clampex (MDS Analytical Technologies, version 10.2.0.14). Series resistance was monitored throughout voltage clamp experiments and was never compensated (i.e never above 20 MΩ).

2.5.5 Whole cell current clamp recordings

Passive membrane properties - subthreshold

Resting membrane potential was measured immediately after gaining electrical access to the cell in the absence of any current injection. Other membrane properties were measured from the changes in voltage recorded after varying current steps were applied to the cell.

Initial recordings involved holding the cell at their resting membrane potential value. Then later recordings replaced this method and instead took repeated recordings from the same cell held at -70 mV and -55 mV.

The input resistance (R_i) and membrane charging time constant (tau) were measured by fitting an exponential to the 10-95 % portion of the membrane charging curve. Extrapolated R_i (RiExt) was determined with Ohm's law from an infinite time extrapolation of this fit. The RiExt is a measure of resting R_i before the activation of I_h that happens with hyperpolarisation. R_i was also calculated from the steady state voltage change at the end of the current step (RiSS), and this value includes the activation of I_h. Measures of R_i and tau were used to calculate an approximate value for the capacitance (C_m) of the cell (C_m = tau/R_i). It is an approximate measure as this equation makes an assumption that the cell is spherical and does not take into account dendrites and that the voltage change across the whole cell is uniform. For a visual example of how these measures were taken see figure 2.5.

The sag current (% sag), due to activation of I_h was measured from the same -100 pA, hyperpolarising current steps and is calculated as follows: % sag = (extrapolated voltage change - steady state voltage change/extrapolated voltage change)*100. See figure 2.5 to see how these values were obtained from a hyperpolarising current step.

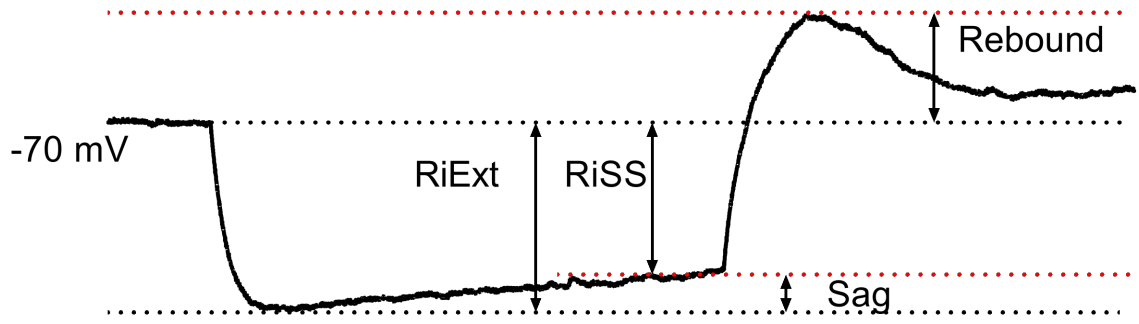

Figure 2.5: Measuring subthreshold properties

Trace shows a cell held at -70 mV being administered a 500 ms current step of -100 pA. Arrows indicate the subthreshold measures that can be calculated from a hyperpolarising current.

Suprathreshold properties

Action potentials and firing properties are dependent on membrane potential so cells were held at -55 mV and -70 mV to measure the different firing properties exhibited by thalamic relay cells and depolarising current injections were applied to evoke firing.

The AP properties were measured at the first spike evoked from a 300 pA current injection. The peak of the AP was measured as the absolute voltage peak and the width was measured at both -15 mV and at threshold. AP threshold was measured as the voltage where the first derivative of the spike waveform exceeded 15 mV.ms-1. The maximum rate of rise was the maximum value of the first derivative of the AP waveform.

As a result of applying 300 pA current injections, the cells would fire multiple APs which were counted. The interval between each AP (inter-spike interval) was measured from the same current step and the reciprocal of these values were calculated to give the instantaneous frequency.

The latency to first spike (AP) was measured at current steps 50 pA - 300 pA in 50 pA increments, and compared between cells held at both -70 mV and -55 mV.

Short term plasticity at the mPFC-MD synapse

To assess the properties of the corticothalamic synapse, mPFC fibres were optically excited and evoked EPSPs were recorded in MD neurons. The optical stimulus (470 nm) was delivered through the objective. The optical pulse duration was adjusted within a range of 0.1 ms - 2 ms, along with light intensity, to evoke EPSPs approximately that were similar in size for each experiment. This size was normally between 2 - 10 mV depending on viral expression. Once achieved, these parameters were constant throughout experiments. Each experiment began with a five-minute baseline of EPSPs being evoked every ten seconds. Cells were discarded if a stable baseline was not maintained. The data were normalised between cells when analysing to account for the differences in response size in each cell.

To investigate short term plasticity at the mPFC-MD synapse, prefrontal fibres were optically stimulated, and evoked responses were recorded from MD neurons. Trains of ten stimuli were delivered at frequencies of 5, 10 and 20 Hz. The order in which cells received the different frequencies was randomised to eliminate any order confounds. EPSP

summation was analysed by measuring the peak of each EPSP relative to the baseline of the first EPSP. Data were normalised to accommodate differences between cells before averaging and quantifying. EPSP summation was measured by dividing the size of a peak in the train by the size of the very first peak (i.e. P2/P1, P3/P1 and so on).

For pharmacological manipulations, drugs were added after the baseline and effects measured fifteen minutes after he drug had been applied. Both EPSPs and trains were recorded in the presence of either AP-5, RJR-oxalate or RJR-oxalate and DHβE.

2.5.6 Whole cell voltage clamp recordings

Voltage clamp recordings were used specifically to measure AMPA and NMDA receptor mediated synaptic currents. Picrotoxin was added to the aCSF to block inhibitory transmission and ensure that all evoked currents were excitatory. Single optical stimuli were delivered at holding potentials of -70 mV, +40 mV, and 0 mV.

AMPA- and NMDA- receptor mediated synaptic currents

To measure the relative contribution of AMPA and NMDA receptors at the corticothalamic synapse a ratio of the peak amplitudes of excitatory postsynaptic currents (EPSC) from AMPA and NMDA receptors was calculated.

Prior to calculating EPSC peak amplitude or decay time, data were baseline-subtracted. EPSCs were evoked by optical stimuli and an average of six EPSCs were taken for both AMPA and NMDA mediated EPSCs.

To isolate AMPAR currents cells were held at -70 mV. Cells were held at + 40 mV to evoke EPSCs that contained both AMPAR and NMDAR currents. AMPAR current was either blocked pharmacologically by bath applying NBQX and then the peak amplitude was measured from the isolated NMDAR current. If AMPARs were not blocked then the amplitude measurement was taken from the time point at which the AMPAR EPSC at -70 mV had returned to baseline (see Figure 2.6).

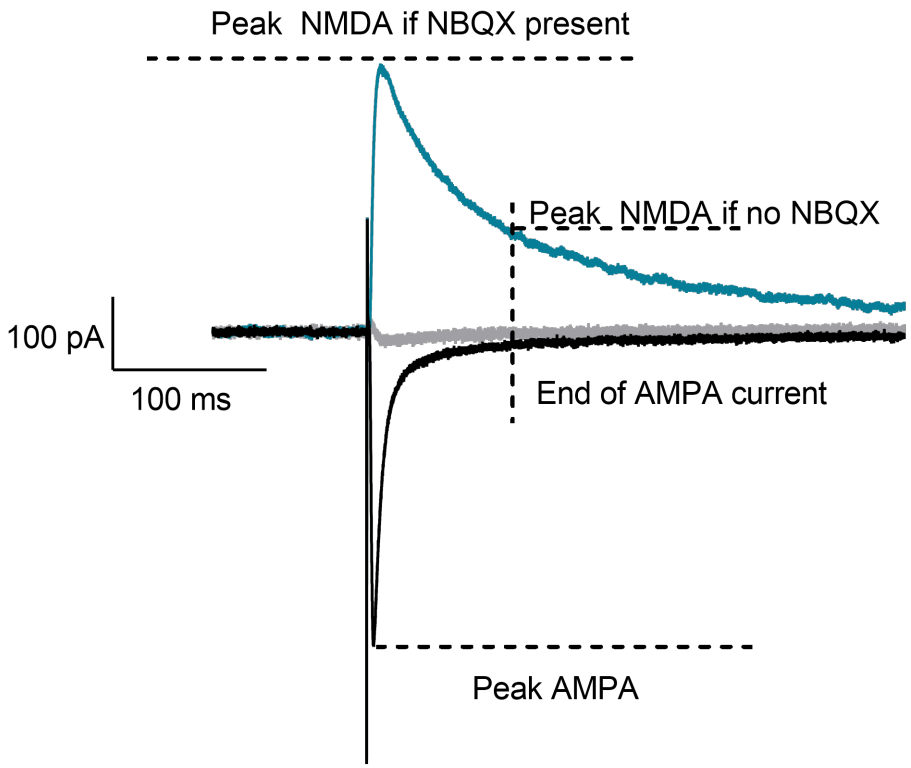

Figure 2.6: Measuring AMPA and NMDA EPSCs

A diagram to illustrate how measures of peak amplitude were obtained for AMPA and NMDA EPSCs dependent on whether AMPARs had been blocked by NBQX or not.

NMDAR antagonism

For the experiments investigating the effects of specific NMDAR subunits, NMDAR EPSCs were isolated by bath applying NBQX to block AMPAR current first. Experiments were also conducted in the presence of picrotoxin to isolate glutamatergic responses. Once NMDAR EPSCs had been isolated, subunit specific antagonists were bath applied and an average of six NMDAR EPSCs were recorded every 5 minutes for 30 minutes.

To measure the effect the drug had on the NMDAR EPSC, the peak amplitude values from each cell were normalised to allow for comparisons.

2.5.7 Statistical analysis: Electrophysiology Data

Data were analysed separately after recording using WinLTPr230 a7 reanalysis software (WinLTP Ltd. and The University of Bristol, version 2.30) or MATLAB (The Math Works, R2019a) using analysis scripts written by Dr Clair Booth. Statistical tests were then performed on IBM® SPSS® Statistics (IBM Corp, Version 24) and all graphs constructed using GraphPad Prism (GraphPad Software, version 8.4.3) and Inkscape (Inkscape Project, version 0.92.4).

Normality of the data was assessed, and provided this condition was met along with test assumptions, then parametric tests were used to analyse the data. In the case of normality or other test violations, then non-parametric tests were used. Details of specific tests are detailed within the results section. The significance value was set at $p = 0.05$.

Chapter 3

Role of Acetylcholine In the MD During Associative Memory Retrieval

3.1 Introduction

As outlined previously in the main introduction, the mediodorsal thalamus (MD) is crucial for supporting associative recognition memory retrieval [1, 4, 18, 25, 28]. Within the network of brain regions required to support such memory, it shares dense reciprocal connections with the mPFC, and previous work has shown that information flow between these regions is crucial during the retrieval of associative recognition memory [4, 18, 20, 28, 42].

Acetylcholine is a widespread neurotransmitter in the brain and evidence shows it has a crucial role in learning and memory [67, 109, 110]. Cholinergic neuromodulation has been well studied in the mPFC [69, 73], however very little is known about cholinergic neuromodulation in the MD. This study aimed to define the contribution of cholinergic receptors in the MD during associative memory retrieval.

Both nAChRs and mAChRs have been shown to be expressed in the thalamus [111–115]. Nicotinic $\alpha4\beta2$ and $\alpha7$ receptors have been found specifically in the MD, whereas muscarinic receptors have been characterised generally across the thalamus, with M1 and

M2 subtypes being most prevalent [75, 76]. The experiments presented in this chapter targeted the $\alpha 7$ and $\alpha 4\beta 2$ subtypes of nAChRs specifically, and targeted all subtypes of mAChRs to determine their role in associative recognition memory retrieval in the MD.

3.2 Methods

This section covers a brief overview of the methods used for the contents of this chapter. For the full description see chapter 2.

3.2.1 Subjects

The subjects for this chapter were from cohort 1 and cohort 3 (see 2.2.1. Cohort 1 consisted of 12 adult male Lister Hooded rats (300 g - 450 g) that had received bilateral guide cannula implants aimed at the MD (see section 2.2.1). Cohort 3 consisted of four rats that were not involved in behaviour but received infusions of fluorescent muscimol. From cohort 1, one animal was removed from testing following cannula blockage and one was removed from analysis due to incorrect cannula placement. The loss of these subjects is reflected by a decrease in n number and degrees of freedom in the statistical reports.

3.2.2 Behavioural experiments

Spontaneous exploration tasks were used to measure recognition memory following pharmacological manipulations in the MD. For a full description of the tasks and arena set up see sections 2.3 and 2.4. Recognition memory was tested using the novel object recognition (OR) task and associative recognition memory was tested using an object in place (OiP) task. Drug and vehicle infusions were delivered 15 minutes prior to the sample or test phase of these tasks to investigate effects on encoding or retrieval, respectively.

Each experiment was conducted using a cross-over experimental design whereby each animal received both vehicle and drug infusions on separate trials, thus each animal was its own control and data were paired across conditions. Placement of the novel object (for the OR task) or novel object configuration (for the OiP task) in the arena was counterbalanced.

3.2.3 Drugs

To confirm previous findings that the MD is required for associative recognition memory retrieval and not novel object recognition, animals were tested on the OiP and OR tasks after receiving infusions of muscimol to inactivate the MD.

To explore the role of cholinergic modulation in the MD during associative recognition memory retrieval, specific antagonists for nicotinic and muscarinic acetylcholine receptors were infused (see table 3.1)

For a full description of how drugs were prepared for infusions, see section 2.3.3.

Table 3.1: Drugs used for cohort 1 and cohort 3

Drug	Function	Concentration	Solvent	Cohort
DHβE	$\alpha4\beta2$ nAChR antagonist	1 μM	Saline	1
MLA	$\alpha7$ nAChR antagonist	100 nM	Saline	1
Muscimol	$GABA_A$ agonist	2.4 mM	Saline	1
Muscimol BODIPY TMR-X	$GABA_A$ agonist	2.4 mM	25% DMSO, 75% PB	3
Scopolamine	mAChR antagonist	26 mM	Saline	1

Agonists

Muscimol the $GABA_A$ receptor agonist was used to inhibit MD neurons. It was used at a concentration of 2.4 mM (unpublished work, Laura Cross, Gareth Barker). It has also been used at this concentration to inactivate other regions without causing off target effects [93]. Infusions of fluorescent muscimol were given to animals in cohort 3, who did not undergo any behavioural tests, in order to quantify the spread of the infusions within the MD.

Antagonists

Scopolamine is a non-specific muscarinic acetylcholine receptor antagonist and was infused into the MD to target all mAChR subtypes. Scopolamine was infused at a concentration of 26 mM, a dose which has previously been infused into other regions to block associative recognition memory [81, 93, 116].

DHβE is a selective antagonist at the α4 subunit containing nAChRs and was infused at a concentration of 1 μM. This concentration was chosen to ensure a high level of receptor block without off target effects at other nAChR subtypes at higher concentrations [73].

MLA is an antagonist of α7 nAChRs and was infused at 100 nM. This dose was chosen as its higher than its K_i value of 0.87 nM but below the level shown to have off target motor effects [73].

3.2.4 Statistical analysis

Statistical comparisons between drug and control conditions were assessed by paired t-tests or a two-way repeated measures ANOVA, by comparing the mean discrimination ratios across conditions. A one-sample t-test was used to compare the mean discrimination ratio against a value of 0 to determine if animals had significantly discriminated between novel and familiar object configurations. These parametric tests were used after first checking the normality of the data, or standardised residuals (for ANOVA). Statistical significance was set at $p < 0.05$. Data are presented as mean $\pm$ SEM unless stated otherwise.

3.3 Results

3.3.1 Cannula placement

Histological analysis confirmed the cannula placement within the MD, as shown in Figure 3.1. Cannula placement was determined by the deepest dorso-ventral point of the cannula tip. One animal was excluded from the analysis due to incorrect cannula placement.

Cannula tips were predominantly located in the medial MD (MDM, n = 6) and the rest were located in the central (MDC, n = 1) and lateral MD (MDL, n = 3).

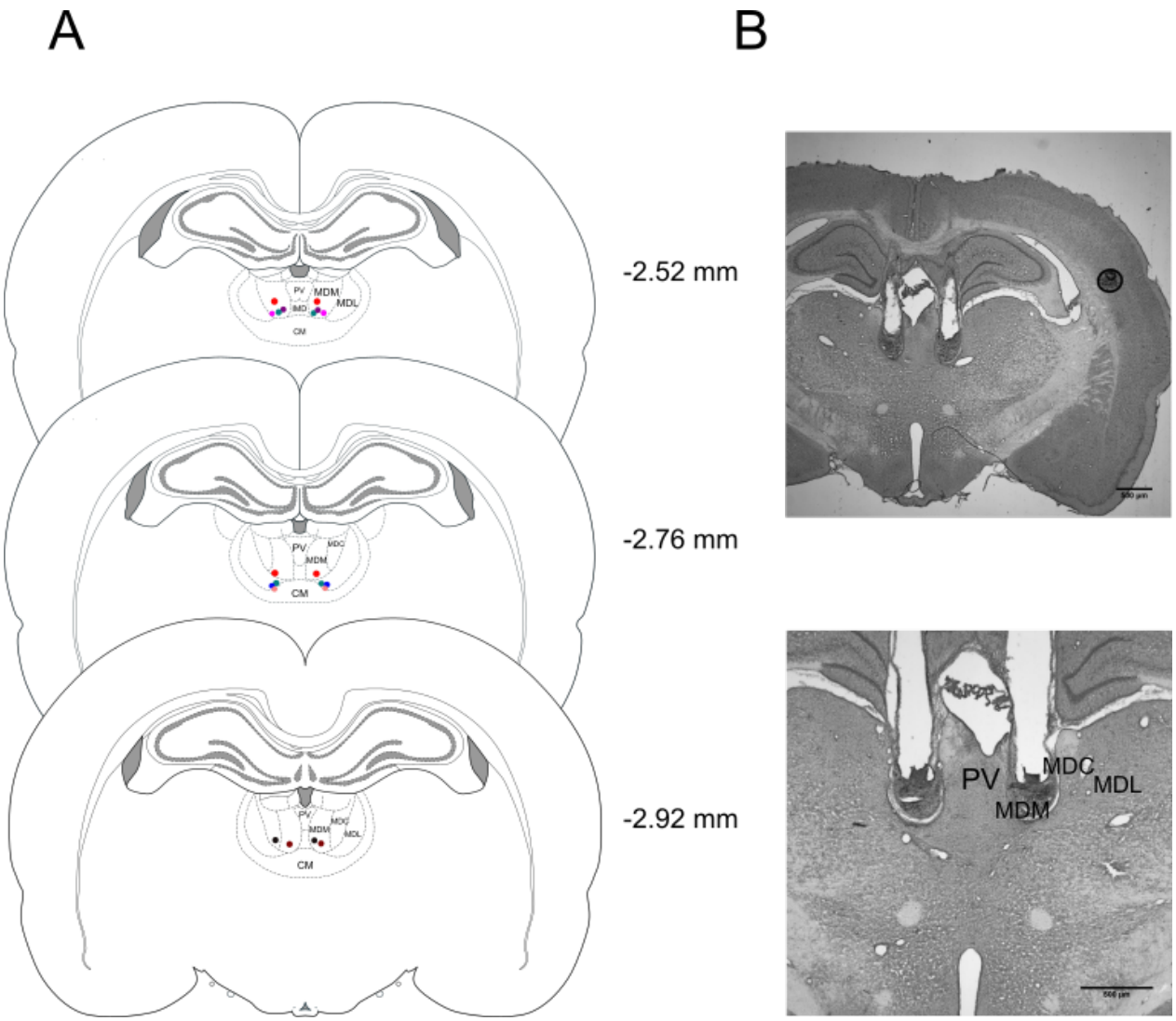

Figure 3.1: Cannula placement in the MD

A: A diagrammatic representation of cannula placement within the MD, this includes medial, central and lateral subsections of the MD (MDM, MDC and MDL). Coloured dots represent location of bilateral cannula tips within the MD (n = 10). Where cannula tip locations overlapped, matching colours were used to demonstrate where bilateral tips were located. Surrounding structures include the paraventricular nucleus (PV), intermedialdorsal nuclei (IMD) and the centromedial nucleus (CMD). Numbers along the right-hand side indicate the section's location relative to bregma. Brain sections were taken and reconstructed from the Paxinos and Watson Brain Atlas [108]. **B:** Images show an example of a cresyl stained section at 2.5x (top) and 5x magnification (bottom) from one animal to identify cannula location. Scale bars are 500 μm.

3.3.2 Drug infusion spread within the medial dorsal thalamus

The $GABA_A$ receptor agonist muscimol conjugated to an orange fluorescent dye was infused bilaterally into the MD to assess the overall spread of drug infusion. The infusions of fluorescent muscimol were timed to match the experimental infusion procedure. Infusions occurred over 2 minutes and 15 minutes after the infusion animals were perfused. Image analysis showed fluorescent labelling was present across the MD over approximately 1.4 mm across the anterior-posterior length of coronal sections. The overall spread of drug was detected across approximately 1.67 mm^3.

Fluorescent muscimol was observed strongly in the medial segment of the MD and moderately in the central and lateral segments of the MD (Figure 3.2.) Some presence of fluorescent muscimol was also found in the dorsal parts of the CMD, IMD, paraventricular nucleus and ventral parts of the habenula.

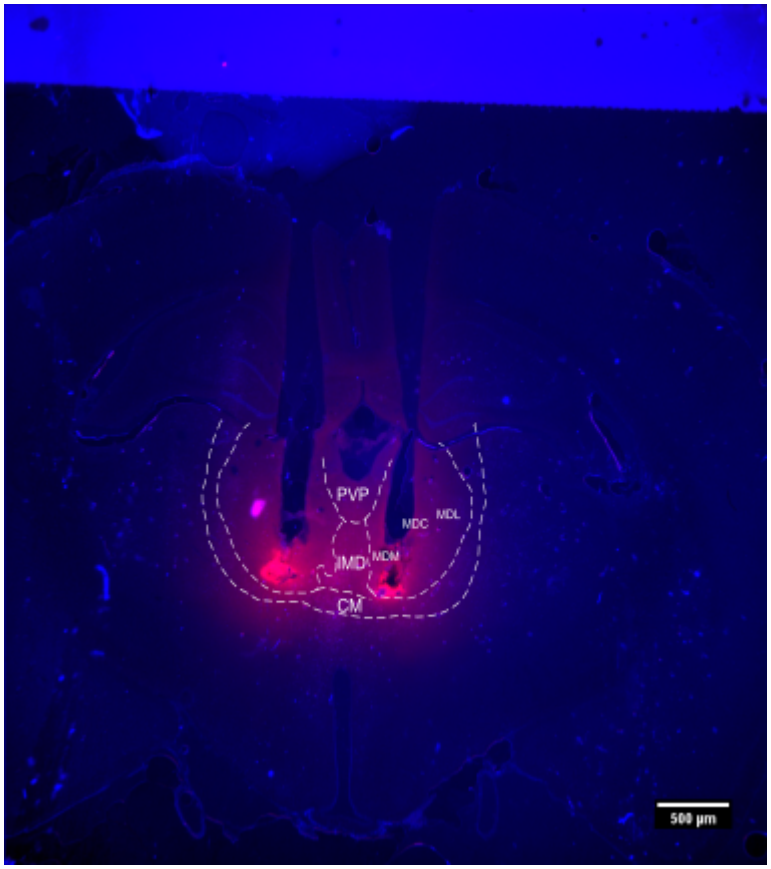

Figure 3.2: Drug spread from cannula tip

Figure shows a representative image of a coronal section, approximately -2.92 mm relative to bregma, containing the cannula implant and spread of fluorescent muscimol. Abbreviations on the diagram are as follows: paraventricular nucleus (PV), intermedialdorsal nuclei (IMD), centromedial thalamus (CM), medial mediodorsal thalamus (MDM), central mediodorsal thalamus (MDC), and lateral mediodorsal thalamus (MDL). Scale bar is 500 μm.

3.3.3 Saline control experiments

Animals were initially tested on the OR task with saline infusions only. This was to ensure the rats were able to complete the task and there were no significant impacts of stress or the infusion procedure on their ability to discriminate.

Analysis revealed that animals had a mean discrimination ratio of 0.26 $\pm$ 0.08 which was statistically significant from 0 ($t_9 = 3.158$, $p = 0.012$, $n = 10$) (Figure 3.3A). Mean exploration at test phase was 37.91 s $\pm$ 3.08 s (Figure 3.3B). No animals were excluded as no animal's exploration time was below 10 seconds.

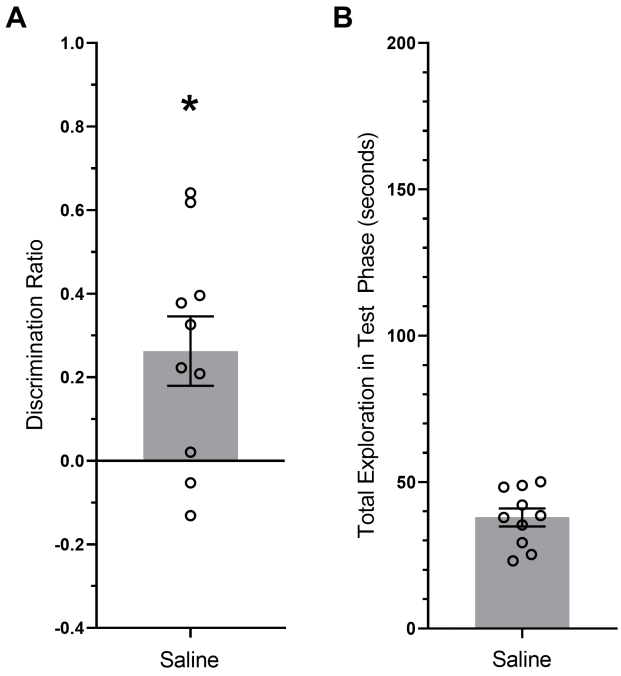

Figure 3.3: Animals successfully performed OR task with saline

A: Animals successfully discriminated between novel and familiar items above chance levels (p = 0.012, n = 10). Statistical significance labelled with asterisk. **B**: Total exploration during the test phase, all animals passed the object exploration time criteria of 10 seconds (n = 10). Graphs display the mean ± SEM with each circle representing data from individual animals.

3.3.4 MD is required for associative memory retrieval but not novel object recognition

To examine the role of the MD in the retrieval of associative and non-associative recognition memory, infusions of muscimol were given prior to the test phase in the OR and OiP tasks.

Analysis of memory performance in the OR task revealed no significant differences in discrimination ratios between vehicle (0.18 ± 0.05) and muscimol (0.25 ± 0.07) groups (t_9 = -0.719, p = 0.491, n = 10) (Figure 3.4 Ai). Both groups significantly discriminated between the novel and familiar objects (Vehicle: t_9 = 3.860, p = 0.004, n = 10; Muscimol: t_9 = 3.461, p = 0.007, n = 10). There were no significant differences in total exploration time at the test phase when animals received vehicle (39.01 s ± 3.51 s) or muscimol (32.08 s ± 3.31 s) (t_9 = 1.796, p = 0.106, n = 10) (Figure 3.4 Aii).

In the object in place task, there was a significant difference in discrimination ratios between vehicle (0.20 ± 0.07) and muscimol (-0.01 ± 0.04) groups (t_9 = 3.678, p = 0.005, n = 10) (Figure 3.4 Bi). The vehicle group significantly discriminated between the novel and familiar objects (t_9 = 3.056, p = 0.014, n = 10) whereas the muscimol group did not (t_9 = -0.455, p = 0.660, n = 10). There were no significant differences in total exploration time at the test phase when animals received vehicle (55.08 s ± 2.26 s) or muscimol (58.70 s ± 3.39 s) (t_9 = -0.867, p = 0.409, n = 10) (Figure 3.4 Bii).

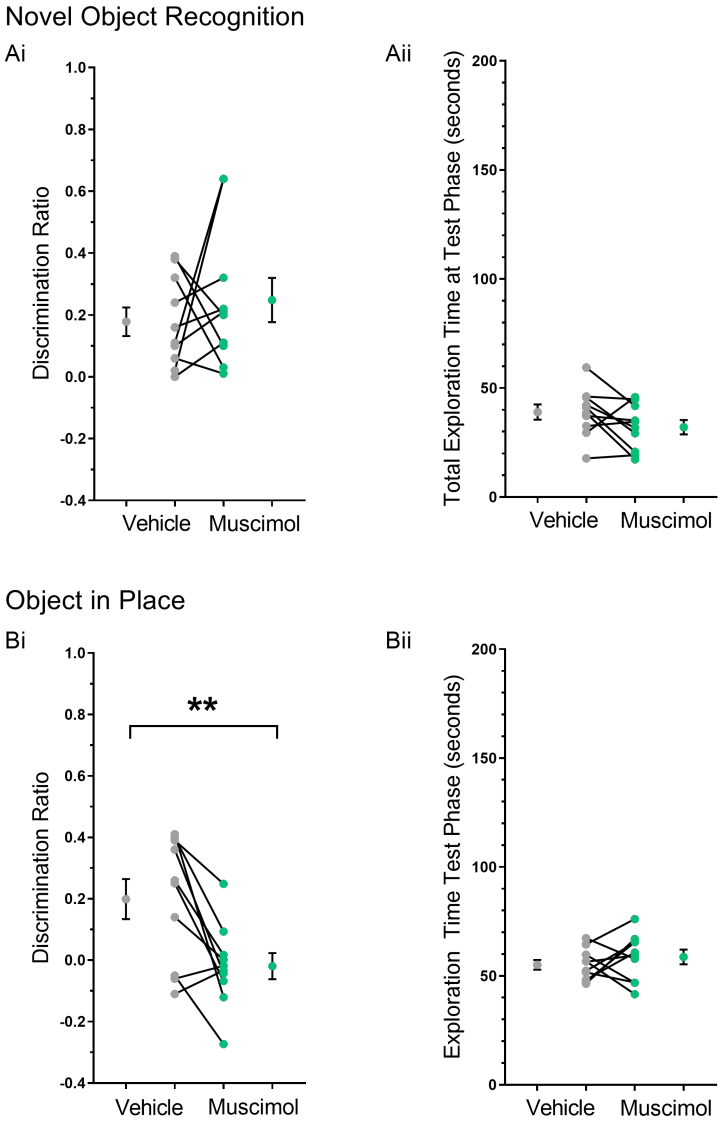

Figure 3.4: MD required for associative recognition memory but not object recognition memory

Ai: Infusions of muscimol before retrieval had no effect on performance in the object recognition task. There were no significant differences between the groups ($p > 0.05$, $n = 10$). Both groups significantly discriminated between novel and familiar objects ($p < 0.05$, $n = 10$). **Aii**: No significant differences in total exploration time during the test phase between vehicle and muscimol receiving groups ($p > 0.05$, $n = 10$). **Bi**: Infusions of muscimol before retrieval significantly impaired performance in the object in place task compared to vehicle infusions ($p = 0.005$, $n = 10$). **Bii**: No significant differences in total exploration time during the test phase between vehicle and muscimol receiving groups ($p > 0.05$, $n = 10$). The graphs display individual data points paired across conditions alongside the group means ± SEM. Statistical differences between groups indicated with asterisks.

3.3.5 $\alpha 4\beta 2$ receptor required for associative memory retrieval but not encoding in the mediodorsal thalamus

To determine the role of $\alpha 4\beta 2$ nAChRs in encoding or retrieval of object-in-place memory, infusions of DHβE were administered prior to the sample or test phase. A two-way repeated measures ANOVA, with drug and infusion timing as factors, revealed a significant effect of drug ($F_{(1,9)} = 8.554$, $p = 0.017$, $n = 10$) and infusion timing ($F_{(1,9)} = 7.779$, $p = 0.021$, $n = 10$), but no significant interaction between the two ($F_{(1,9)} = 3.636$, $p = 0.089$, $n = 10$). Although there were no significant interactions between conditions, further simple effects analysis, with the Bonferroni correction, were conducted to explore differences between the conditions at each point. These results showed that the drug had a significant effect on task performance when given prior to the test phase ($p = 0.001$) (Figure 3.5 C), but not the sample phase ($p = 0.867$) (Figure 3.5 A).

Comparison of the groups' discrimination ratios against chance showed that infusions of vehicle (DR = 0.22 ± 0.09) or DHβE (DR = 0.20 ± 0.05) prior to the sample did not impair discrimination between novel and familiar configurations (Vehicle : $t_9 = 2.344$, $p = 0.044$, $n = 10$; DHβE: $t_9 = 3.975$, $p = 0.003$, $n = 10$). There were no significant differences in the mean total exploration time during the sample phase for vehicle (117.69 s ± 7.18 s) or DHβE (115.06 s ± 9.48 s) receiving groups ($t_9 = 0.449$, $p = 0.664$, $n = 10$) (Figure 3.5 B).

In contrast, when infusions were administered prior to the test phase, the vehicle group (DR = 0.24 ± 0.07) but not the DHβE (DR = -0.09 ± 0.06) group significantly discriminated above chance levels (Vehicle: $t_9 = 3.632$, $p = 0.005$, $n = 10$; DHβE: $t_9 = -1.521$, $p = 0.162$, $n = 10$). There were no significant differences in the mean total exploration time for vehicle (65.68 s ± 3.33 s) or DHβE (67.59 s ± 3.19 s) groups ($t_9 = -0.550$, $p = 0.596$, $n = 10$) (Figure 3.5 D).

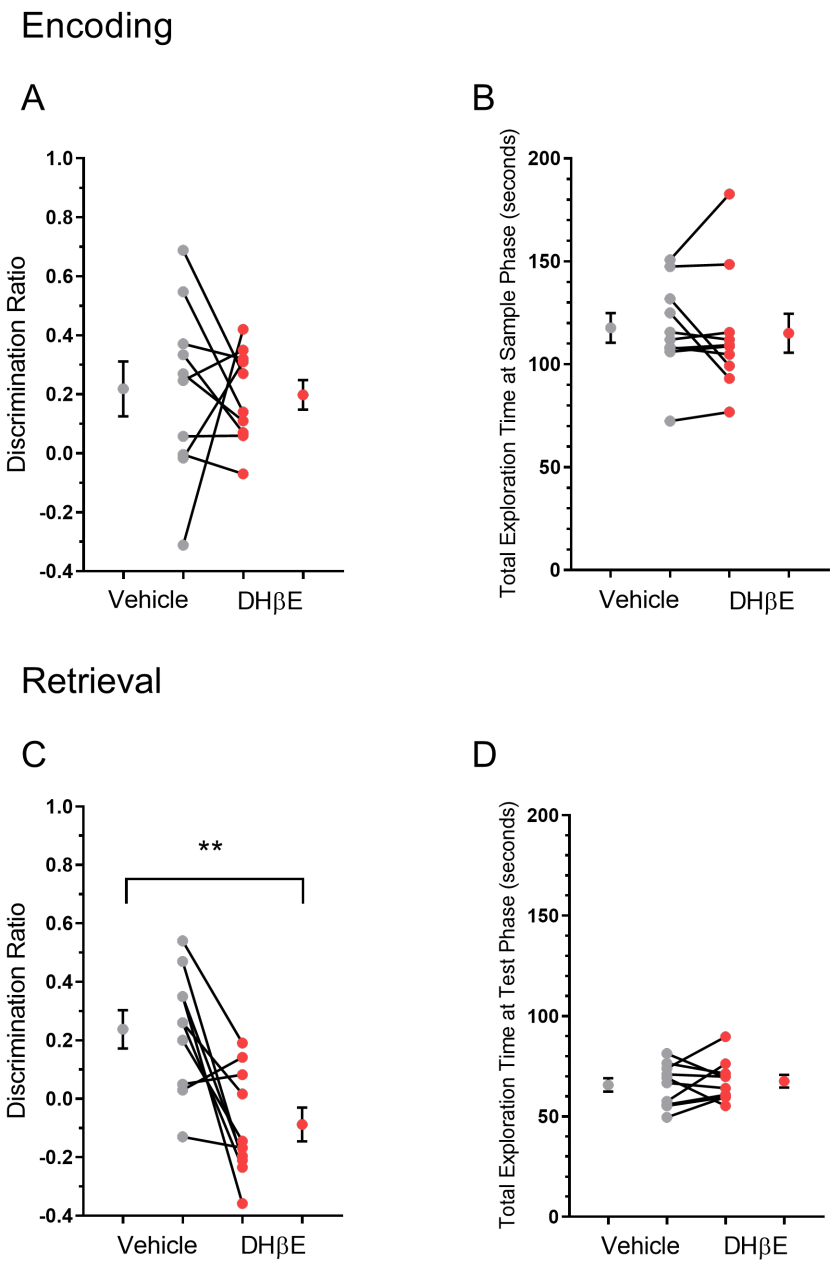

Figure 3.5: Blocking $\alpha 4\beta 2$ nAChRs impairs memory retrieval but not encoding. **A**: DHβE had no effect on OiP performance when infused before the sample phase ($p > 0.05$, $n = 10$). **B**: No differences in total exploration time during the sample phase after vehicle or DHβE infusions ($p > 0.05$, $n = 10$). **C**: DHβE significantly impaired OiP performance when infused prior to the test phase ($p = 0.001$, $n = 10$). **D**: No differences in total exploration time during the test phase after vehicle or DHβE infusions ($p > 0.05$, $n = 10$) The graphs display individual data points paired across conditions alongside the group means ± SEM. Statistical differences between groups indicated with asterisks.

3.3.6 α7 nAChRs not required for associative recognition memory encoding or retrieval in the MD

A two-way repeated measures ANOVA, with drug and infusion timing as factors, revealed no significant effects of drug ($F_{(1,8)} = 0.505$, $p = 0.497$, $n = 9$) or infusion timing ($F_{(1,8)} = 0.027$, $p = 0.874$, $n = 9$).

Comparison of the groups' discrimination ratios against chance showed that the infusions of vehicle (DR = 0.18 ± 0.08) or MLA (DR = 0.15 ± 0.06) prior to the sample phase did not impair discrimination between novel and familiar configurations (Vehicle: $t_8 = 2.380$, $p = 0.045$, $n = 9$; MLA: $t_8 = 2.660$, $p = 0.029$, $n = 9$) (Figure 3.6 A). There were no significant effects in mean total exploration time during the sample phase between vehicle (120.71 s ± 9.13 s) and MLA (104.93 s ± 8.29 s) groups ($t_8 = 1.575$, $p = 0.154$, $n = 9$) (Figure 3.6 B).

Infusions of vehicle (DR = 0.12 ± 0.03) or MLA (DR = 0.23 ± 0.04) prior to the test phase also had no effects on animals' ability to discriminate between novel and familiar configurations (Vehicle: $t_8 = 4.177$, $p = 0.003$; MLA: $t_8 = 6.047$, $p < 0.001$, $n = 9$) (Figure 3.6 C). There were no significant differences in total exploration time at test phase between vehicle (70.42 s ± 4.76 s) and MLA (59.53 s ± 5.13 s) groups ($t_8 = 2.288$, $p = 0.051$, $n = 9$) (Figure 3.6 D).

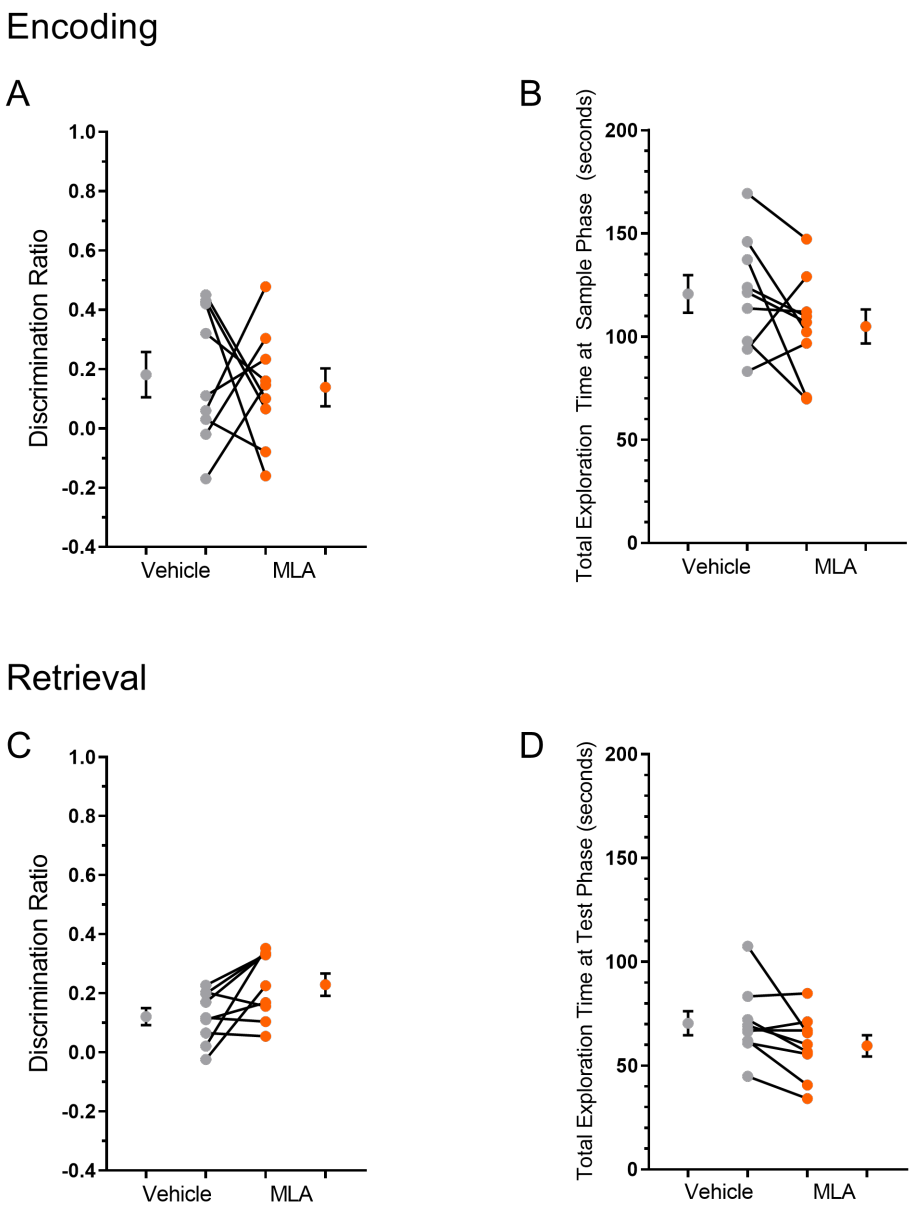

Figure 3.6: $\alpha 7$ nAChRs are not essential for associative memory in the MD

A: Infusions of MLA, prior to the sample phase, had no effect on OiP performance ($p > 0.05$, $n = 9$). **B**: There were no effects on total exploration time at sample phase following infusions of either vehicle or MLA ($p > 0.05$, $n = 9$). **C**: Infusions of MLA prior to the test phase had no effect on OiP performance ($p > 0.05$, $n = 9$). **D**: There were no effects on total exploration time at test phase following infusions of vehicle or MLA ($p > 0.05$, $n = 9$). The graphs display individual data points paired across conditions, alongside the group means ± SEM.

3.3.7 Muscarinic acetylcholine receptors are not required for associative recognition memory retrieval in the MD

To assess the contribution of mAChRs in associative memory retrieval in the MD, scopolamine was infused into the MD prior to the test phase. Analysis revealed no significant differences in DR values between vehicle (DR = 0.20 ± 0.07) and scopolamine (DR = 0.14 ± 0.05) groups (t_8 = 0.535, p = 0.607, n = 9). Both groups were able to significantly discriminate between novel and familiar configurations above chance levels (Vehicle: t_8 = 2.863, p = 0.021, n = 9; Scopolamine: t_8 = 2.692, p = 0.027, n = 9) (Figure 3.7 A). Analysis of the overall exploration time at the test phase showed there were no significant differences between vehicle (66.70 s ± 4.20 s) and scopolamine (66.57 s ± 4.67 s) groups (t_8 = 0.018, p = 0.986, n = 9) (Figure 3.7 B).

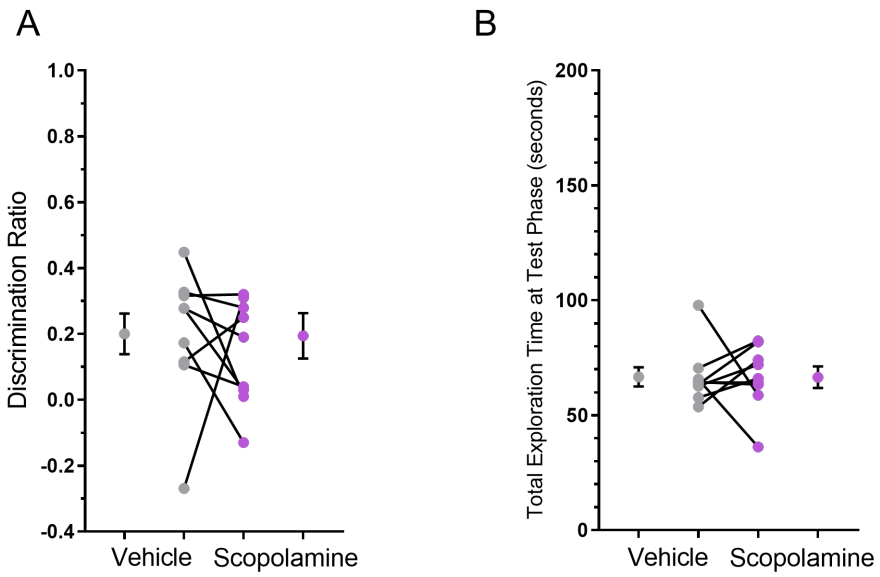

Figure 3.7: mAChRs not essential for associative memory retrieval

A: Infusions of scopolamine, prior to the test phase, had no effect on OiP performance (p >0.05, n = 9). **B**: There were no effects on total exploration time at test phase following infusions of either vehicle or scopolamine (p >0.05, n = 9). The graphs display individual data points paired across conditions, alongside the group means ± SEM.

Table 3.2: Mean Exploration Times Across Experiments

Drug	**Infusion Timing**	**Mean Exploration Time at Sample Phase (s)**	**Mean Exploration Time at Test Phase (s)**	**Mean DR**
DHβE	Pre-Sample OiP	115.06 ± 9.48	59.95 ± 3.87	0.20 ± 0.05
Saline	Pre-Sample OiP	117.69 ± 7.18	54.64 ± 6.19	0.22 ± 0.09
DHβE	Pre-Test OiP	102.68 ± 7.22	67.59 ± 3.19	-0.07 ± 0.06
Saline	Pre-Test OiP	104.71 ± 6.17	68.68 ± 3.33	0.24 ± 0.06
MLA	Pre-Sample OiP	104.93 ± 8.29	56.92 ± 2.62	0.14 ± 0.06
Saline	Pre-Sample OiP	120.71 ± 9.13	46.29 ± 6.31	0.16 ± 0.07
MLA	Pre-Test OiP	110.23 ± 8.16	59.53 ± 5.13	0.22 ± 0.03
Saline	Pre-Test OiP	112.52 ± 9.55	70.42 ± 4.76	0.12 ± 0.03
Muscimol	Pre-Test OiP	100.30 ± 3.39	58.70 ± 3.39	-0.02 ± 0.04
Saline	Pre-Test OiP	107.82 ± 5.55	55.08 ± 2.26	0.20 ± 0.07
Muscimol	Pre-Test OR	37.05 ± 2.06	32.08 ± 3.31	0.25 ± 0.07
Saline	Pre-Test OR	39.86 ± 0.17	39.01 ± 3.51	0.18 ± 0.05
Saline	Pre-Test OR	40.03 ± 0.00	37.91 ± 3.08	0.26 ± 0.08
Scopolamine	Pre-Test OiP	110.58 ± 5.63	66.57 ± 4.67	0.14 ± 0.05
Saline	Pre-Test OiP	105.02 ± 7.46	66.70 ± 4.20	0.20 ± 0.07

3.4 Discussion and conclusions

3.4.1 Main findings

Experiments in this chapter confirmed that inactivation of the MD with muscimol impaired associative recognition memory retrieval but spared object recognition memory. These results are in line with previous data which demonstrate the role of the MD in the OiP task and not the OR tasks [4] (unpublished work L Cross, G Barker).

The data in this chapter also showed for the first time that cholinergic transmission in the MD is essential during associative memory retrieval. Specifically, retrieval was shown to require the activation of $\alpha4\beta2$ nicotinic acetylcholine receptors, but not activation of $\alpha7$ or mAChRs. Further experiments showed that infusions of MLA or DHβE prior to the encoding phase had no effect on task performance, confirming the effects of $\alpha4\beta2$ nAChR antagonism are specific to memory retrieval.

3.4.2 $\alpha4\beta2$ nAChRs in the MD are required for associative recognition memory retrieval but not $\alpha7$ nAChRs

The data presented in this chapter showed that infusions of the $\alpha4\beta2$ nAChR antagonist, DHβE, impaired performance on the OiP when infused prior to the test phase. In comparison, infusions of the $\alpha7$ nAChR antagonist, MLA, produced no impairments on the OiP when infused prior to the sample or test phase of the OiP task. These experiments demonstrate a significant and retrieval dependent requirement of $\alpha4\beta2$ nAChRs activation in the MD during associative recognition memory.

Infusions of MLA or DHβE into the mPFC produce impairments during OiP encoding or retrieval, respectively [73]. It could be speculated that a similar function of these receptors occurs in the MD also. As the MD is not required for memory encoding, this could explain why there were no impairments observed after infusions of MLA. This result could be interpreted alongside the hypothesis that different modes of acetylcholine release occur during encoding and retrieval [73, 82]. As the MD is not involved in encoding, it might not receive the same release of acetylcholine as the mPFC during memory encoding, hence $\alpha7$ nAChRs are not activated and blocking them has no effect. In comparison, diffuse, tonic release of acetylcholine is associated with memory retrieval and perhaps both the

mPFC and MD are recipient to this mode of release which favours the activation of $\alpha4\beta2$ nAChRs; hence blocking these receptors impairs memory retrieval in both the mPFC and the MD.

It could also be argued that no effects were observed with MLA infusions due to $\alpha7$ nAChRs not being present in the MD. In the literature there is mostly evidence for $\alpha4\beta2$ nAChRs mRNA expressed in the MD, and sparse mention of $\alpha7$ [112, 113]. A study by Cannady et al conducted experiments where rodents received infusions of DHβE and MLA into the MD, but during a working memory task instead [86]. Their results showed that infusions of DHβE impaired performance on the working memory task but these effects could be attenuated by infusing MLA [86]. The data from Cannady et al's study could be used to argue that $\alpha7$ nAChRs are in fact present and they are required in working memory [86].

3.4.3 Muscarinic acetylcholine receptors are not required in MD during associative recognition memory retrieval

Infusions of scopolamine had no effect on OiP task performance suggesting that there is no essential requirement for these receptors during associative recognition memory retrieval in the MD. This experiment only tested the effects of infusing scopolamine on memory retrieval and not encoding. The rationale behind this is that previous studies using infusions of both NBQX or muscimol into the MD had no effect on encoding, but impaired memory retrieval (unpublished work L Cross, G Barker). The data in this chapter also demonstrated that infusions of DHβE or MLA had no effect on encoding either. Combined, these data demonstrate there is no requirement for the MD during memory encoding, thus only effects on memory retrieval were tested during the scopolamine experiment and during the experiments within chapter 5.

Previously, experiments targeting muscarinic receptors in the mPFC only produced impairments in memory encoding. Similarly, infusions of scopolamine into the PRH and NRe have impaired the encoding, but not retrieval of OiP memory [81, 93]. As discussed earlier with the $\alpha7$ nAChRs, it could be that mAChRs respond to different modes of acetylcholine release and differ in their sensitivity to acetylcholine compared to $\alpha4\beta2$ nAChRs. As phasic release of ACh is hypothesised to favour memory retrieval [73, 82], this could explain why mAChRs are not activated despite acetylcholine being released in

the MD during associative memory retrieval.

3.4.4 Cholinergic modulation in the thalamus

The MD receives cholinergic input mostly from the LDT and PPT but it also receives cholinergic projections from the BF which provides cholinergic input to the mPFC [49, 79, 80]. The present experiments examined the effects of blocking $\alpha4\beta2$ nAChRs throughout the MD but it is unknown whether the acetylcholine release is predominantly from the LDT, PPT, or the BF. An interesting experiment for the future could be to specifically target cholinergic cells from the LDT, PPT or BF using optogenetics. This would allow fine spatial and temporal manipulations to be made to explore whether input from these regions are required in the MD during retrieval.

The effect of acetylcholine on the firing of MD neurons has not been studied, however acetylcholine has been applied to thalamic relay cells in the lateral geniculate nucleus [60]. Bath applying acetylcholine resulted in a depolarisation of the cell membrane. As thalamic relay cells change their firing pattern depending on their membrane potential, this depolarisation caused cells to switch from burst firing, to tonic firing [60]. Burst firing has been largely hypothesised to occur during sleep states and not capable of encoding sensory information, whilst tonic firing relays more specific information to the cortex [64, 117]. In the present experiment, blockade of $\alpha4\beta2$ nAChRs could be preventing depolarisation of the cell membrane of MD cells and thus disrupting the incoming signals from the mPFC. The study by McCormick et al did not use specific agonists however, so the general effect of acetylcholine at both nAChRs and mAChRs is depolarising, but the effect of applying a specific $\alpha4\beta2$ nAChR agonist was not investigated [60]. As the location of these receptors in the MD is unknown, it is unclear how their activation affects the MD neurons.

There is increasing speculation in the literature that burst firing may be encoding more information from the cortex than previously thought [57, 64, 118], so another possibility is that the $\alpha4\beta2$ nAChRs are located on GABAergic terminals arising from the basal forebrain and the thalamic reticular nucleus (TRN). These are the two regions that supply inhibitory input to the MD. There is also evidence from the cortex that $\alpha4\beta2$ nAChRs are typically expressed on inhibitory neurons [73]. With this in mind, it could be that the $\alpha4\beta2$ nAChRs are expressed on these inhibitory terminals and that blocking them results in a disinhibition of MD neurons. This would switch them from burst firing to tonic firing

due to less GABA being released and hyperpolarising MD neurons.

As both nAChRs and mAChRs have an important role in attentional processes, it could be argued that the impairment observed after blocking these receptors is a result of an attentional deficit. Infusions of DHβE or MLA had no significant effect on rat's overall exploration time of novel and familiar object configurations. Also, if the impairments produced by DHβE were caused by an effect on attention, it would be expected that an impairment would have been observed when DHβE was infused prior to the sample phase also. Infusions of scopolamine had no significant effect on rat's overall exploration times either. Therefore, the impairments observed from infusions of DHβE are most likely from targeting mnemonic processes and not attentional, yet the precise synaptic location of the $\alpha4\beta2$ nAChRs in the MD requires investigation.

3.4.5 Study caveats

Scoring of behaviour

Spontaneous recognition tasks measure recognition by calculating a discrimination ratio that uses exploration time of novel and familiar objects. What constitutes exploration has been debated in the literature and overall, there is not an agreed standard [119]. Measures of exploration are consistent throughout our group and other groups and have been determined as outlined in the methods in chapter two. There are trends heading towards using automated software to measure exploratory behaviour, such as DeepLabCut^{TM}. However, these software are a long way off for providing an accurate measure of exploration. We define exploration as the animal directing its head toward an object <2 cm away, but do not count biting of the object. It would be difficult for this software to distinguish between these two behaviours. Additionally, sometimes animals will sit on the objects and groom and direct their head downwards. Such minute details in behaviour are easy for a human to notice and respond to but would require complex programming for automation. Whilst automated software would certainly be an excellent way to make scoring of exploration consistent across experimenters, it does not improve on current methods at present.

Naturally, there will be differences in scoring due to variations in reaction times that can introduce a small human error, but this is negligible within the data, as re-scoring the

videos gave no differences to the overall result. To reduce the possibility of human error, videos were re-scored and compared against original scores to check the consistency of scoring.

Between-subject variability

The nature of spontaneous exploration tasks results in an increase in variance between subjects and a decrease in statistical power [119]. The amount of exploration given to an individual object (novel or familiar) can be biased by the subjects' individual preferences for a particular object. To reduce the effect of this bias, the novel and familiar objects are counterbalanced across trials. Objects are also designed to be equivalent in interest and all objects made have been used in previous experiments that found consistent and relatively equal levels of exploration.

The stress to the animal in an open arena and being handled is also important to consider. Stressful experiences before the test phase can impair recognition memory at long intervals. These issues are reduced by regular handling of the animals to habituate them to the experimenter. Additionally, habituation to the arena and infusion process reduces the levels of stress this may cause. However, it is never stress-free and the natural variability in an animal's stress level day to day will contribute to the variance in exploration times across trials. As infusions of drugs prior to the test phase did also get null results, and that infusions of saline gave a null result, it is unlikely that impairments observed following DHβE infusions are due to stress.

Drug spread

The drug spread from the cannula tip was approximately 1.67 mm^3 across approximately 1.44 mm over the anterior-posterior length of the MD. This meant there was a reasonable spread of drug present across the length of the MD, and also throughout all subdivisions.

Whilst the presence of fluorescent muscimol was observed strongly in the medial MD, there was evidence of drug present in surrounding thalamic nuclei. As the cannula tips were quite ventral in cohort 1, it is likely that drug spread included the CMD. The CMD is thought to be involved in nociceptive transmission and also aid in the regulation of sleep cycles and attention [120]. As none of the cholinergic antagonists significantly affected exploration

times, it is unlikely they caused any effects in the CMD during the task. However, the role of the CMD during associative recognition memory has not been explored, and, whilst the impairments observed in this chapter are most likely due to the antagonists targeting the MD, it is not possible to rule out the involvement of the CMD.

Time delays

Throughout this study, the behaviour tests used a three-hour delay between the initial sample phase and the test phase. As infusions must be administered to the rat 15 minutes prior to entering the arena, it is not possible to have delays much shorter than an hour. A delay of five minutes has been used in other studies, but these studies have used animals with lesions, or optogenetic techniques allowing finer temporal control. Thus, it was not possible to study the effects of blocking acetylcholine on short term memory.

An optogenetic study conducted by G Barker demonstrated that the specific mPFC - MD input is crucial for memory retrieval (unpublished work, G.Barker). Impairments in OiP performance were seen at both 5 minute and 3 hour delays, suggesting that the MD is important for both short and longer term memory recall. Following on from these experiments, it would be interesting to find out if cholinergic modulation is required during these shorter delays also. As the MD receives cholinergic input from several sources, it would require a complex experiment to determine which cholinergic loci are supporting the MD during retrieval. One possible way to investigate this would be to use a transgenic rat line using ChAT and Cre recombinase, so Cre recombinase is present only in cholinergic neurons [121]. Then, these neurons could be targeted for optogenetic experiments. Viral injections could be administered into one of the three regions that supply cholinergic fibres to the MD; the BF, the PPT, or the LDT. The virus used would drive the expression of channel rhodopsin in Cre recombinase containing neurons, which, in this example would specifically be cholinergic neurons [121]. Then, optrodes implanted into the MD would allow for optogenetic manipulations to be made during the test phase where cholinergic fibres from the BF, for example, could be inactivated and effects on the behaviour could be observed.

Longer time points were not studied in the experiments in this chapter, so it is unknown whether the MD is required for longer term associative recognition memory retrieval. Most evidence in the literature points toward the MD being important for short term and

working memory [31, 32, 122, 123], however the MD's role in long term memory has not been tested sufficiently to rule this out. This could be tested by conducting the same experiment as presented in this chapter but extending the delay period to 24 hours.

3.4.6 Conclusion

The data presented in this chapter demonstrate for the first time that associative recognition memory retrieval in the mediodorsal thalamus is dependent on $\alpha 4\beta 2$ nicotinic acetylcholine receptors and that there are no requirements for muscarinic acetylcholine receptors.

Chapter 4

Properties of MD Neurons and the Corticothalamic Synapse

4.1 Introduction

The mPFC and MD share dense reciprocal connections with each other, and damage to either of these regions impairs associative recognition memory in rodents [4, 19]. Corticothalamic neurons arising in layers V and VI project across the MD [20, 30]. These projections are reciprocated by neurons in the MD that return projections to superficial cortical layers and thus complete reciprocal feedback loops between the MD and mPFC [45, 124]. There is little known about synaptic transmission between the mPFC and MD and whether any particular properties of this transmission may be critical for the behavioural response during associative recognition memory retrieval. A study by Bolkan et al showed that the mPFC and MD synchronise within the beta frequency range, and this coherence occurred during the retrieval phase of a delayed non-matching to sample test (DNMS) investigating communications between the mPFC and MD in working memory [123]. As it is unknown how the mPFC and MD transmit information during associative memory retrieval in the live animal, the experiments in this chapter explored how MD neurons respond to incoming mPFC input within theta and beta frequency ranges.

How neurons respond to incoming signals is determined by their intrinsic properties, and there is little known about the properties of MD neurons. Studies have suggested that

MD neurons exhibit similar firing profiles to other thalamic relay neurons, in that they display both burst and tonic firing [45, 58], however their intrinsic properties have not been extensively characterised. The experiments in this chapter sought to characterise the properties of MD neurons and confirm whether they exhibit the same firing patterns as neurons in other thalamic nuclei.

In the previous chapter, experiments demonstrated that the MD is required for memory retrieval and not formation during the OiP task. The data also showed that memory retrieval depends on the activation of $\alpha4\beta2$ nAChRs in the MD. Thus, the experiments in this chapter aimed to explore whether manipulating $\alpha4\beta2$ receptors affected transmission between the mPFC and MD *in vitro*.

4.2 Methods

This section will cover a brief overview of the methods for the experiments in this chapter. For a more detailed description see Chapter 2.

4.2.1 Subjects

All *in vitro* electrophysiology experiments were conducted on adult male Lister-Hooded rats (300-500g). All subjects received viral injections of AAV9 : CaMKIIα : hChR2$_{(E123T/T159C)}$: mCherry in to the mPFC 2-4 weeks prior to recordings (see section 2.2.2).

4.2.2 Electrophysiology recordings

Whole cell patch clamp recordings were taken from MD neurons located in the medial or central subdivisions of the MD. These regions receive their main projection from the prelimbic cortex. For the experiments presented in this chapter, all recordings were conducted in current clamp and so a potassium gluconate internal solution was used throughout.

To investigate the intrinsic properties of MD neurons, cells were administered 500 ms current steps ranging from -100 pA - +300 pA, in 50 pA increments. For a detailed

explanation of how various properties were calculated from these steps, see sections 2.5 and 2.5.5. Initially these depolarising steps were taken while the cell was held at its resting membrane potential. Then subsequent recordings were taken from the same cell held at -55 mV and -70 mV.

To investigate the properties of the mPFC - MD synapse, EPSPs were evoked by an optical stimulus shone through the objective and onto the slice. Short term plasticity was investigated by administering trains of ten stimuli at 5 Hz, 10 Hz and 20 Hz stimulation frequencies. For a full description of how these data were analysed, see section 2.5.5.

4.2.3 Drugs

To explore the contribution of NMDA and $\alpha4\beta2$ nAChRs at the mPFC - MD synapse, AP-5 or DHβE were applied to the bath during experiments. For a full description of how drugs were dissolved see section 2.5.2.

AP-5 was used to specifically target NMDA receptors and assess their contribution to the short term plasticity at the mPFC - MD synapse. It was applied to the bath at a concentration of 50 μM.

RJR-oxalate (RJR) is an agonist of $\alpha4\beta2$ nAChRs and was used to explore the effects of manipulating these receptors on the short term plasticity at the mPFC - MD synapse. It was bath applied at a concentration of 3 μM.

DHβE is an antagonist of $\alpha4\beta2$ nAChRs and was used to block the potential effects observed by RJR-oxalate during short term plasticity experiments. It was bath applied at a concentration of 1 μM.

Table 4.1: Drugs used in vitro

Drug	**Function**	**Concentration**
AP-5	NMDAR antagonist	50 μM
DHβE	$\alpha4\beta2$ nAChR antagonist	1 μM
RJR-oxalate	$\alpha4\beta2$ nAChR agonist	3 μM

4.2.4 Statistical analysis

Data analysis was conducted using WinLTPr230 a7 reanalysis software (WinLTP Ltd. and The University of Bristol, version 2.30), custom scripts in MATLAB (The Math Works, R2019a) written by Dr Clair Booth, and Microsoft Excel (Microsoft Corporation, version 2110). IBM® SPSS® Statistics (IBM Corp, Version 24) was used for statistical analysis. Parametric or non-parametric tests were used after first assessing the normality of the data with the Shapiro-Wilk test. Any violations of normality resulted in the relevant non-parametric test being used instead. Use of non-parametric tests are indicated within the results section and data are reported as the median and interquartile range (IQR). Otherwise, data are presented as the mean ± the SEM if not stated otherwise. P value set at 0.05.

4.3 Results

4.3.1 Viral expression in the mPFC

To confirm that the virus had been injected in to the mPFC, sections were observed on the microscope (Figure 4.1 A). Viral expression was found across all layers of the mPFC and in the PL and IL cortices.

Cells in the MD were filled with biocytin via the patch pipette. Visualising cells filled with biocytin was used to confirm the cell patched was located in the MDM or MDC. The morphology of cells were observed, and cells were a stellate or fusiform shape (Figure 4.1 B).

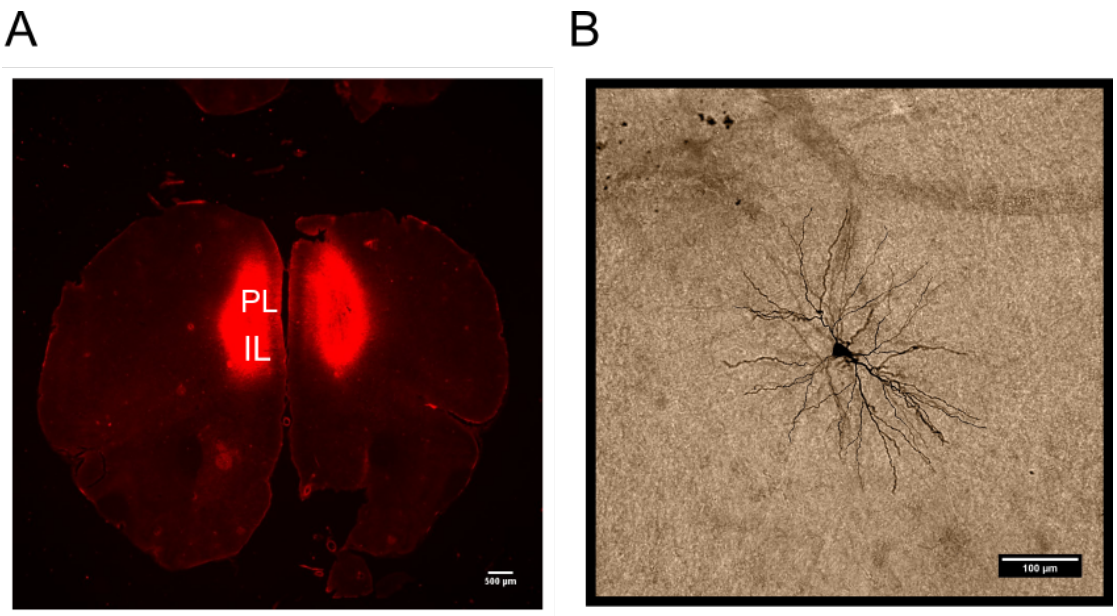

Figure 4.1: Confirmation of viral injection and patched cell

A: Expression of AAV9 : CaMKIIα : hChR2$_{(E123T/T159C)}$: mCherry confirmed in the mPFC using mCherry to visualise the injection site. Expression found in all cortical layers across the PL and IL cortices. Scale bar 500 μm **B:** Example of a biocytin filled stellate cell located in the MDM. Scale bar 100 μm.

4.3.2 Intrinsic properties of MD neurons

Neurons were injected with 500 ms current steps ranging from -100 pA - +300 pA in 50 pA increments. Changes in voltage were used to measure a range of intrinsic properties.

Firing properties

Firing properties were recorded from cells held at their resting membrane potential. Depolarising current injections revealed that MD neurons have two different spiking properties depending on their resting membrane potential. Cells more hyperpolarised than -65 mV would fire bursts of APs in response to depolarising current injection whereas cells resting more depolarised (-50 mV - -65 mV) would fire a succession of single APs. This firing pattern is observed in relay cells situated in other thalamic nuclei and is often referred to as "burst" and "tonic" firing, respectively. See figure 4.2 for examples of burst and tonic firing.

In lieu of this finding, further experiments were conducted where cells were held at both

-70 mV and -55 mV in order to compare how their intrinsic properties shape the difference in their firing profiles.

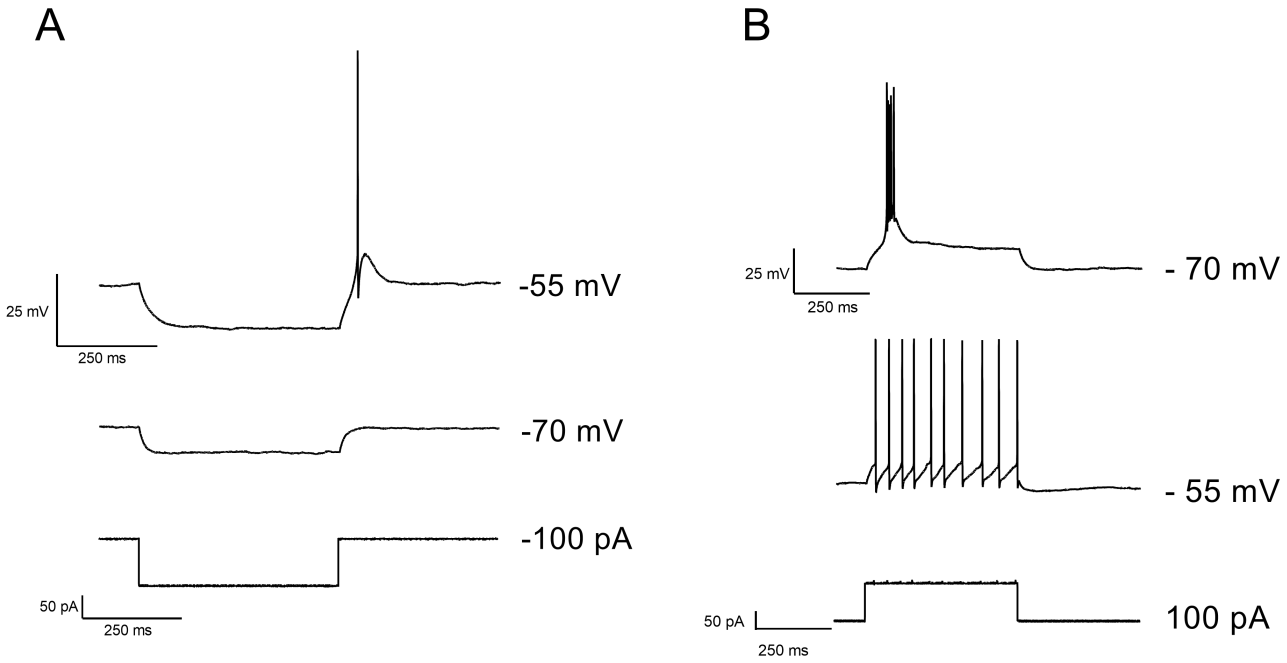

Figure 4.2: Firing properties depend on membrane potential

A: Representative recording from one cell receiving a 500 ms hyperpolarising current injection of -100 pA and held at -55 mV and -70 mV. **B:** Representative recording from the same cell shown in A, receiving a 500 ms depolarising current injection of 100 pA at -70 mV and -55 mV.

4.3.3 Subthreshold properties

Overall MD neurons had an average RMP of -62.5 mV ± 0.44 mV and cells patched could vary from -50 mV to -76 mV, but most cells rested at -60 mV and lower (Figure 4.3 A).

Comparisons of subthreshold properties were made between cells at -70 mV and the same cells then held at -55 mV in response to hyperpolarising (-100 pA) current steps (Figure 4.3). The input resistance measured at steady state was significantly lower in cells held at -70 mV (median = 75.90 MΩ, IQR = 43.23 MΩ) compared to -55 mV (median = 162.98 MΩ, IQR = 87.28 MΩ) ($Z = 6.073$, $p < 0.001$, $n = 49$, Wilcoxon signed ranks test) (Figure 4.3 C). This input resistance is the value obtained by measuring the change in voltage at the fixed current step at steady state (RiSS). The input resistance calculated from extrapolated data (RiExt), prior to the sag current, was also compared between

conditions. A Wilcoxon signed ranks test showed that there were significant differences between the median RiExt of cells held at -70 mV (84.62 MΩ, IQR = 41.53) and at -55 mV (194.96 MΩ, IQR = 92.25) (Z = 6.093. p <0.001, n = 49) (Figure 4.3 D).

Comparisons of the membrane charging constant, tau (ms), using a paired t test showed that when cells were held at -70 mV their tau value was significantly lower (12.53 ms ± 0.46 ms) compared to -55 mV (29.49 ms ± 1.32 ms) (t_{48} = -14.168, p <0.001, p = 49) (Figure 4.3 E). An approximate value of the cells' membrane capacitance was obtained using the values of tau and RiSS and cells had a mean capacitance of 0.17 nF ± 0.01 nF (Figure 4.3 B).

The percentage sag current was calculated as described in chapter 2 methods. A Wilcoxon signed ranks test showed that cells held at -70 mV a significantly lower median sag % (7.92 %, IQR = 10.20 %) compared to when they were held at -55 mV (15.71 %, IQR = 15.30 %) (Z = 4.302, p <0.001, n = 49) (Figure 4.3 F).

These cells exhibited a rebound potential once the current step had terminated. However, in cells at -55 mV, the rebound potential was enough to bring these cells to their AP threshold and as a result they would exhibit rebound firing in response to current step termination. This meant an accurate measurement of the rebound potential at -55 mV was not possible and accurate comparisons could not be made.

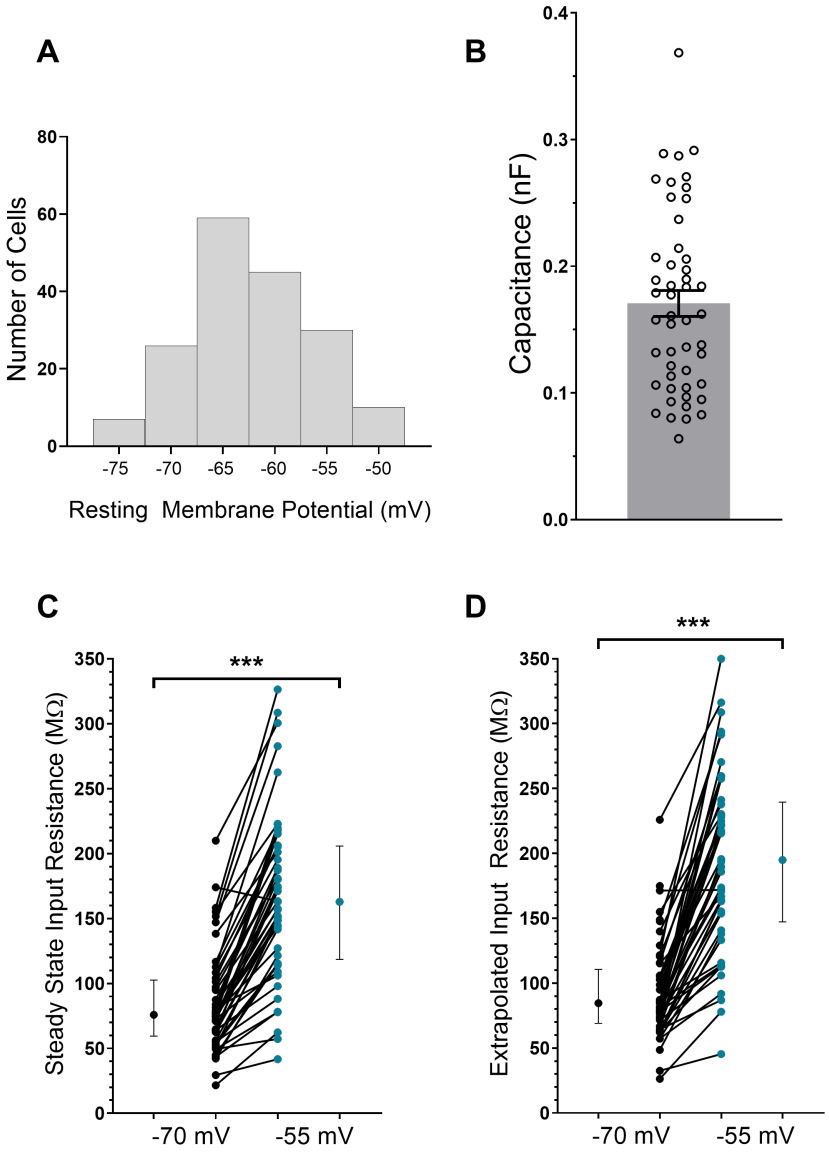
A
Number of Cells
80
60
40
20
0
-75
-70
-65
-60
-55
-50
Resting Membrane Potential (mV)
B
Capacitance (nF)
0.4
0.3
0.2
0.1
0.0
C
***
Steady State Input Resistance (MΩ)
350
300
250
200
150
100
50
0
-70 mV
-55 mV
D
***
Extrapolated Input Resistance (MΩ)
350
300
250
200
150
100
50
0
-70 mV
-55 mV

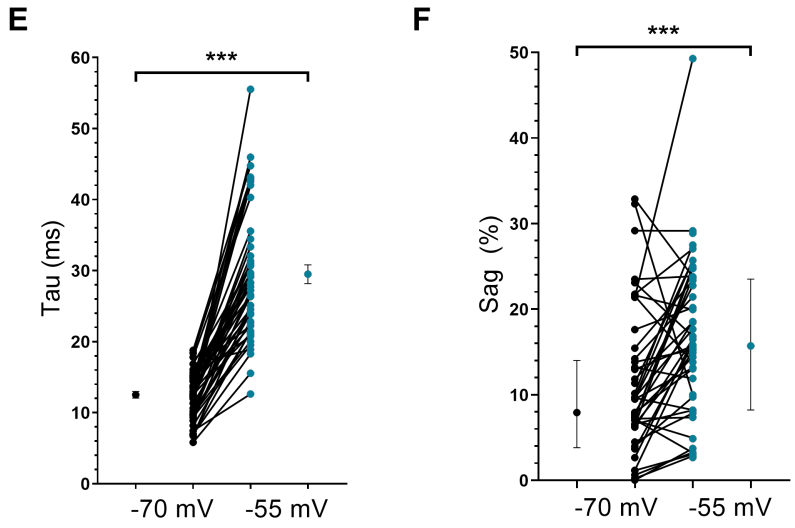

Figure 4.3: Subthreshold properties of MD neurons differ depending on membrane potential

A: A histogram representing the variance in resting membrane potential across MD neurons (n = 177). **B:** A bar plot showing the capacitance of individual MD neurons represented by circles. Bar indicates the mean ± the SEM (n = 49). **C:** Steady state input resistance significantly differed between holding potentials ($p < 0.001$, n = 49, Wilcoxon). **D:** The extrapolated input resistance significantly differed between holding potentials ($p < 0.001$, n = 49, Wilcoxon). **E:** Tau significantly differed between holding potentials ($p < 0.001$, n = 49, paired t test) **F:** Sag % significantly differed between holding potentials ($p < 0.001$, n = 49, Wilcoxon). **C-D, F:** Paired data from individual cells for each condition plotted alongside the group median ± the IQR. **E:** Paired data plotted alongside the group means ± the SEM.

4.3.4 AP properties

To analyse the differences in AP properties, cells were administered depolarising current steps when held at -55 mV and -70 mV.

Example AP waveforms show that, on average, cells at -70 mV have faster and larger APs in response to depolarising current compared to cells at -55 mV (Figure 4.4 A). These observations are reflected by the statistical comparisons made between the AP peaks, the AP half-width and the rate of rise of the AP (Figure 4.4 B-D). Cells at -70 mV had a median AP peak of 33.85 mV (IQR = 8.69 mV) compared to a median of 30.18 mV (IQR = 9.83 mV) when held at -55 mV. A Wilcoxon signed ranks test showed these differences

were statistically significant (Z = -3.926, p <0.001, n = 47) (Figure 4.4 B). The AP half width (speed which half of AP has happened) was significantly higher in cells at -55 mV (median = 0.64, IQR = 0.19) compared to cells at -70 mV (median = 0.53, IQR = 0.08) (Z = 4.633, p <0.001, n = 41, Wilcoxon signed ranks test) (Figure 4.4 C). Additionally, cells at -70 mV had a significantly higher median AP rate of rise with the median being 297.97 mv/ms (IQR = 74.95) compared to 236.45 mv/ms (IQR = 114.38) at -55 mV (Z = -5.714, p <0.001, n = 47, Wilcoxon signed ranks test) (Figure 4.4 D). Whilst APs at -70 mV were faster and higher in amplitude compared to -55 mv, the threshold to fire an AP was higher in cells at -70 mV. When cells were held at -70 mV their median AP threshold was significantly higher than when they were held at -55 mV (-70 mV: -34.45 mV (IQR = 5.26); -55 mV: -29.15 mV (IQR = 7.80) (Z = 5.556, p <0.001, n = 47, Wilcoxon signed ranked test) (Figure 2.5.5 E).

Cells would fire multiple APs in response to depolarising current, and the AP peaks of 15 APs were measured in cells receiving a 300 pA current (Figure 4.4 F). The peak of the first AP in cells at -70 mV was the highest and rapidly decreased before recovering over the course of the current step. In comparison when cells were at -55 mV the peak of APs started off high and gradually decreased over the current step. A repeated measures ANOVA with Greenhouse-Geisser correction using spike number (1-15) and membrane potential as factors revealed a significant interaction between membrane potential and spike number ($F_{(1.901, 49.425)}$ = 26.544, p <0.001, n = 11). Further pairwise comparisons, with Bonferroni correction showed that the significant differences were between response 1 (p = 0.034), 2 (p <0.001), 3 (p <0.001), 4 (p <0.001), and 5 (p = 0.007).

The latency to fire the first AP (spike) varied between cells held at different membrane potentials (Figure 4.4 F). Wilcoxon signed ranks tests between the groups medians showed that there were significant differences at 100 pA steps (-70 mV: median = 38.51 ms, IQR = 22.19 ms; -55 mV: median = 74.65, IQR = 120.83) (Z = 2.830, p = 0.005, n = 13), 150 pA (-70 mV: median = 25.73 ms, IQR = 12.01 ms; -55 mV: median = 32.64 ms, IQR = 35.75 ms) (Z = 2.504, p = 0.012, n = 18), 250 pA (-70 mV: median = 17.21 ms, IQR = 6.52 ms; -55 mV: median = 20.18 ms, IQR = 30.76 ms) (Z = 2.159, p = 0.031, n = 22).

The number of APs fired at each depolarising step also varied between cells held at -70 mV and -55 mV (Figure 4.4 H). A Wilcoxon signed ranks test between the group medians showed that there were significant differences at the 50 pA current step (-70 mv: median = 3.5, IQR = 4.75; -55 mV: median = 0, IQR = 0) (Z = -3.243, p = 0.001, n = 30,

Wilcoxon signed ranks test) and at 300 pA (-70 mV: median = 7, IQR = 17.5; -55 mV: median = 19, IQR = 21) (Z = 2.682, p = 0.007, n = 27, Wilcoxon signed ranks test).

To compare the time between each spike, the instantaneous frequency was measured from cells receiving a 300 pA current injection. This was calculated by the reciprocal of the inter-spike interval. As cells burst fire at -70 mV they fire several APs within close succession (Figure 4.5 B-C), and this is reflected by an increase in instantaneous frequency when compared to cells at -55 mV whose instantaneous frequency remains steady across the depolarising step (Figure 4.5 A). The time between the first 15 spike pairs from a 300 pA current injection were compared across the two holding potentials. A mixed model ANOVA, with a Greenhouse-Geisser correction applied, using spike pair (1-15) and membrane potential as factors revealed that there was a significant interaction between the two factors ($F_{(1.386, 33.256)}$ = 62.790, p <0.001, -70 mV: n = 11; -55 mV: n =15). Further pair wise comparisons revealed that these differences occurred between spike pair numbers 1 (p <0.001), 2 (p <0.001), 3 (p <0.001), 4 (p <0.001), 5 (p = 0.001), and 6 (p = 0.028) (Figure 4.5 A).

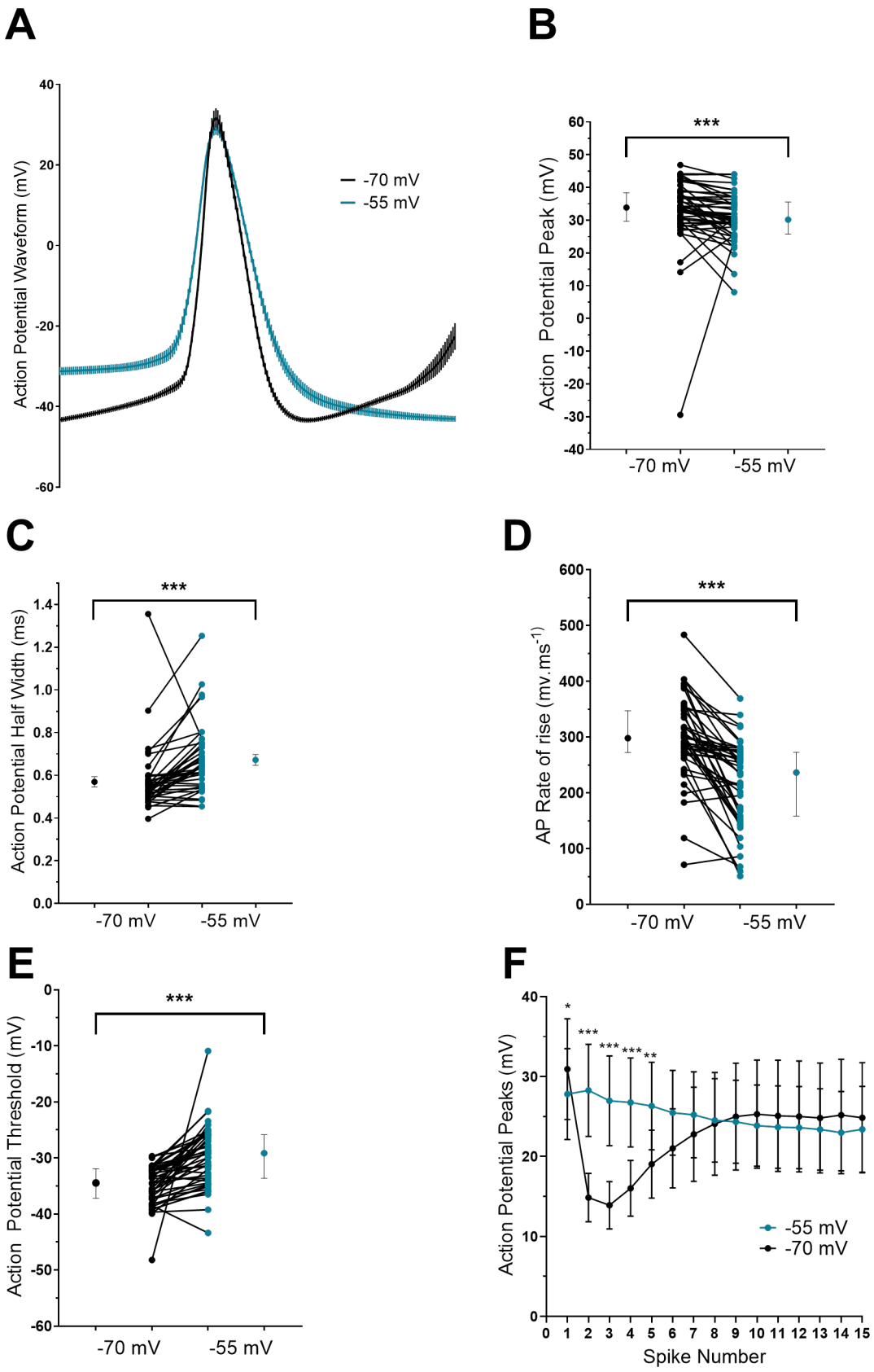
A
Action Potential Waveform (mV)
-70 mV
-55 mV
B
Action Potential Peak (mV)
***
-70 mV
-55 mV
C
Action Potential Half Width (ms)
***
-70 mV
-55 mV
D
AP Rate of rise (mv.ms-1)
***
-70 mV
-55 mV
E
Action Potential Threshold (mV)
***
-70 mV
-55 mV
F
Action Potential Peaks (mV)
-55 mV
-70 mV
Spike Number

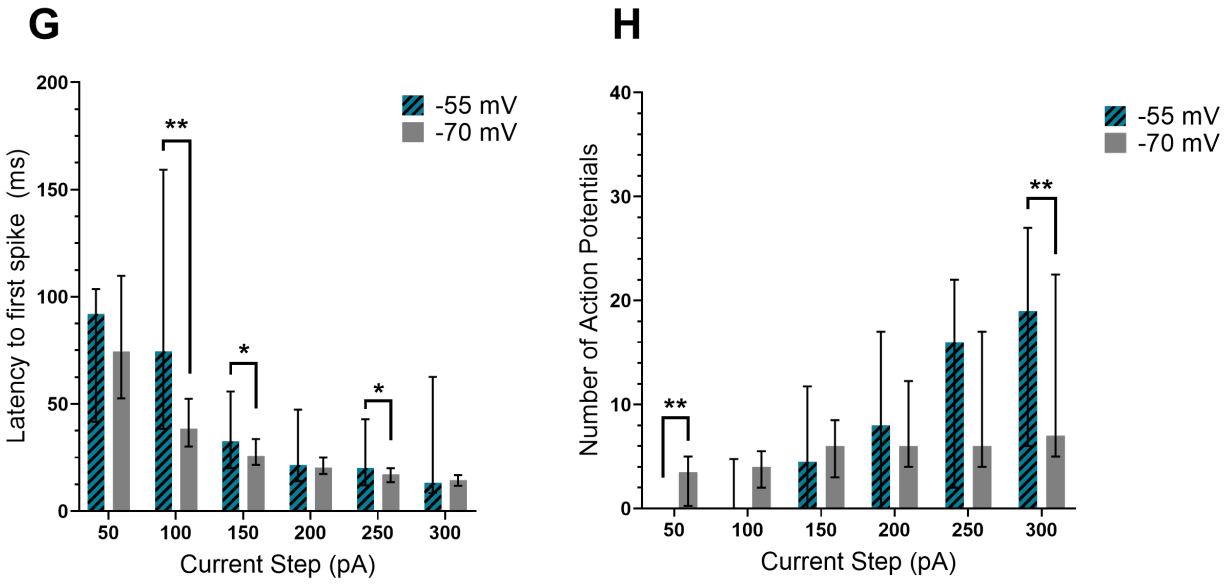

Figure 4.4: AP properties differ dependent on membrane potential

A: Example AP waveforms at -70 mV and -55 mV. The line shows the mean of 31 cells with vertical lines showing the spread of the SEM. **B:** AP peak was significantly higher in cells held at -70 mV ($p < 0.001$, $n = 47$, Wilcoxon). **C:** The AP half width was significantly lower in cells held at -70 mV ($p < 0.001$, $n = 41$, Wilcoxon). **D:** The AP rate of rise was significantly higher in cells held at -70 mV compared to -55 mV ($p < 0.001$, $n = 47$, Wilcoxon). **E:** Cells held at -70 mV had a significantly lower AP threshold compared to -55 mV ($p < 0.001$, $n = 41$, Wilcoxon). **F:** AP peaks of 15 APs fired in a 300 pA depolarising step when cells held at -70 mV (black) or -55 mV (blue). Significant differences found between the responses 1-5 ($p < 0.05$, $n = 11$). **G:** Latency to first spike differed between the -70 mV and -55 mV groups at 100 pA, 150, pA and 250 pA. **H:** Number of APs was significantly different between groups at 50 pA ($p < 0.01$, $n = 30$, Wilcoxon) and 300 pA current steps ($p < 0.01$, $n = 27$ Wilcoxon). Data displayed in B-E,G,H show individual data points with the median values and interquartile range either side.

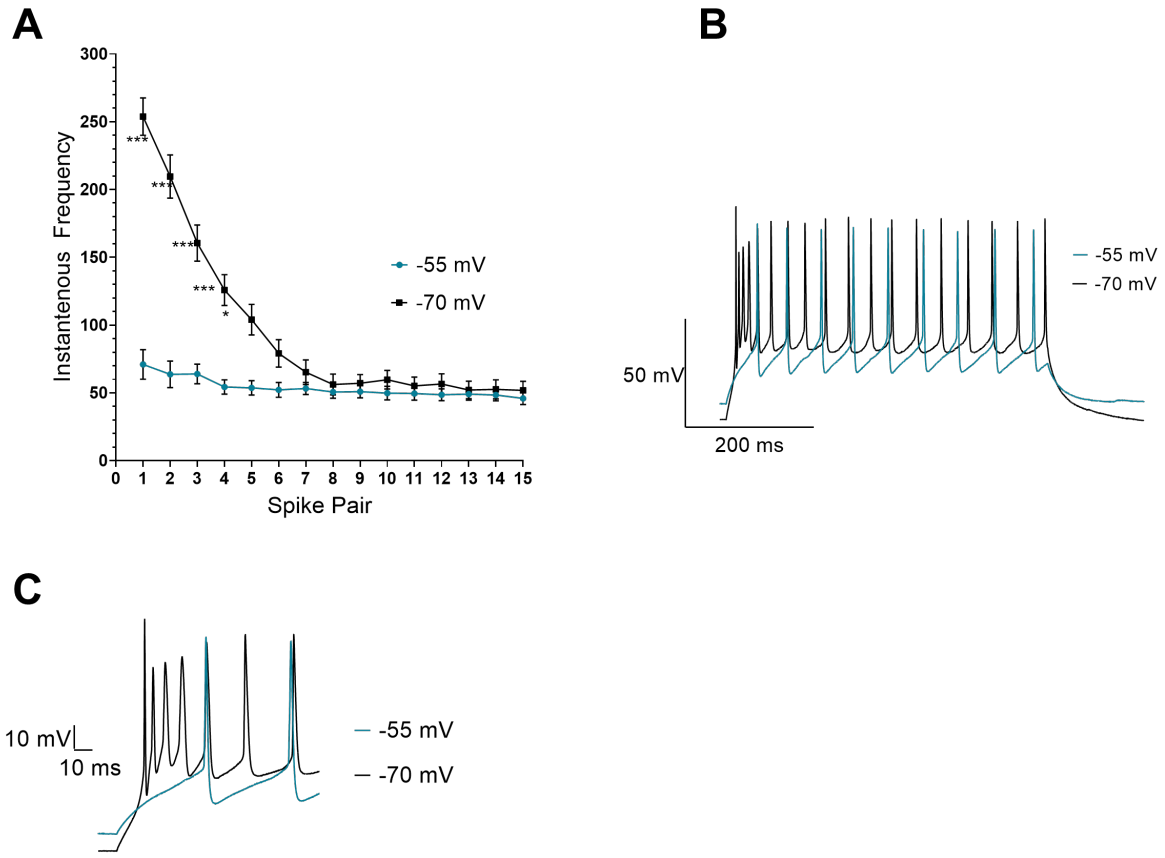

Figure 4.5: Instantaneous frequency

A: Instantaneous frequency was significantly higher between spike pairs 1 - 5 at a holding potential of -70 mV compared to -55 mV ($p < 0.001$ (***), $p < 0.05$ (*), -70 mV: $n = 11$; -55 mV: $n = 15$). Individual points represent the mean with error bars showing SEM. **B:** Representative traces from a single cell held at -55 mV (blue) and -70 mV (black) receiving a 300 pA current injection. **C:** A magnified and cropped version of the trace shown in B.

4.3.5 Evoked EPSPs of the mPFC - MD pathway

EPSPs were induced by optogenetic stimulation and light intensity was controlled to produce EPSPs approximately 2 mV - 15 mV in size (see section 2.5.5). To control for any possible effects of run down in current, or increases in series resistance, a series of experiments were conducted in which baseline EPSPs were recorded for 30 minutes with no drug addition to ensure they were stable for this length of time (Figure 4.6)

Over 30 minutes the average peak amplitude went from 4.90 mV ± 0.53 mV to 4.25 mV

± 0.12 mV (n = 6). Data were normalised to the first response across 30 minutes to allow for comparisons between individual cells (Figure 4.6). A repeated measures ANOVA with the Greenhouse-Geisser correction showed that there was no effect of time on the peak amplitude of evoked EPSPs ($F_{2.049, 10.243} = 1.666$, p = 0.236, n = 6).

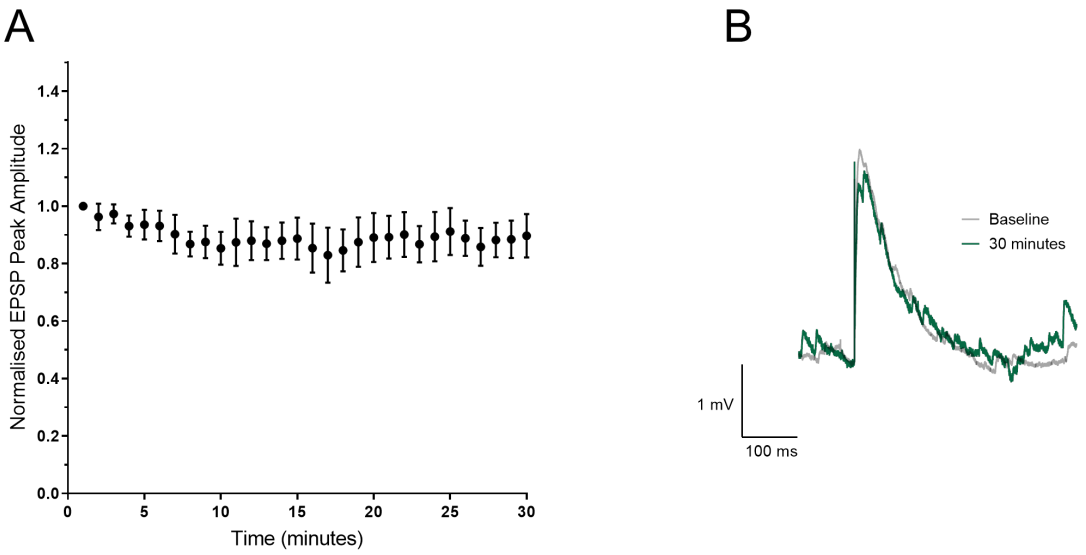

Figure 4.6: EPSPs remain stable over 30 minutes

A: Data points show the average normalised peak amplitude ± the SEM of EPSPs every minute for 30 minutes (n = 6, animals = 6). No significant change in normalised peak amplitude after thirty minutes. **B:** Representative trace of a cell held at -70 mV showing evoked EPSPs in the first minute and thirtieth minute of experiment.

4.3.6 Short term plasticity is unaltered by different membrane potentials

To investigate short term plasticity at the mPFC - MD synapse, cells were administered trains of ten stimuli that were given at 5 Hz, 10 Hz or 20 Hz. Due to differences in firing properties depending on membrane potential, the short term plasticity properties were investigated with cells being held at -55 mV and - 70 mV to compare. A mixed-model ANOVA, with the Greenhouse-Geisser correction applied, was conducted separately for 5 Hz, 10 Hz and 20 Hz groups with membrane potential and stimulus number treated as a factors. At 5 Hz there was a significant effect of the train stimulation ($F_{(2.439, 87.796)} = 41.698$, p <0.001, n = 19) but no effect of membrane potential ($F_{(2.439, 87.769)} = 0.288$, p = 0.793, n = 19). At 10 Hz there was a significant effect of train stimulation ($F_{(1.881, 67.716)}$

= 48.323, p <0.001, n = 19) but no effect of membrane potential ($F_{(1.881, 67.716)} = 0.221$, p = 0.789, n = 19). At 20 Hz there was a significant effect of train stimulation ($F_{(1.866, 67.174)} = 67.659$, p <0.001, n = 19) but no effect of membrane potential ($F_{(1.866, 67.174)} = 0.915$, p = 0.400, n = 19). Overall, administering trains of stimuli at 5 Hz, 10 Hz and 20 Hz resulted in short term facilitation of the evoked EPSPs, but this was unaffected by the cell's membrane potential.

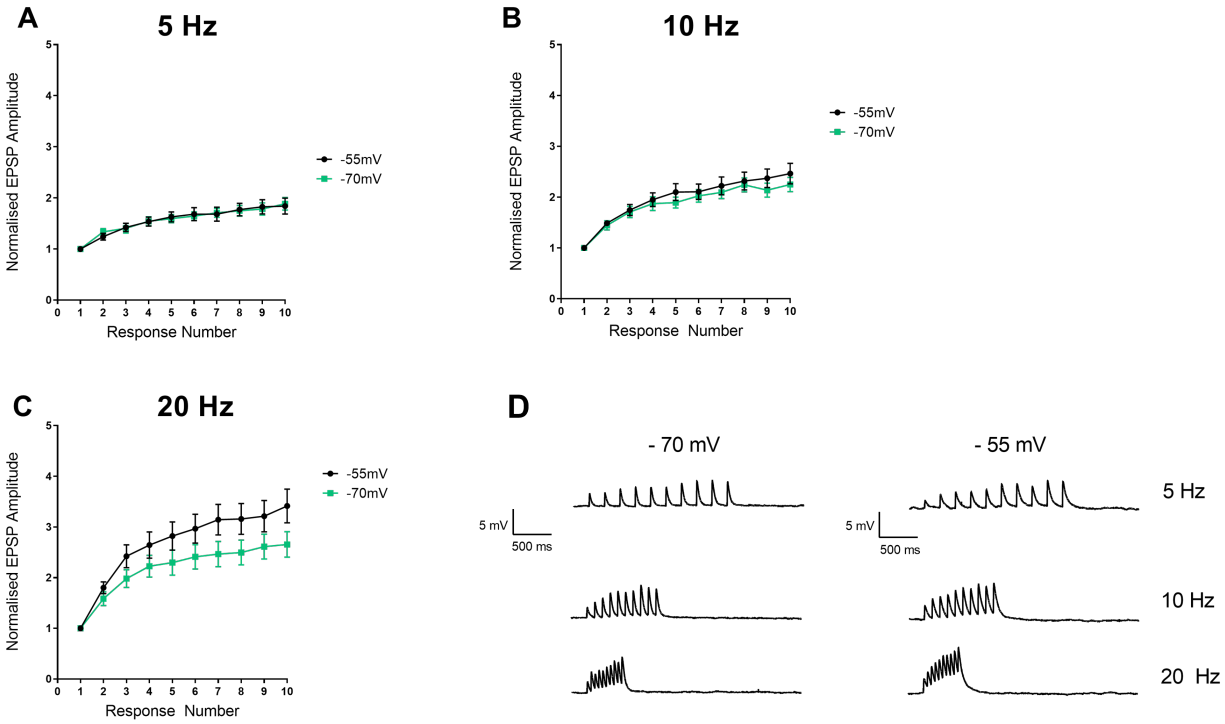

Figure 4.7: Short term plasticity unchanged by membrane potential

A-C Short term facilitation significantly increased with the frequency of stimulation (p <0.001). The size of facilitation was not affected by the cell's membrane potential. Data represent the mean normalised EPSP amplitude ± the SEM, n = 19, animals = 15. **D:** Representative traces from a cell held at -70 mV and -55 mV and administered trains at 5 Hz, 10 Hz and 20 Hz.

4.3.7 Blocking NMDA receptors reduces EPSP facilitation

The next experiments tested whether the short term facilitation would be impacted after application of AP-5, the NMDA receptor antagonist. Trains were first run at the two different membrane potentials and then repeated in the presence of AP-5. A mixed-model ANOVA with Greenhouse-Geisser correction was conducted with stimulus number and

drug as factors. Cells were held at -55 mV and -70 mV and effects of facilitation in the presence of AP-5 and at 5 Hz, 10 Hz and 20 Hz stimulation, was analysed separately (Figure 4.8, 4.9).

When cells were held at -55 mV, analysis showed that there was no significant interaction between 5 Hz stimuli and drug treatment ($F_{(2.891, 46.251)} = 0.814$, $p = 0.489$, $n = 9$) (Figure 4.8 A). However, with the 10 Hz and 20 Hz protocols there was a significant interaction between stimulus and drug (10hz: $F_{(1.941, 31.055)} = 4.492$, $p = 0.020$, $n = 9$; 20 Hz $F_{(2.000, 31.998)} = 9.633$, $p = 0.001$, $n = 9$). Further pairwise comparisons, with the Bonferroni correction applied, in the 10 Hz condition revealed significant differences between baseline and AP-5 occurred at response numbers 5 ($p = 0.035$), 6 ($p = 0.033$), 7 ($p = 0.019$), 8 ($p = 0.033$), 9 ($p = 0.023$), 10 ($p = 0.013$) (Figure 4.8 B).To assess the effect on facilitation, pairwise comparisons were used to compare the first response to the 10th response in baseline and in the presence of AP-5. In baseline conditions there was a significant difference between the first and tenth response ($p = 0.018$) whereas there was no significant difference in the presence of AP-5 ($p = 0.058$) In the 20 Hz condition, further pairwise comparisons with the Bonferroni correction revealed the significant differences occurred at response numbers 3 ($p = 0.045$), 4 ($p = 0.017$), 5 ($p = 0.041$), 6 ($p = 0.013$), 7 ($p = 0.009$), 8 ($p = 0.008$), 9 ($p = 0.006$), and 10 ($p = 0.006$) (Figure 4.8 C). To assess the effect on facilitation, pairwise comparisons were used to compare the first response to the tenth response in baseline and in the presence of AP-5. In baseline conditions there was a significant difference between the first and tenth response ($p = 0.013$) and this was also significant in the presence of AP-5 ($p = 0.009$)

Similarly, when the same cells were held at -70 mV, there was no significant effect of drug when cells were administered stimuli at 5 Hz ($F_{(3.490, 55.846)} = 0.283$, $p = 0.513$, $n = 9$) (Figure 4.9 A), or at 10 Hz ($F_{(2.219, 35.502)} = 1.612$, $p = 0.128$, $n = 9$) (Figure 4.9 B). However there was a significant interaction at 20 Hz $F_{(1.741, 27.861)} = 6.201$, $p = 0.008$, $n = 9$). Further pairwise comparisons, with Bonferroni correction, revealed that the differences between baseline and AP-5 occurred at response numbers 3 ($p = 0.045$), 4 ($p = 0.017$), 5 ($p = 0.041$), 6 ($p = 0.013$), 7 ($p = 0.009$), 8 ($p = 0.008$), 9 ($p = 0.006$), and 10 ($p = 0.006$) (Figure 4.9 C). To assess the effect on facilitation, pairwise comparisons were used to compare the first response to the tenth response in baseline and in the presence of AP-5. In baseline conditions there was a significant difference between the 1st response and the tenth ($p = 0.032$) whereas this difference was not significant in the presence of

AP-5 (p = 0.068)

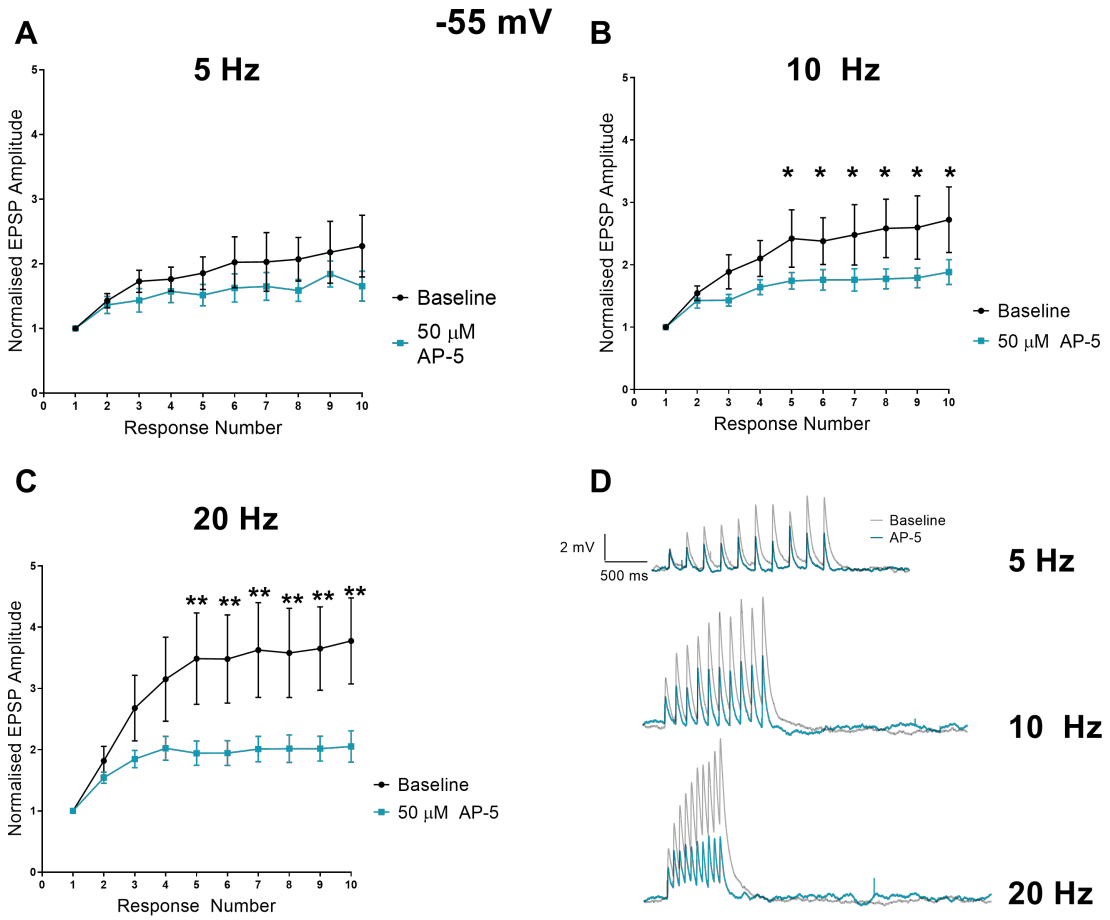

Figure 4.8: Effect of AP-5 on trains when cell held at -55 mV

A: No significant differences between control 5 Hz stimulation and in the presence of AP-5 (p >0.05, n = 9). **B:** At 10 Hz stimulation there was a significant decrease in EPSP amplitude in the presence of AP-5 (p = 0.020, n = 9). **C:** During 20 Hz stimulation there was a significant decrease in EPSP amplitude in the presence of AP-5 (p<0.001, n = 9). Stars represent where the EPSP amplitude differed significantly from the control recordings. All data shown represent the mean normalised EPSP amplitude ± SEM, n = 9, animals = 9.

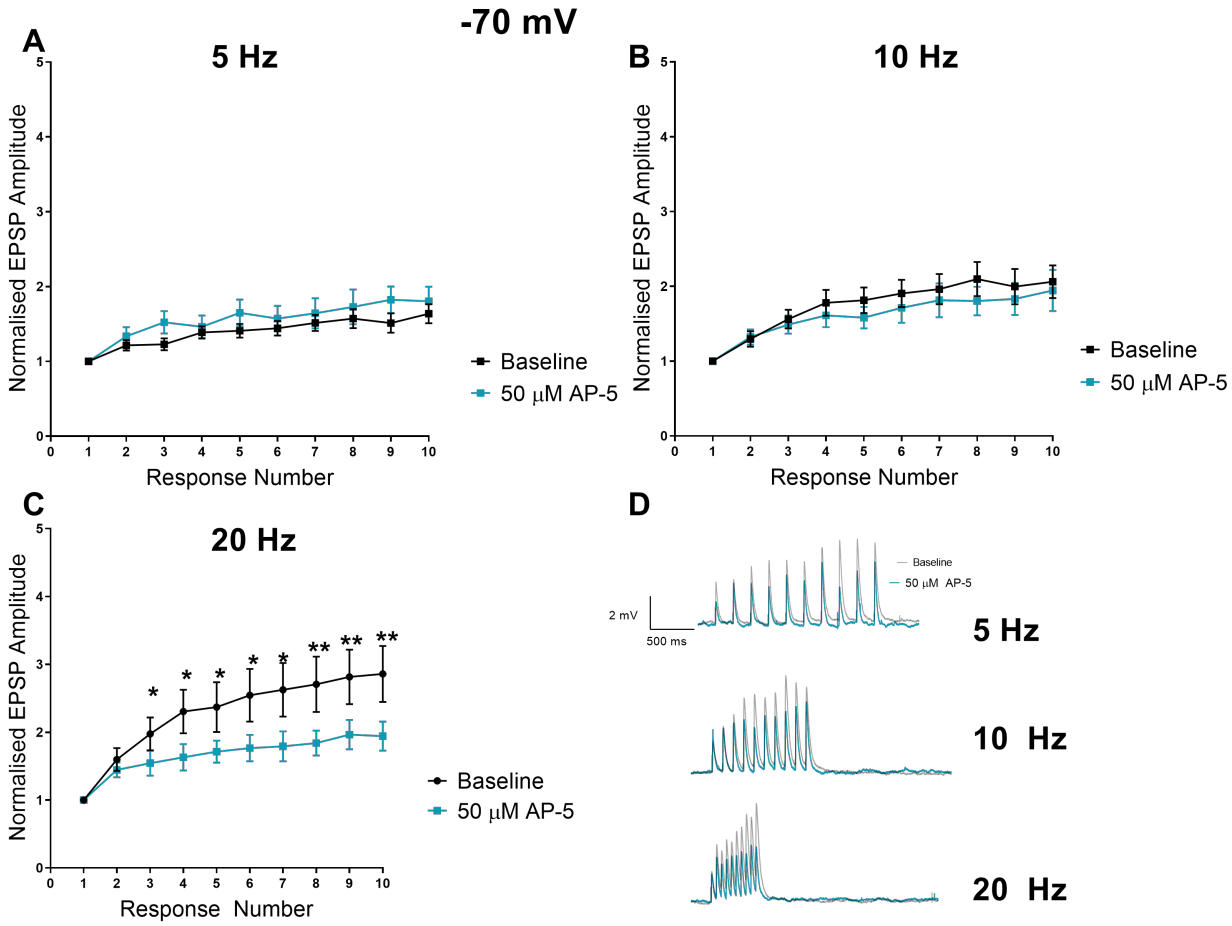

Figure 4.9: Effect of AP-5 on trains when cells held at -70 mV

A: There were no significant differences between control 5 Hz stimulation and in the presence of AP-5 ($p > 0.05$, $n = 9$). **B:** There were no significant differences between control 10 Hz stimulation and in the presence of AP-5 ($p > 0.05$, $n = 9$). **C:** At 20 Hz stimulation there was a significant decrease in EPSP amplitude in the presence of AP-5 ($p < 0.001$, $n = 9$). Stars represent where the EPSP amplitude differed significantly from the control recordings. All data shown represent the mean normalised EPSP amplitude ± SEM, $n = 9$, animals = 9.

4.3.8 Effect of AP-5 on evoked EPSPs at mPFC-MD synapse

During the train experiments, evoked EPSPs were averaged over one minute during the initial baseline, with EPSPs being evoked once every 10 seconds. Averages were taken when cells were held at -55 mV and at -70 mV in control conditions and then in the presence of AP-5 (Figure 4.10 D, 4.10 H).

Data were normalised and expressed as a percentage. Drug conditions were compared against normalised data with a one sample t test, set to a value of 100 %. When cells were held at -55 mV, there was no significant effect of AP-5 on normalised EPSP peak amplitude (83.11 % ± 10.35 %) (t_6 = -1.632, p = 0.154, n = 7) (Figure 4.10 A). AP-5 had a significant effect on the normalised decay time of the EPSP (89.94 % ± 3.34 %) (t_6 = -3.010, p = 0.024, n = 7) (Figure 4.10 B). There was no significant effect on normalised input resistance (85.23 % ± 12.12 %) in the presence of AP-5 (t_4 = -1.220, p = 0.289, n = 5) (Figure 4.10 C).

Cells were also held at -70 mV and the same measures were taken before and after AP-5 application. Again, data were normalised and so the normalised group means in the presence of AP-5 were compared using a one sample t test with the test value set to 100 %. Adding AP-5 had a significant effect on both the normalised EPSP peak amplitude (77.17 % ± 5.26 %) (Figure 4.10 E) and the normalised decay time (92.52 % ± 3.09 %) (Peak amplitude: t_8 = -4.343, p = 0.002, n = 9; Decay time: t_8 = -2.419, p = 0.042, n = 9) (Figure 4.10 F). There was no significant effect of AP-5 on normalised input resistance (133.23 % ± 16.67 %) (t_5 = 1.993, p = 0.103, n = 6) (Figure 4.10 G).

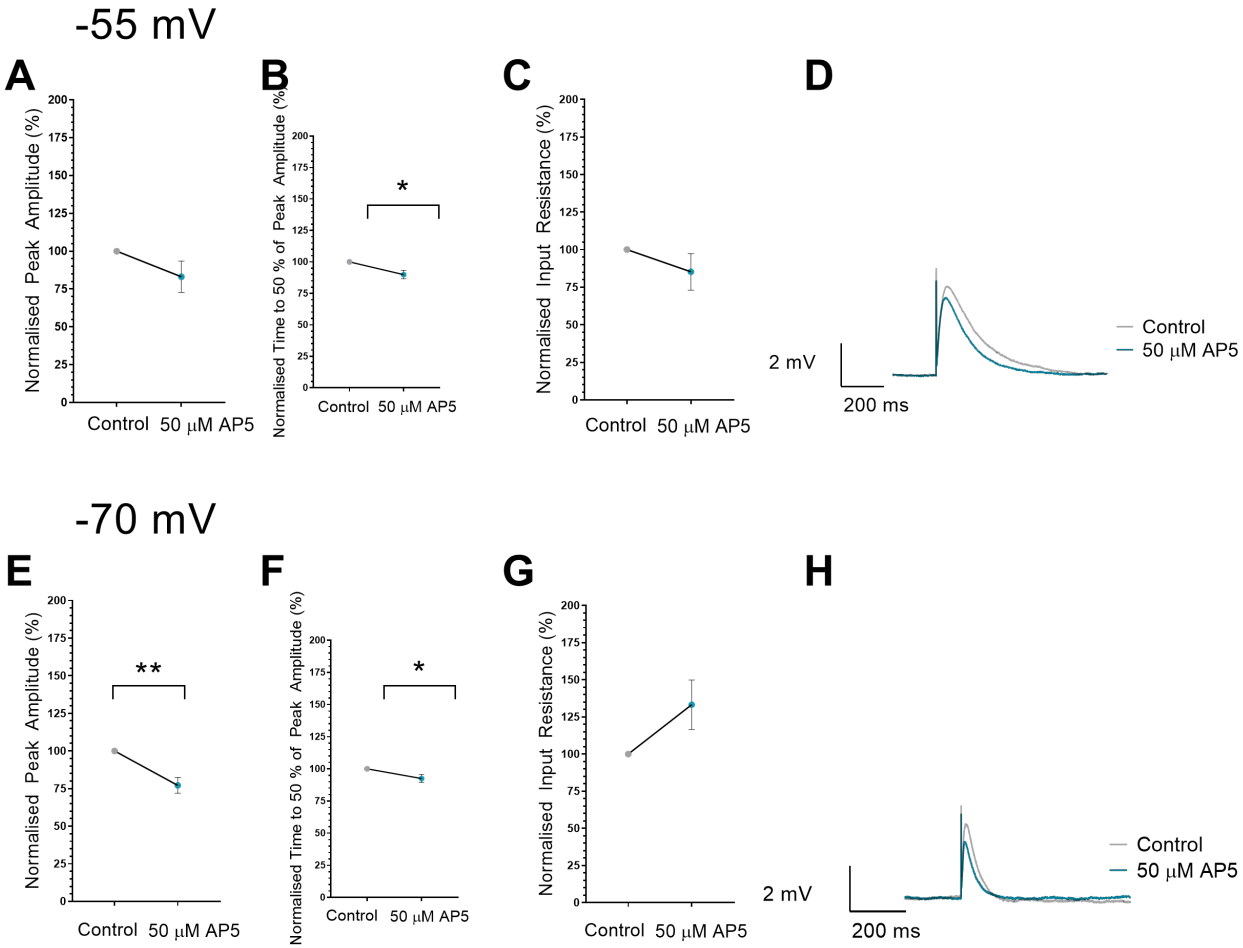

Figure 4.10: Effect of AP-5 on evoked EPSPs

A: AP-5 had no significant effect on normalised peak amplitude of EPSPs of cells held at -50 mV ($p > 0.05$, $n = 7$). **B:** AP-5 significantly decreased the normalised time to fall to 50 % of the peak amplitude of EPSPs in cells held at -50 mV ($p = 0.024$, $n = 7$). **C:** AP-5 had no effect on the normalised input resistance of cells held at -50 mV ($p > 0.05$, $n = 5$). **D:** Representative traces of EPSPs recorded from a single cell during control conditions and in the presence of AP5. **E:** AP-5 significantly decreased the normalised peak amplitude of EPSPs when cells were held at -70 mV ($p = 0.002$, $n = 9$). **F:** AP-5 significantly decreased the normalised time to fall to 50 % of the peak amplitude of EPSPs in cells held at -70 mV ($p = 0.042$, $n = 9$). **G:** AP-5 had no significant effect on the normalised input resistance of cells held at -70 mV ($p > 0.05$, $n = 6$). **H:** Representative traces of EPSPs recorded from a single cell (a different cell to D) during control conditions and in the presence of AP-5. Data are presented as the mean ± SEM. Statistical significance indicated by asterisks. Number of animals matches the n number in all cases.

4.3.9 Nicotinic receptor modulation of the medial prefrontal cortex - mediodorsal thalamus pathway

Train experiments were conducted again, but this time in the presence of RJR-oxalate and then DHβE, with cells held at -55 mV (Figure 4.11 D) and -70 mV (Figure 4.12 D). This was to test the effects of activating and then blocking $\alpha4\beta2$ nAChRs on the short term plasticity at the mPFC-MD synapse. Trains were delivered to cells held at -55 mV and then -70 mV, then they were repeated in the presence of RJR, then finally repeated for a third time in the presence of both RJR and DHβE. A mixed-model ANOVA was conducted with stimulus number (1-10) and drug as factors.

When cells were held at -55 mV and administered trains at 5 Hz, a mixed model ANOVA with Greenhouse-Geisser correction applied showed that there was no significant interaction between the stimulus and drug treatments ($F_{(3.931, 39.314)} = 0.562$, p = 0.689, Control n = 9, RJR n = 9, RJR & DHβE n = 5) (Figure 4.11 A. The same test showed that there were no significant interactions between stimulus and drug at 10 Hz stimulation ($F_{(2.626, 26.264}$, p = 0.825, Control n = 9, RJR n = 9, RJR & DHβE n = 5) (Figure 4.11 B) or at 20 Hz ($F_{(3.511, 31.600)}$, p = 0.717, Control n = 8, RJR n = 8, RJR & DHβE n = 5) (Figure 4.11 C).

When the same cells were held at -70 mV and administered trains at 5 Hz, a mixed model ANOVA with Greenhouse-Geisser correction showed that there was no significant interaction between the stimulus and drug treatments ($F_{(2.872, 30.159)} = 0.562$, p = 0.637, Control n = 9, RJR n = 9, RJR & DHβE n = 6) (Figure 4.12 A). The same statistical test also showed that there were no significant interactions between stimulus and drug at 10 Hz stimulation ($F_{(2.355, 24.726)} = 0.282$, p = 0.791, Control n = 9, RJR n = 9, RJR & DHβE n = 6) (Figure 4.12 B) and 20 Hz stimulation ($F_{(3.062, 30.616)} = 1.245$, p = 0.311, Control n = 9, RJR n = 8, RJR & DHβE n = 6) (Figure 4.12 C).

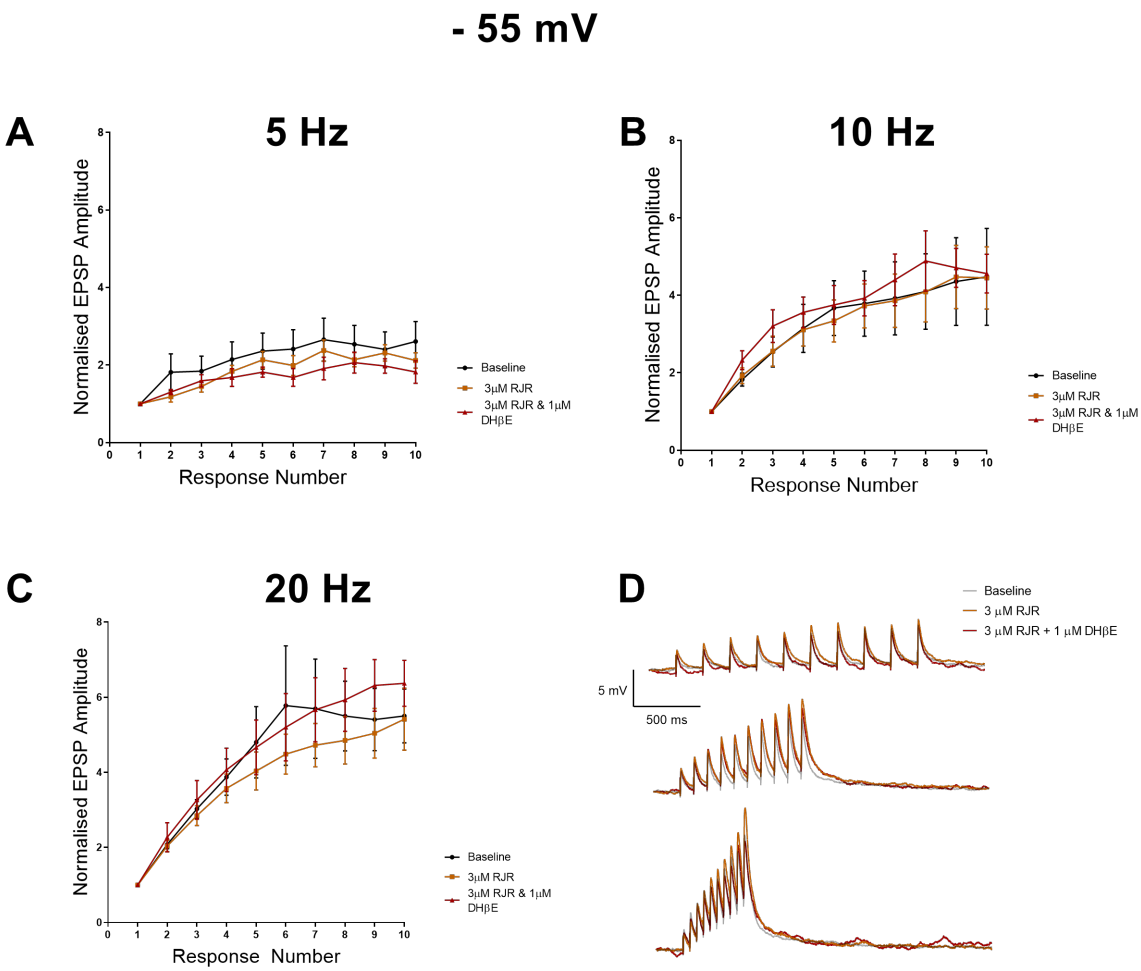

Figure 4.11: Effect of manipulating $\alpha 4\beta 2$ nAChRs on short term plasticity when cells held at -55 mV.

A: There were no significant differences between control 5 Hz stimulation and in the presence of RJR, or RJR & DHβE ($p > 0.05$, Control n = 9, RJR n = 9, RJR & DHβE n = 5). **B:** There were no significant differences between control 10 Hz stimulation and in the presence of RJR, or RJR & DHβE ($p > 0.05$, Control n = 9, RJR n = 9, RJR & DHβE n = 5)). **C:** There were no significant differences between control 20 Hz stimulation and in the presence of RJR, or RJR & DHβE ($p > 0.05$, Control n = 9, RJR n = 9, RJR & DHβE n = 5))($p > 0.05$, Control n = 8, RJR n = 8, RJR & DHβE n = 5)). Data from A-C are represented as the mean normalised EPSP amplitude ± SEM. **D:** Representative traces recorded from one cell held at -55 mV during 5 Hz, 10 Hz, and 20 Hz stimulation in control conditions and in the presence of RJR, and RJR & DHβE. Animal numbers matched the n numbers.

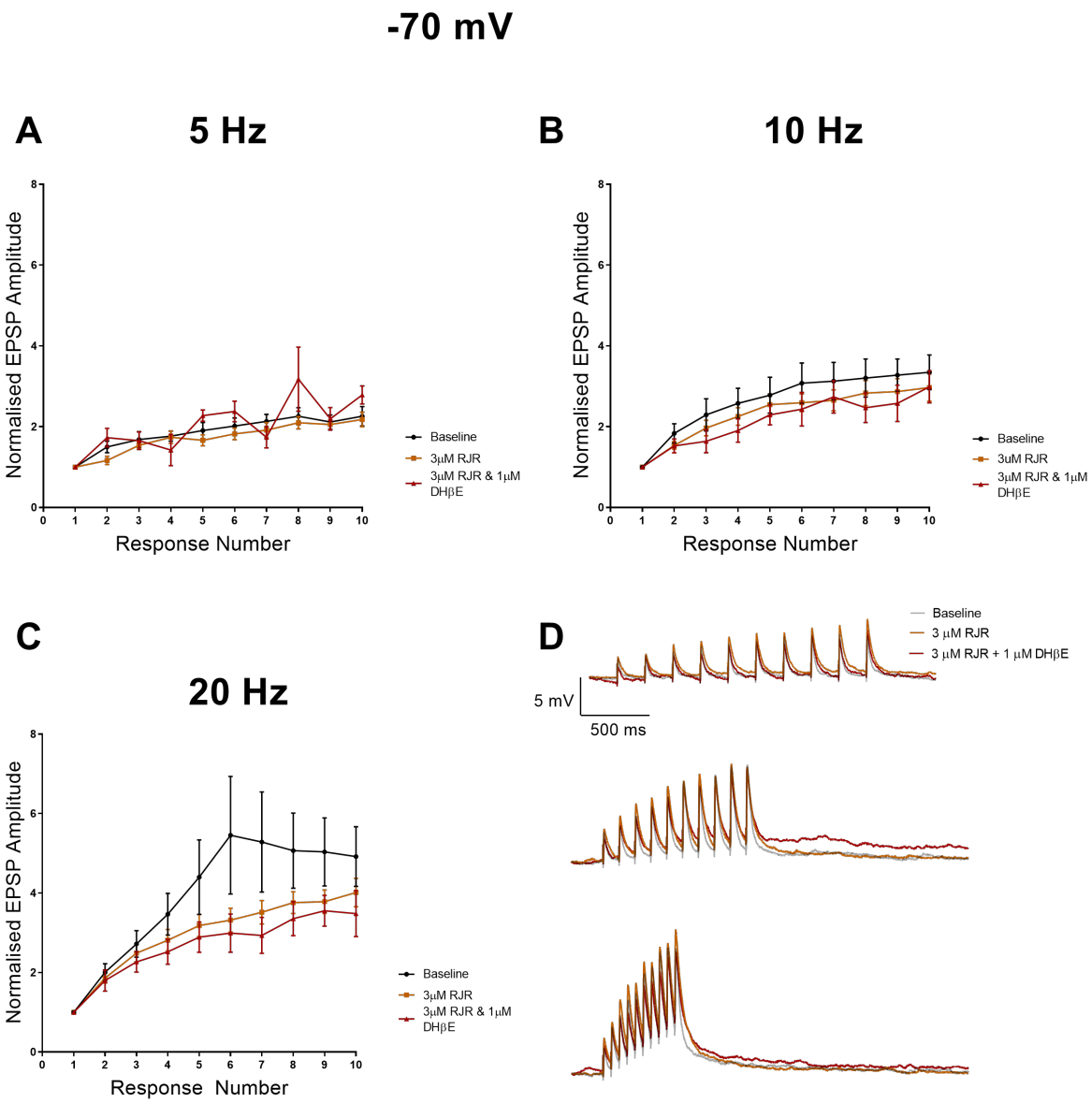

Figure 4.12: Effect of manipulating $\alpha 4\beta 2$ nAChRs on short term plasticity when cells held at -70 mV

A: There were no significant differences between control 5 Hz stimulation and in the presence of RJR, or RJR & DHβE ($p > 0.05$, Control n = 9, RJR n = 9, RJR & DHβE n = 6). **B:** There were no significant differences between control 10 Hz stimulation and in the presence of RJR, or RJR & DHβE ($p > 0.05$, Control n = 9, RJR n = 9, RJR & DHβE n = 6). **C:** There were no significant differences between control 20 HZ stimulation and in the presence of RJR, or RJR & DHβE ($p > 0.05$, Control n = 9, RJR n = 8, RJR & DHβE n = 6). Data from A-C represent the mean normalised EPSP amplitude ± SEM **D:** Representative traces recorded from one cell held at -70 mV during 5 Hz, 10 Hz, and 20 Hz stimulation in control conditions and in the presence of RJR, and RJR & DHβE. Animal numbers matched the n numbers.

4.3.10 Effect of manipulating $\alpha 4\beta 2$ nAChRs on evoked EPSPs

During the train experiments, evoked EPSPs were averaged over one minute during the baseline, with EPSPs being evoked once every 10 seconds. Averages were taken when cells were held at -55 mV and at -70 in control conditions and then in the presence of RJR-oxalate (RJR), then RJR and DHβE (Figure 4.14, 4.14).

Data were normalised and expressed as a percentage. Drug conditions were compared against normalised data with a repeated measures ANOVA. When cells were held at -55 mV, there was no significant effect of applying RJR, or RJR and DHβE, on the mean normalised EPSP peak amplitude (RJR: 97.46 % ± 14.80; RJR & DHβE: 84.67 % ± 15.15 %) ($F_{(2,8)} = 0.739$, $p = 0.507$) (Figure 4.13 A). There were also no changes in the mean across conditions for the normalised mean time taken for the EPSP to fall to 50 % of its peak amplitude (RJR : 93.18 % ± 6.61 %; RJR & DHβE: 89.32 % ± 6.88 %) ($F_{(2,8)} = 1.615$, $p = 0.258$) (Figure 4.13 b), or for the normalised mean input resistance (RJR: 97.29 % ± 5.87 %; RJR & DHβE: 92.08 % ± 8.39 %) ($F_{(2,8)} = 0.642$, $p = 0.551$) (Figure 4.13 C).

When cells were held at -70 mV there were also no significant differences in the means across all conditions. A repeated measures ANOVA with the Greenhouse-Geisser correction applied showed no significant effect of adding RJR, or RJR & DHβE on the normalised mean peak amplitudes of EPSPs (RJR: 96.96 % ± 5.15 %; RJR & DHβE: 87.68 % ± 14.09 %) ($F_{(1.061,5.303)} = 0.774$, $p = 0.425$) (Figure 4.14 A). Repeated measures ANOVA with no corrections applied also showed that there was no significant effect of RJR, or RJR & DHβE on the normalised mean time taken for the EPSP to fall to 50 % of its peak amplitude (RJR: 102.83 % ± 3.04; RJR & DHβE: 94.98 % ± 5.88 %) ($F_{(2,10)} = 1.402$, $p = 0.290$) (Figure 4.14 B). Similarly, there was no significant effect of RJR, or RJR & DHβE on normalised mean input resistance (RJR: 111.68 % ± 10.52 %; RJR & DHβE: 107.51 % ± 17.00 %) ($F_{(2,10)} = 0.420$, $p = 0.668$) (Figure 4.14 C).

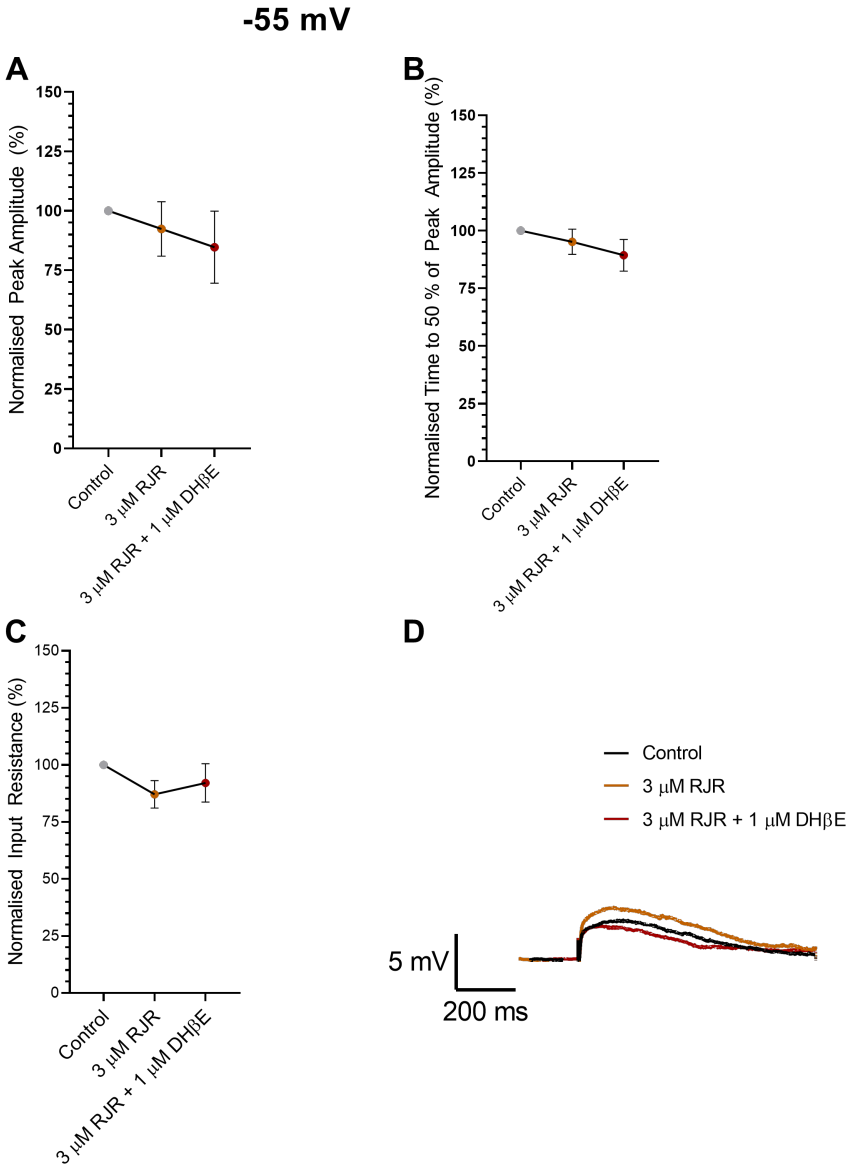

Figure 4.13: Effect of manipulating $\alpha 4\beta 2$ nAChRs on evoked EPSPs when cells were held at -55 mV

A: Application of RJR or DHβE had no significant effect on normalised mean peak amplitude of EPSPs of cells held at -55 mV ($p > 0.05$, Control n = 9, RJR n = 9, RJR & DHβ n = 6). **B:** Application of RJR or DHβE had no significant effect on normalised mean time to reach 50% of peak amplitude when cells were held at -55 mV ($p > 0.05$, Control n = 9, RJR n = 9, RJR & DHβE n = 6). **C:** Application of RJR or DHβE had no significant effect on normalised input resistance of cells held at -50 mV ($p > 0.05$, Control n = 9, RJR n = 9, RJR & DHβ n = 6). **D:** Representative traces of EPSPs recorded from one cell during control conditions then in the presence of RJR, and RJR with DHβE. Animal numbers matched the n numbers.

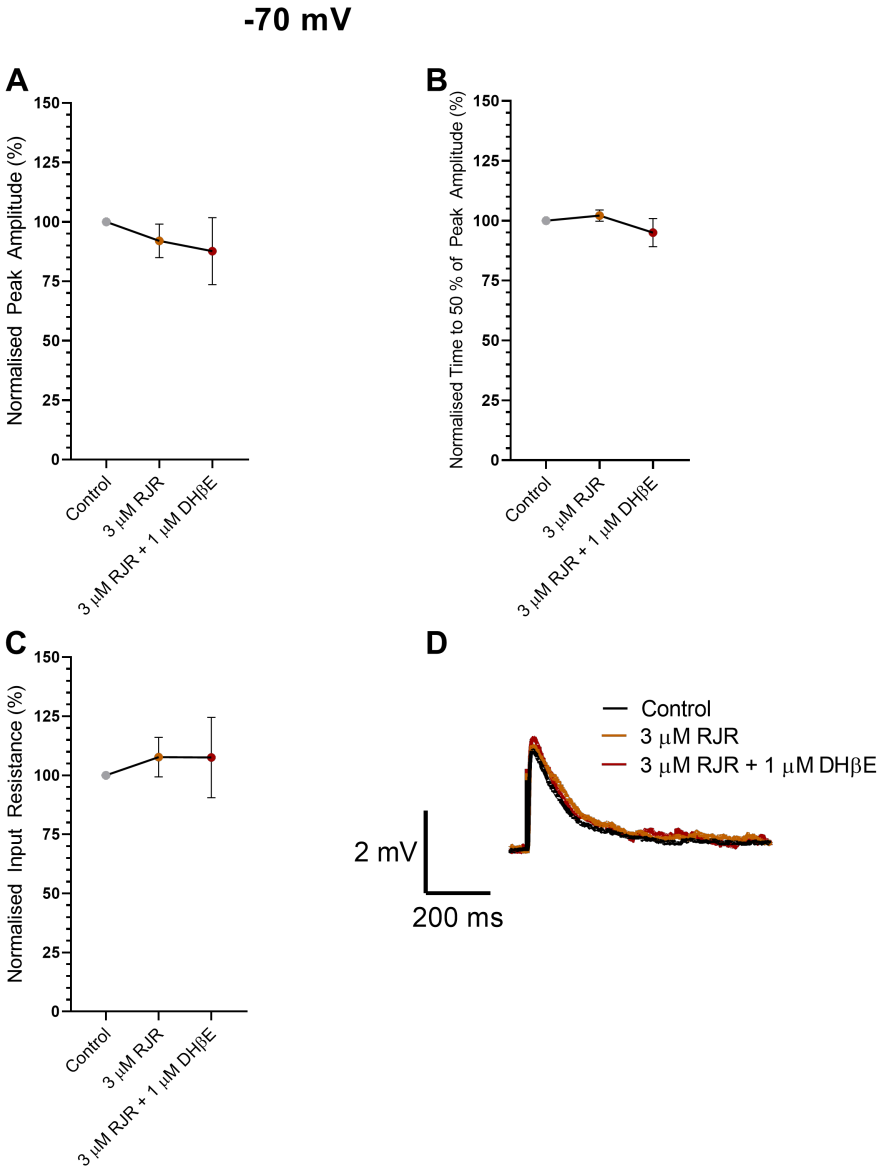

Figure 4.14: Effect of manipulating $\alpha 4\beta 2$ nAChRs on evoked EPSPs when cells were held at -70 mV

E: There was no significant effect of RJR or DHβ on the normalised mean peak amplitude of EPSPs when cells were held at -70 mV ($p > 0.05$, Control n = 9, RJR n = 9, RJR & DHβE n = 6). **F:** There was no significant effect of RJR or DHβE on the normalised, mean time to reach 50 % of peak amplitude of EPSP in cells held at -70 mV ($p > 0.05$, Control n = 9, RJR n = 9, RJR & DHβE n = 6). **G:** There was no significant of RJR or DHβE on the normalised mean input resistance of cells held at -70 mV ($p > 0.05$, Control n = 9, RJR n = 9, RJR & DHβE n = 6). **H:** Representative traces of EPSPs recorded from one cell during control conditions and in the presence of RJR, and RJR & DHβE. Data are presented as the mean ± SEM. Animal numbers matched the n numbers.

4.4 Discussion

The experiments in this chapter provide the first overview of the intrinsic properties of MD neurons. The data also show that the mPFC - MD synapse exhibits short term plasticity, with evoked responses facilitating proportionally to stimulation frequency. This facilitation is reduced by blocking NMDARs but is unchanged by manipulating $\alpha4\beta2$ nAChRs.

4.4.1 Differences in intrinsic and firing properties depending on membrane potential

Firing properties

Similar to other thalamic neurons, MD neurons, in the present study, exhibited two types of firing profiles, "burst" and "tonic". The mode of firing is determined by their membrane potential and is a result of specific voltage gated ion channels [60]. Whilst the experiments in this chapter didn't pharmacologically identify the channels responsible, the general consensus in the literature is that thalamic relay cells possess T-type calcium channels which are responsible for eliciting burst firing [57, 60, 65, 125, 126]. These channels also typically work alongside HCN channels that give rise to the I_H current [57]. Burst firing in the MD was shown to increase during theta frequency transmission between MD and mPFC [126]. A study using mice with a knock-out of the T type calcium channel gene ($Ca_V3.1$) found that theta frequency transmission was reduced between MD and mPFC [126]. This study suggests that T-type calcium channels are present in the MD, and likely result in burst firing.

As mentioned in the introduction, burst firing is often orchestrated by the presence of both T-type calcium channels and HCN channels [57, 60]. HCN channels are also activated at more hyperpolarised membrane potentials and allow non specific cations across the membrane [60]. The current through HCN channels can be identified by the presence of sag currents [57]. As the results in this chapter demonstrated that MD neurons possess this sag current, it is likely that HCN channels are working in concert with T-type calcium channels in MD neurons to produce burst firing.

HCN channels are slow to activate, so in response to a hyperpolarising current injection,

they activate and allow cations in to the cell, resulting in a small depolarisation of the cell membrane [60]. As a result, there is a slow depolarisation after the initial hyperpolarising step before the membrane reaches a steady state. Similarly, when the current step is terminated, I_H is slow to inactivate and so there is a slight depolarisation above the baseline membrane potential before I_H inactivates, and this is known as the rebound potential. Both the sag and rebound potential were observed in MD neurons and differed between cells held at -70 mV and -55 mV. The percentage of sag current was higher in cells at -55 mV due to more driving force across the cell membrane after the hyperpolarising current injection. The rebound potential was also difficult to measure in cells held at -55 mV. This was because the rebound potential was sufficient to bring the cell over threshold and would result in the cell burst firing. The brief hyperpolarising step activated I_T and I_H, and once the step was over and the cell returned to -55 mV, and burst firing was triggered riding on the rebound potential mediated by I_H. Thus whilst the experiments in this chapter did not pharmacologically block either I_T or I_H, the presence of the above mentioned properties indicates that these channels are present in MD neurons.

Passive membrane properties

The passive membrane properties of a neuron determine how it responds to changes in voltage across the cell membrane, and this shapes how the cell will process incoming signals. MD neurons showed that they switch between burst and tonic firing, and the underlying passive membrane properties set them up perfectly for this.

Hyperpolarising steps allowed for the analysis of subthreshold cell properties such as the input resistance, membrane charging constant, capacitance and can identify the presence of I_H. The results in this chapter showed that cells held at -70 mV had a lower input resistance and higher membrane charging constant in comparison to when they were held at -55 mV. These measures are dependent on the size of the cell, but also the ion channels along the membrane. As recordings were taken from the same cell, effects due to cell size can be ruled out. When cells are at -70 mV their change in voltage relative to the current step is higher, thus their input resistance is lower, and this is likely due to more ion channels being active at this holding potential. As there is less resistance across the cell membrane, the change in voltage relative to current step is also faster, thus explaining why the membrane charging constant is faster at this holding potential.

Considering these initial properties, it can then explain how cells at -70 mV had different responses to depolarising current steps, and differences in AP properties. At a holding potential of -70 mV these cells had a faster membrane charging constant, and this was reflected in the AP with a faster rate of rise and a smaller AP half width. These differences are likely due to different electrochemical driving forces when the cells are held at -70 mV compared to -55 mV.

4.4.2 The mPFC - MD synapse undergoes short term plasticity

Activating mPFC fibres with trains of ten stimuli resulted in a facilitation of EPSPs recorded in MD neurons. This facilitation increased proportionally with the speed of the stimulation applied. Frequencies of 5 Hz, 10 Hz and 20 Hz were chosen as the mPFC and MD have been shown to cohere at both theta frequency and beta frequency ranges during cognition. Unfortunately, frequency ranges any higher than 20 Hz could not be reliably tested due to the limits of the channel kinetics of the channel rhodopsin variant (unpublished work, Paul Banks).

Despite MD neurons showing unique firing profiles depending on their membrane potential, no differences in the short term facilitation were observed between the two different holding potentials. This suggests that neurons will respond similarly to small, depolarising signals coming from the cortex and amplify them at similar levels.

Short term facilitation is a typical characteristic of corticothalamic modulator inputs [26].The thalamus receives both driver and modulator inputs from the cortex [26, 45]. Driver inputs will have a large first response then the response will depress rapidly whereas modulator inputs start weak and facilitate [26, 45]. A study by Collins et al demonstrated this in a very similar set of experiments. They patched MD neurons and optically stimulated mPFC fibres, however they specifically activated corticothalamic neurons in cortical layer V or layer VI [45]. They found that inputs from layer V evoked short term facilitation in the same manner that this chapter presents [45]. In comparison inputs from layer VI displayed a “driver” style response [45]. The study presented in this thesis will have activated both inputs from layer V and VI, and all cortical inputs facilitated. This could be explained by the fact that 80 % of cortical input comes from modulator inputs, so there was a higher chance of seeing these responses. It could be also that different subregions of MD receive different proportions of input and that the

medial region receives very little driver input.

4.4.3 Corticothalamic short term plasticity requires NMDA receptors

The short term plasticity elicited by train frequency stimulation was greatly reduced in the presence of AP5, a NMDAR antagonist, showing that this plasticity requires NMDA receptors. As corticothalamic projections are predominantly glutamatergic, this confirmed the hypothesis that blocking NMDA receptors would interfere with incoming signals from the mPFC.

The short term plasticity appears to be due to short term facilitation of the EPSPs. This is considered a pre-synaptic mechanism where the pre-synaptic cell releases increasing levels of neurotransmitter. Whilst the facilitation was reduced in the presence of AP-5 it is not clear whether the AP-5 is acting on pre- or post- synaptic NMDARs. The response still facilitated in the presence of AP-5, so perhaps the amplitude of the response was decreased due to blocking post-synaptic NMDARs. To be certain, the experiment could be repeated but with loading the internal solution with an NMDAR antagonist so it only effects the post-synaptic cell.

Blocking NMDARs also decreased the time course and amplitude of single evoked EPSPs. Current through NMDARs is slower than AMPARs, and thus, applying AP5 typically reduces the EPSP decay time rather than the peak. However, both amplitude and latency were decreased in cells held at -70 mV and only EPSP latency was decreased at -55 mV. It could be argued that reductions in peak amplitude are not a real effect of the drug and is caused by increased series resistance over the course of the recording instead. However, the control experiment of evoked EPSPs over 30 minutes didn't show the changes to be significantly lower over the course of the control experiment. This suggests that the decrease in amplitude is a real effect of the drug and not confounded by series resistance.

4.4.4 No effect on manipulating $\alpha 4\beta 2$ receptors on mPFC - MD transmission

As the results of Chapter 3 showed that blocking $\alpha 4\beta 2$ nAChRs in the MD blocked memory retrieval, the experiments in this chapter aimed to investigate whether this occurs at the mPFC – MD synapse. Endogenous acetylcholine release was mimicked by applying the

$\alpha4\beta2$ agonist RJR which had no effect on evoked EPSPs, or on short term plasticity. Similarly, there was no effect of DHβE on EPSPs or short-term plasticity. Overall it is unclear from these whether the effects of blocking $\alpha4\beta2$ nAChRs on memory retrieval is effecting mPFC – MD transmission or acting elsewhere.

The experiments in this chapter may have not sufficiently replicated endogenous acetylcholine release. As these recordings were taken in acute MD slices, the background level of neurotransmitter release is clearly not the same as that in the live animal. Acetylcholine release was mimicked via bath application of RJR, however the level of acetylcholine present in the MD during memory retrieval is unknown. There is speculation in the literature that phasic release of acetylcholine favours activation of $\alpha4\beta2$ nAChRs as they desensitise to high levels of acetylcholine [69]. Prolonged bath application with RJR could potentially have desensitised the $\alpha4\beta2$ nAChRs before any effect on mPFC – MD transmission was observed.

It could be better to explore other ways of replicating endogenous acetylcholine release for future studies. An option could be to use puff application of RJR so only small volumes of drug are applied directly in to the bath over the slice rather than being continuously perfused [127]. This would allow finer manipulation of agonist release.

Another consideration is that cells were patched from the medial and sometimes central MD due to these subdivisions receiving afferents from the PL cortex, however, the lateral MD receives the most extensive cholinergic input [20, 79, 85]. The infusions of DHβE *in vivo* will have targeted all subdivisions of the MD during retrieval, so it is not possible to know whether the effect of blocking $\alpha4\beta2$ nAChRs is predominantly occurring in one subdivision over another. There are hypotheses in the literature speculating that due to each subdivision having its own distinct anatomical afferents and efferents, that they have separate roles in cognition [34, 128]. Whilst it would be difficult to isolate the subdivisions *in vivo*, it would be interesting to patch cells in the lateral MD and compare with the data collated in this chapter.

4.4.5 Experimental limitations and considerations

Whilst this study enables more specific questions to be considered with the optogenetics, it does have its drawbacks. Patching single cells and recording the single mPFC input is quite a linear approach and doesn't really help understand how ensembles of MD cells

respond to mPFC input.

As previous papers have mentioned the mPFC and MD synchronising in beta frequency range [123], that was the focused replication here. However, *in vivo* recordings of cell population activity have not been conducted in the mPFC or the MD during the object in place task, and so it cannot be confidently concluded that the same level of communication is happening and whether this study adequately replicates what is occurring in the live animal.

Cells were patched mostly from the medial MD and central MD, but it would be useful to get data from all regions of MD. Infusions in behaviour will have affected all regions of the MD and so whilst these data show effects for medial and central MD, it would be important to look at other regions of MD and see if any comparison can be made. As all three regions have diverse inputs and outputs there are several ideas that these three regions serve distinct functions and their distinct roles in recognition memory is unclear.

4.4.6 Conclusion

MD neurons exhibit the same firing characteristics of thalamic relay neurons with their burst and tonic firing modes, orchestrated by T-type calcium channels and HCN channels. The mPFC - MD pathway undergoes short term plasticity irrespective of the cells holding potential, whereby EPSPs facilitate in size proportional to the speed of frequency stimulation. This plasticity is dependent on NMDARs but there does not seem to be a requirement of $\alpha 4\beta 2$ nAChRs.

Chapter 5

Investigating the Contributions of NMDARs and Plasticity Mechanisms In the MD During Associative Recognition Memory Retrieval

5.1 Introduction

Associative recognition memory retrieval requires a functional interaction between the mPFC and the MD [4]. Specifically, input from the mPFC to the MD is crucial during associative recognition memory retrieval (unpublished work G. Barker). As the input from the mPFC to the MD is glutamatergic, this chapter aimed to investigate the role of NMDA receptors, and specific NMDAR subtypes, in the MD during associative recognition memory retrieval.

Glutamatergic transmission is the most widespread throughout the brain. NMDA receptors have been shown to be involved in learning and memory and their roles are typically observed during memory encoding [93, 97]. As information flow from the mPFC to the MD is crucial during memory retrieval, we hypothesised that blocking NMDA receptors may interfere with incoming signals from the cortex and as a result,

impair associative recognition memory retrieval.

NMDA receptors are also recognised for their role in synaptic plasticity by supporting both long term potentiation (LTP) and long term depression (LTD). It is unknown whether either form of plasticity occurs at the mPFC-MD synapse, or if it is required to support associative recognition memory retrieval. Infusions of ZIP and TAT-GluR2$_3\gamma$ blocked memory encoding and retrieval mechanisms in the mPFC, respectively. These peptides act intracellularly and have been shown to block specific mechanisms involved in LTP and LTD processes *in vitro* [73]. These peptides were used to investigate LTP- and LTD-like mechanisms within the MD during retrieval.

5.2 Methods

This is a brief overview of the methods applied for this chapter. For the full description refer to Chapter 2.

5.2.1 Subjects

Behaviour

The experiments in this chapter show data from cohort 1 and cohort 2 (see section 2.2.1). The AP-5 experiment was conducted on animals from cohort 1 which consisted of 10 animals at this point due to loss of animals (see section 2.2.1). The rest of the behavioural experiments in this chapter were conducted on cohort 2 which consisted of 12 animals.

Animals from both cohorts received bilateral guide cannula implants in to the MD (see section 2.2.1). The study was designed so each animal was its own control and received both vehicle and drug infusions.

Electrophysiology

All *in vitro* electrophysiology experiments were conducted on adult male Lister-Hooded rats (300-500g). All subjects received viral injections of AAV9 : CaMKIIα : hChR2$_{(E123T/T159C)}$: mCherry in to the mPFC 2-4 weeks prior to recordings (see

section 2.2.2).

5.2.2 Drugs

To determine the role of NMDARs in the MD during associative memory retrieval, several subunit specific antagonists were infused into the MD. Saline infusions were administered in to the MD initially to ensure animals could perform the task and were not affected by the infusion procedure.

The NMDA receptor antagonist AP-5 was used to selectively target NMDA receptors. It was used at a dose of 50 μM which has previously been infused into the nucleus reuniens and perirhinal cortex, and impaired task acquisition at the same concentrations [93, 129].

NVP AAM077 is a potent antagonist for GluN2A subunit containing NMDARs and was used at a concentration of 10 μM which was used previously in the perirhinal cortex to investigate its potential contribution to encoding during OiP [129].

RO 25-6981 is an antagonist at GluN2B containing NMDARs and again was infused at a concentration of 30 μM used previously in the perirhinal cortex to investigate its potential contribution to encoding during OiP [129].

UBP-791 is a new and selective antagonist at GluN2C and GluN2D containing NMDARs. The compound was provided for this study by Dr Mark Irvine (University of Bristol) and was the first time it has been used *in vivo*. A concentration of 1 μM was selected for infusion to be over the value of the K_i (0.08 μM) at the receptors, but under the K_i of the concentration it interacts with GluN2B subunits (1.38 μM) [91].

The same drugs were used *in vitro* for the electrophysiology experiments. They were dissolved in aCSF and applied to the perfusion system bathing the slice.

5.2.3 Behavioural experiments

Spontaneous exploration tasks in an open field arena were used to assess recognition memory performance, for a full description of the tasks and arena set up see sections 2.3 and 2.4.

Animals were tested on spatial recognition memory using the object location (OL) task

and associative recognition memory using the object in place (OiP) task.

5.2.4 Electrophysiology: whole cell voltage clamp

Cells were voltage clamped and held at -70 mV to evoke AMPA EPSCs. After a 5-minute baseline of stable EPSCs were achieved, 5 μM NBQX was bath applied to block AMPARs and isolate NMDA EPSCs. Once AMPA EPSCs had been abolished, cells were briefly held at +40 mV and NMDA currents were measured. Specific subunit antagonists for NMDARs were bath applied and effects on the NMDAR EPSC were measured over thirty minutes. All experiments were conducted in the presence of 50 μM picrotoxin to eliminate GABAergic currents and isolate glutamatergic currents. In some experiments, only the AMPA/NMDA ratio was investigated, not specific NMDA antagonists. In these experiments, NBQX was not applied, and the NMDA current was measured as the highest peak amplitude after the AMPA current had finished. For the full details of these recordings and how they were analysed see section 2.5.6.

5.2.5 Histology

Animals were perfused and 40 μM sections were cresyl stained and checked under the microscope to locate cannula tips (see section 2.4.7).

Location of cannulae were taken at the deepest point identifiable by the cannulae tracks in the section.

5.2.6 Statistical analysis

Comparisons between drug and control conditions were assessed by paired t tests by comparing the mean discrimination ratios. This is the ratio calculated from the animal's exploration at the novel object versus familiar object divided by total object exploration (see section 2.4.6). One sample t-tests were conducted to assess if animals discriminated between novel and familiar objects above chance levels. Group means were compared against a set value of 0 (discrimination ratio of 0 means no discrimination). Statistical significance was set at $P < 0.05$. Data are presented as mean $\pm$ SEM unless stated otherwise.

5.3 Results

5.3.1 Cannula placement

The position of cannulae tips were identified by comparing cresyl stained sections against sections in the Paxinos and Watson rodent brain atlas. Cannula sites were confirmed in all twelve animals of cohort two with cannula located between -2.28 mm and -3.36 mm relative to bregma (Figure 5.1). Cannula were located across all MD sections, medial (MDM: n = 7), central (MDC: n = 1) and lateral MD (MDL: n = 4). For the location of cannula tips of cohort one, see section 3.3.1.

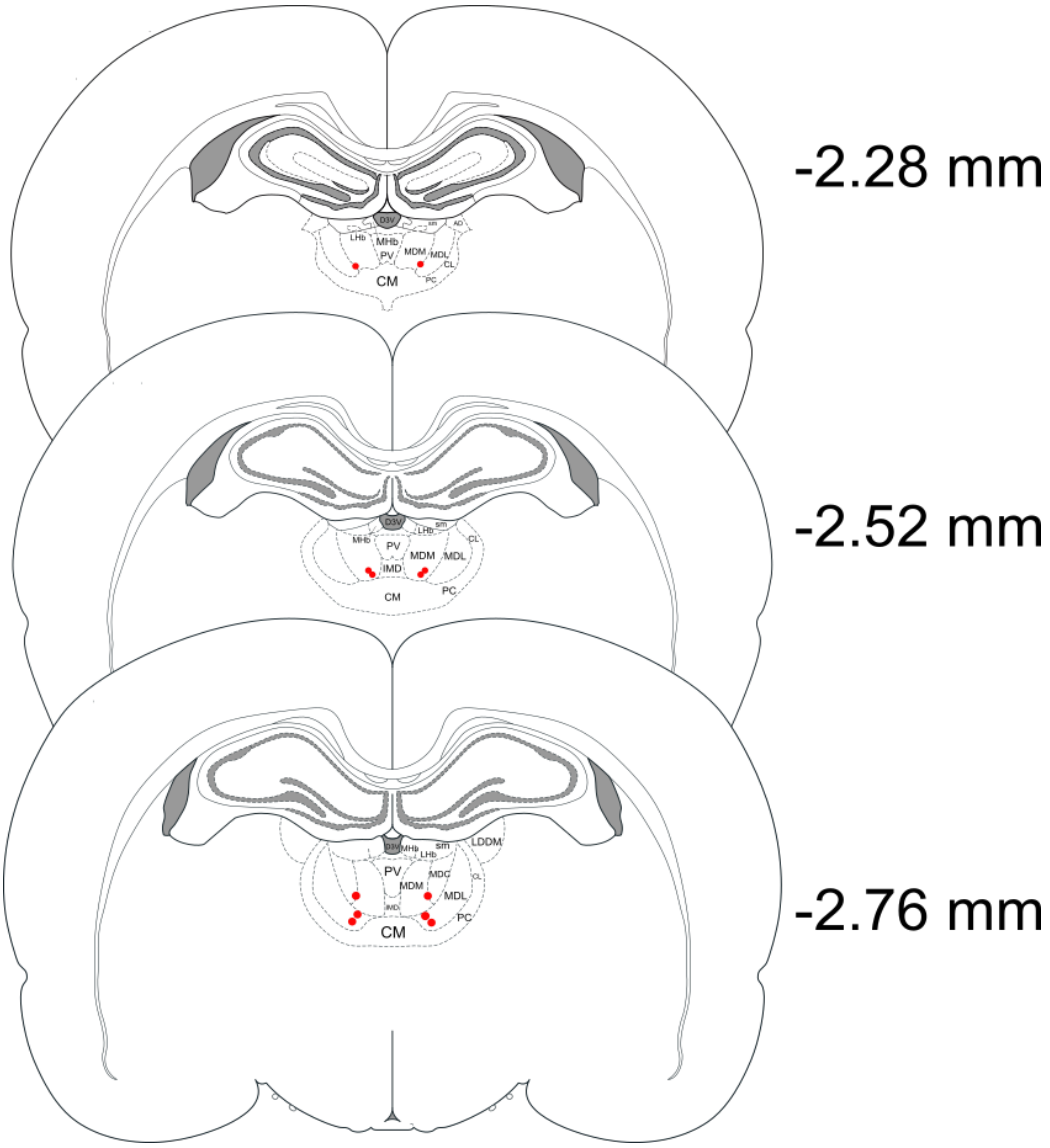

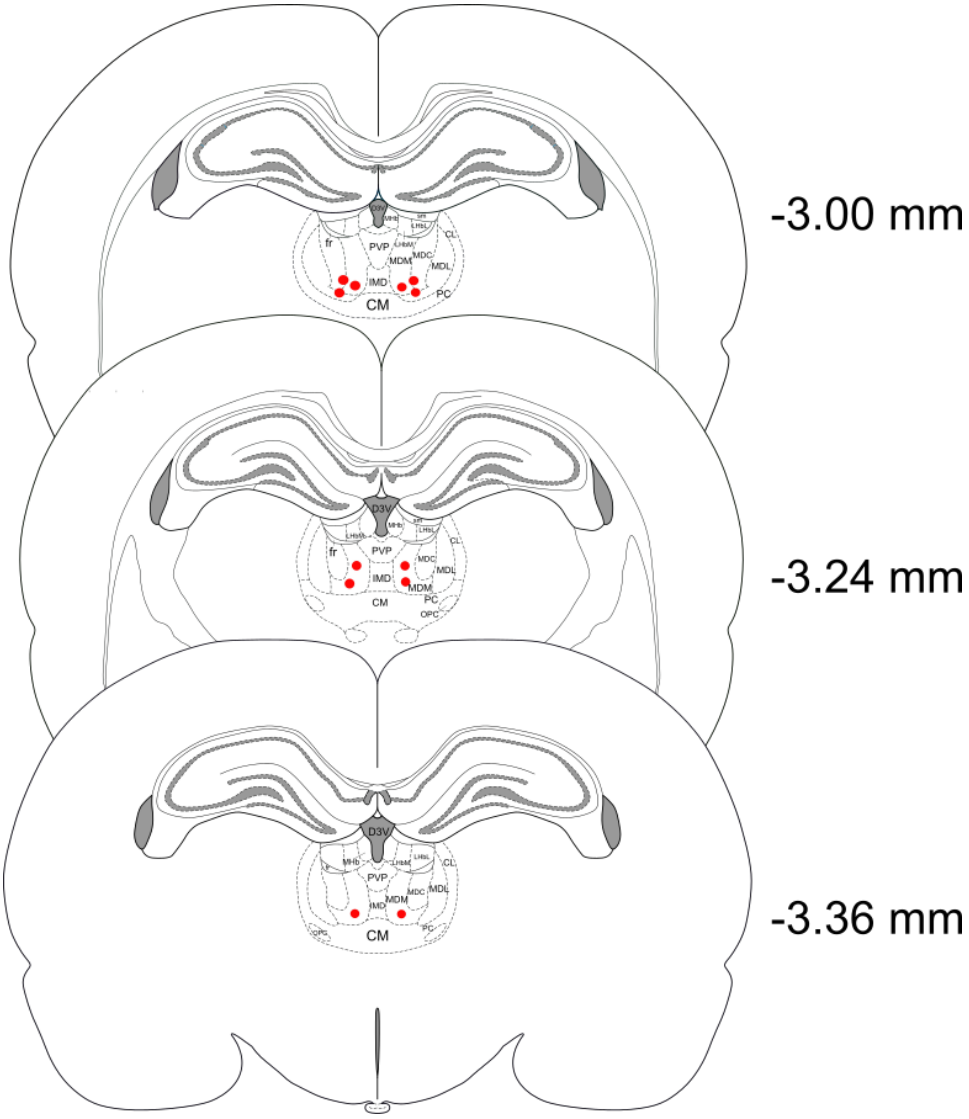

Figure 5.1: Cannula location in MD for Cohort 2

Representative sections of approximate cannula tip locations in all sections of the mediodorsal thalamus (MDM, MDC, MDL). Each symmetrical pair of red dots represents cannula tip location (n = 12). Surrounding structures labelled include the PV, IMD, CMD, lateral habenular nucleus, lateral and medial parts (LHbL, LHbM), paracentral thalamic nucleus (PC), stria medullaris of the thalamus (sm), dorsal third ventricle (D3V), and the laterodorsal thalamic nucleus, medial part (LDDM). Numbers indicate the section's location relative to bregma. Images were taken and reconstructed from the Paxinos and Watson atlas [108].

5.3.2 Saline infusions

Animals received saline infusions prior to the test phase. The average discrimination ratio for the group was 0.20 ± 0.06 which meant they significantly discriminated between novel and familiar object configurations (Saline: $t_{11} = 3.214$, $p = 0.008$, $n = 12$). Average exploration during the test phase was 75.91 s ± 2.13 s.

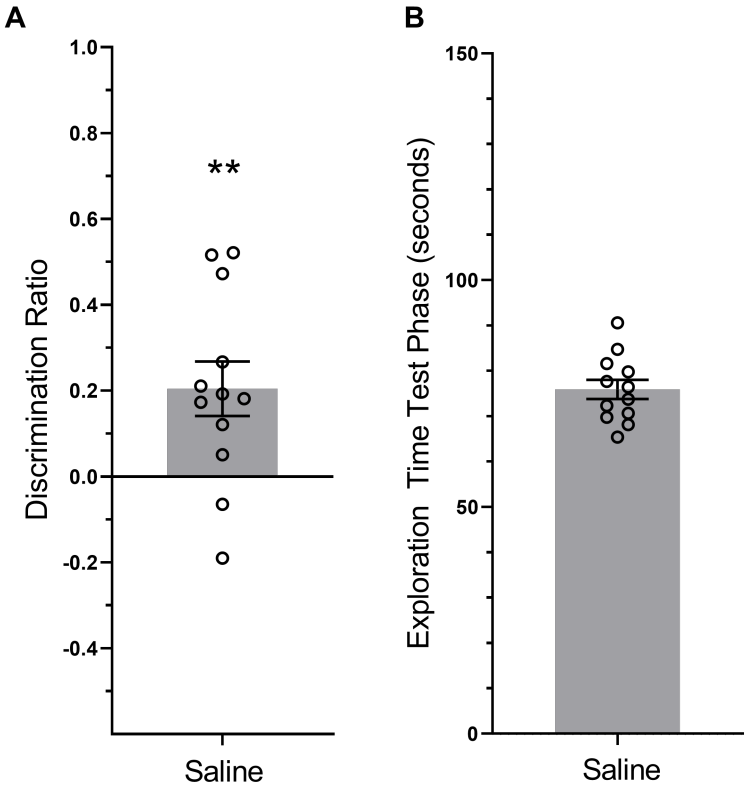

Figure 5.2: Saline infusions did not adversely affect performance in the OiP task
A: Animals receiving saline infusions successfully performed the OiP task and discriminated between objects above chance levels ($p = 0.008$, $n = 12$) **B:** Infusions of saline had no effect on overall exploration time during the test phase and all animals met the exploration time criteria of ten seconds. Graphs display the group mean ± SEM. Symbols represent data from each individual animal. Statistical significance indicated with asterisks.

5.3.3 NMDARs required for associative memory retrieval in the MD

To assess the contribution of NMDA receptors to associative recognition memory retrieval in the MD, infusions of AP-5 were administered prior to the test phase of the OiP task.

Animals receiving AP-5 (DR = -0.06 ± 0.04) had a significantly lower discrimination ratio compared to when they received vehicle (DR = 0.14 ± 0.04) infusions (t_8= 3.920, p = 0.004, n = 9) (Figure 5.3 A). The vehicle group significantly discriminated between novel and familiar object configurations above chance levels, whereas the AP-5 group did not (Vehicle: t_8 = 3.837, p = 0.005, n = 9; AP-5: t_8 = -0.155, p = 0.240, n = 9). Analysis of the overall exploration time at the test phase showed there were no significant differences between vehicle (63.33 s ± 4.81 s) and AP-5 (55.17 s ± 5.65 s) groups (t_8 = 1.008, p = 0.343, n = 9) (Figure 5.3 B).

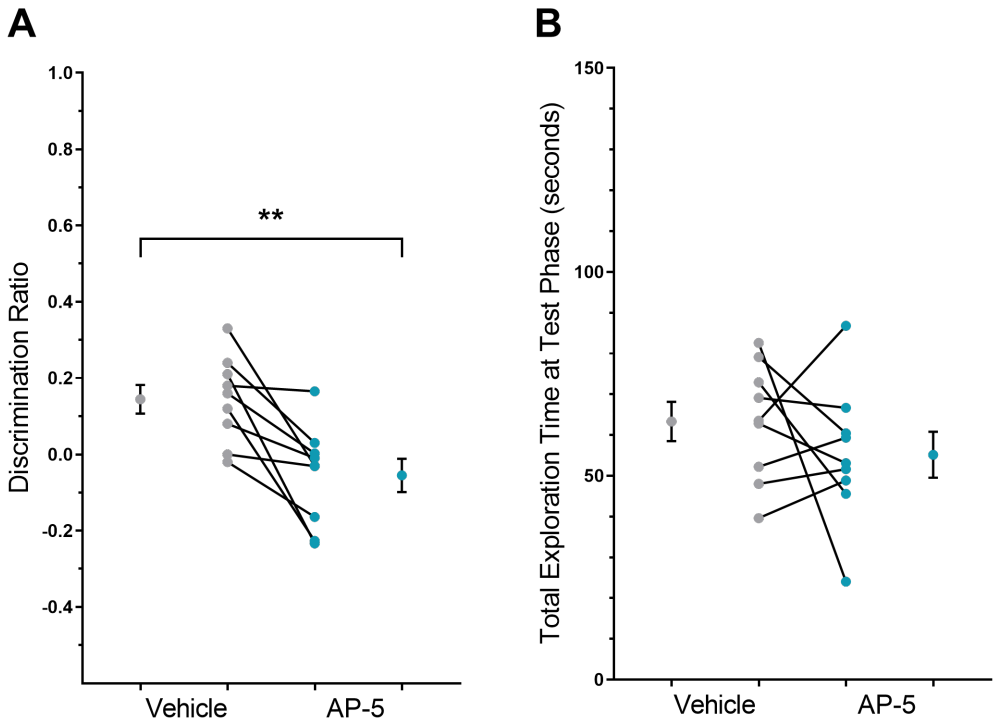

Figure 5.3: Blocking NMDARs impairs OiP performance

A: Infusions of AP-5 before the test phase significantly impaired OiP performance (p = 0.004, n = 9). **B:** No differences in total exploration time at test phase following infusions of vehicle or AP-5 (p >0.05, n = 9). The graphs display individual data points paired across conditions alongside the group means ± SEM. Statistical significance indicated by asterisks.

5.3.4 Blocking GluN2A containing NMDA receptors impairs associative memory retrieval in the MD

Animals which received vehicle infusions (DR = 0.34 ± 0.07) significantly discriminated between novel and familiar object configurations ($t_{11} = 4.784$, $p = 0.001$, $n = 12$). However, when animals received infusions of NVP AAM077 (DR = -0.01 ± 0.07) they did not discriminate successfully (t_{11} = -0.080, p = 0.938, n = 12). There was a significant difference between the two groups ($t_{11} = 2.821$, $p = 0.017$, $n = 12$).

There were no significant differences in mean exploration time between vehicle (58.97 s ± 4.51 s) and NVP AAM077 (58.35 s ± 4.17 s) receiving groups ($t_{11} = 0.200$, $p = 0.845$, $n = 12$)

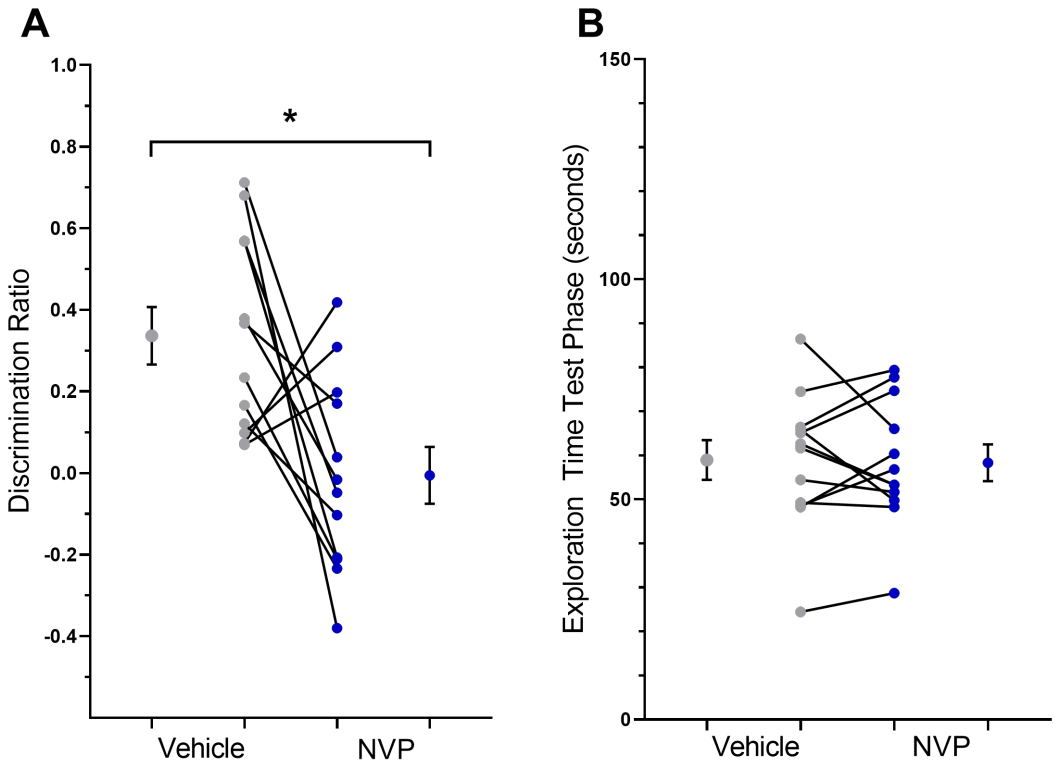

Figure 5.4: Blocking GluN2A containing NMDARs impairs memory retrieval

A: Infusions of NVP AAM077 prior to the test phase significantly impaired OiP performance compared to vehicle infusions ($p = 0.017$, $n = 12$). **B:** There were no effects on total exploration time at test following infusions of NVP compared to vehicle infusions ($p > 0.05$, $n = 12$). Graphs display individual data points paired across conditions alongside the group means ± SEM. Statistical significance indicated by asterisks.

5.3.5 No effect of blocking GluN2B containing NMDARs on memory retrieval in the MD

Animals which received vehicle infusions (DR = 0.25 ± 0.05) and RO 25-6981 (DR = 0.19 ± 0.07) successfully discriminated between novel and familiar object configurations (Vehicle: t_{11} = 4.581, p = 0.001, n = 12; RO 25-6981: t_{11} = 2.641, p = 0.023, n = 12). There were no significant differences in discrimination ratio between the two groups (t_{11} = 0.555, p = 0.590, n = 12). There were no significant differences in mean exploration time between the vehicle (63.10 s ± 3.60 s) and RO 25-6981 (61.48 s ± 4.28 s) groups (t_{11} = 0.462, p = 0.653, n = 12).

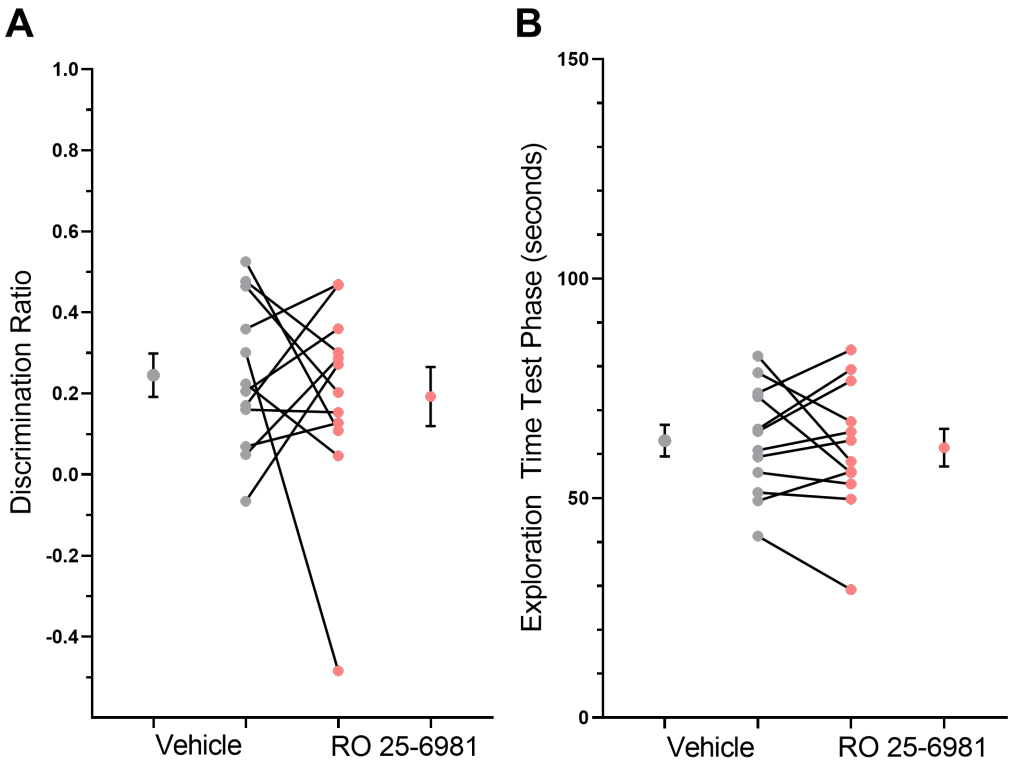

Figure 5.5: Blocking GluN2B containing NMDARs had no effect on memory retrieval **A:** Infusions of RO 25-6981 prior to the test phase had no effect on OiP performance compared to vehicle infusions (p >0.05, n = 12). **B:** There were no effects on total exploration time at test following infusions of RO 25-6981 compared to vehicle infusions (p >0.05, n = 12). Graphs display individual data points paired across conditions alongside the group means ± SEM.

5.3.6 GluN2C/D containing NMDARs are required for associative memory retrieval in the MD

Animals which received vehicle infusions (DR = 0.40 ± 0.07) significantly discriminated between novel and familiar object configurations (t_{11} = 5.952, p <0.001, n = 12). In comparison, animals which received infusions of UBP-791 (DR = -0.084 ± 0.059) could not discriminate successfully (t_{11} = -1.429, p = 0.181, n = 12). A paired t test revealed a significant difference between the two groups (t_{11} = 5.484, p <0.001, n = 12) (Figure 5.6 A). Infusions of UBP-791 had no effect on the animals' overall exploration time during the test phase. There were no significant differences between the mean total exploration times for vehicle (54.29 s ± 5.00 s) and UBP-791 groups (51.38 s ± 4.52 s) (t_{11} = 0.878, p = 0.399, n = 12) (Figure 5.6 B).

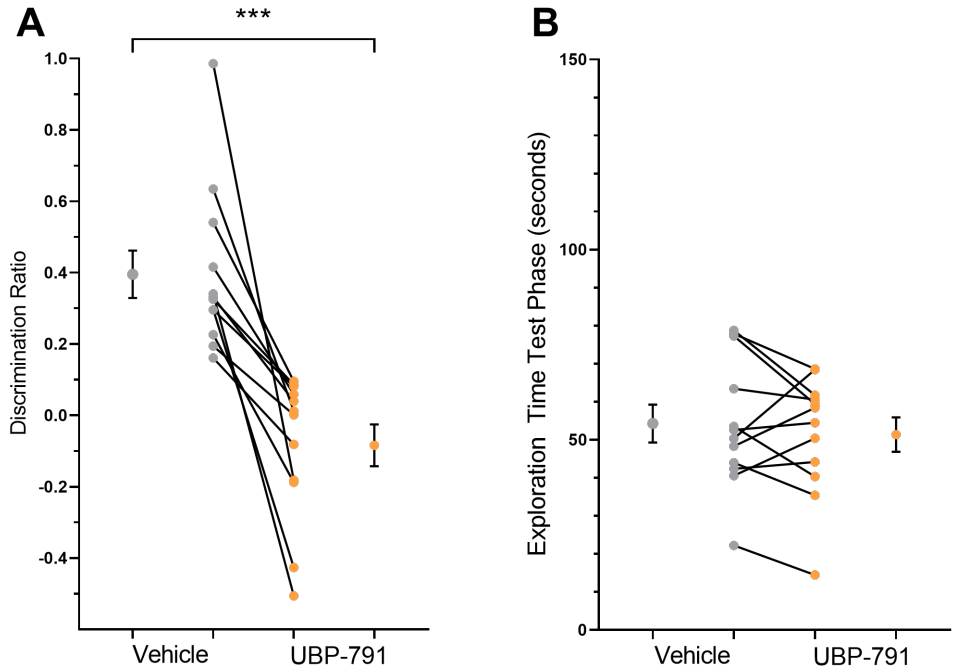

Figure 5.6: Blocking GluN2C/D containing NMDARs impairs memory retrieval in the MD

A: Infusions of UBP-791 in to the MD significantly impaired animals' performance in the OiP task compared to vehicle (p <0.001, n = 12). **B:** Infusions of UBP-791 did not affect animals' overall exploration time during the test phase and was not significantly different to vehicle infusions (p >0.05, n = 12). The graphs display individual data points paired across conditions alongside the group means ± SEM. Statistical differences indicated by asterisks.

5.3.7 No impairments observed in the object location task

To ensure effects observed were not due to drugs affecting the HPC, or damage to the HPC by the cannula implants, animals were run in the OL task. Infusions of UBP-791 and NVP AAM077 were used as these produced deficits in the OiP task.

Firstly, infusions of UBP-791 (DR = 0.29 ± 0.08) prior to the test phase of the OL task produced no deficits in comparison to animals receiving vehicle (DR = 0.29 ± 0.08) infusions. Both groups could successfully discriminate between novel and familiar object configurations (Vehicle: $t_{11} = 3.570$. p = 0.004, n = 12; UBP-791: $t_{11} = 3.496$, p = 0.005, n = 12) (Figure5.7 A). There were no significant differences between the two groups (t_{11} = -0.141, p = 0.890, n = 12). Exploration time during the test phase was unchanged between UBP-791 (49.90 s ± 5.18 s) and vehicle (45.44 s ± 2.55 s) groups. Comparisons between the two conditions were not significant (t_{11} = -0.966, p = 0.355, n =12) (Figure 5.7 B).

Similarly, infusions of NVP AAM077 (DR = 0.35 ± 0.05) prior to the test phase of the OL task produced no deficits compared to vehicle infusions (DR = 0.36 ± 0.069) infusions (Figure 5.8 A). Both groups successfully discriminated between novel and familiar object configurations (Vehicle: $t_{10} = 5.233$, p <0.001, n = 11; NVP AAM077: $t_{10} = 6.933$, p <0.001, n = 12). There were no significant differences between the two groups (t_{10} = 0.063, p = 0.951, n = 11).

Exploration time during the test phase did not differ between NVP AAM077 (51.15 s ± 3.15) and vehicle (50.92 s ± 3.92 s) groups. Comparisons between the two conditions were not significantly different (t_{10} = -0.051, p = 0.960, n = 11) (Figure 5.8 B).

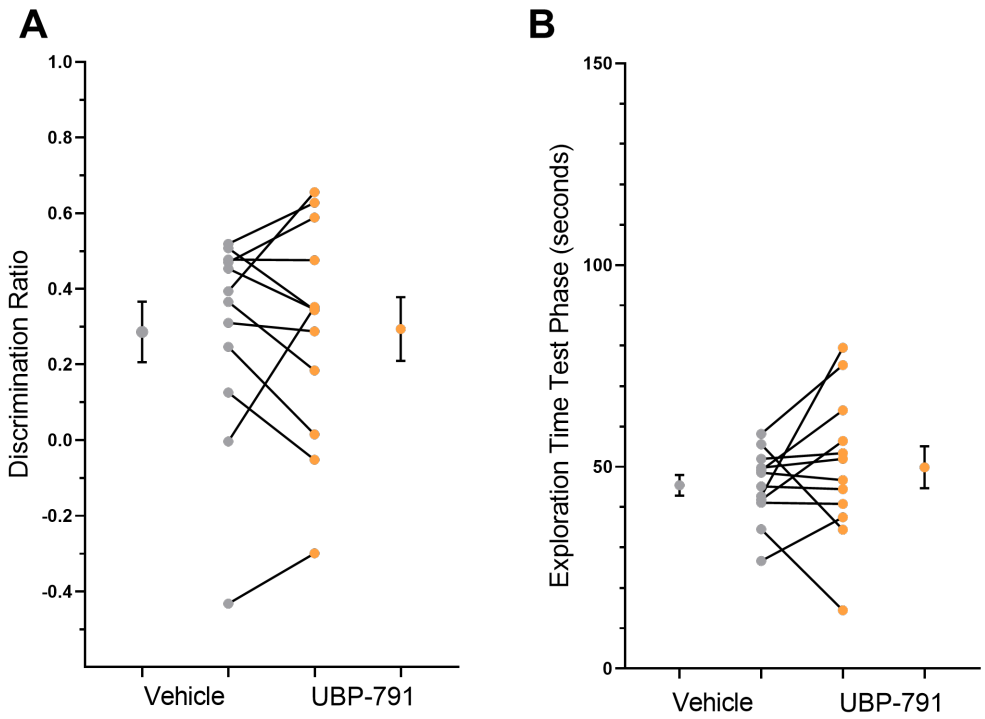

Figure 5.7: Blocking GLuN2C/D containing NMDARs in the MD had no effect on the object location task

A: Infusions of UBP-791 prior to the test phase had no effect on the object location task, there were no significant differences between UBP-791 and vehicle infusions ($p > 0.05$, $n = 12$). **B:** There were no differences between mean total exploration times at the test phase following infusions of UBP-791 or vehicle ($p > 0.05$, $n = 12$). Graphs display individual data points paired across conditions alongside the group means ± SEM.

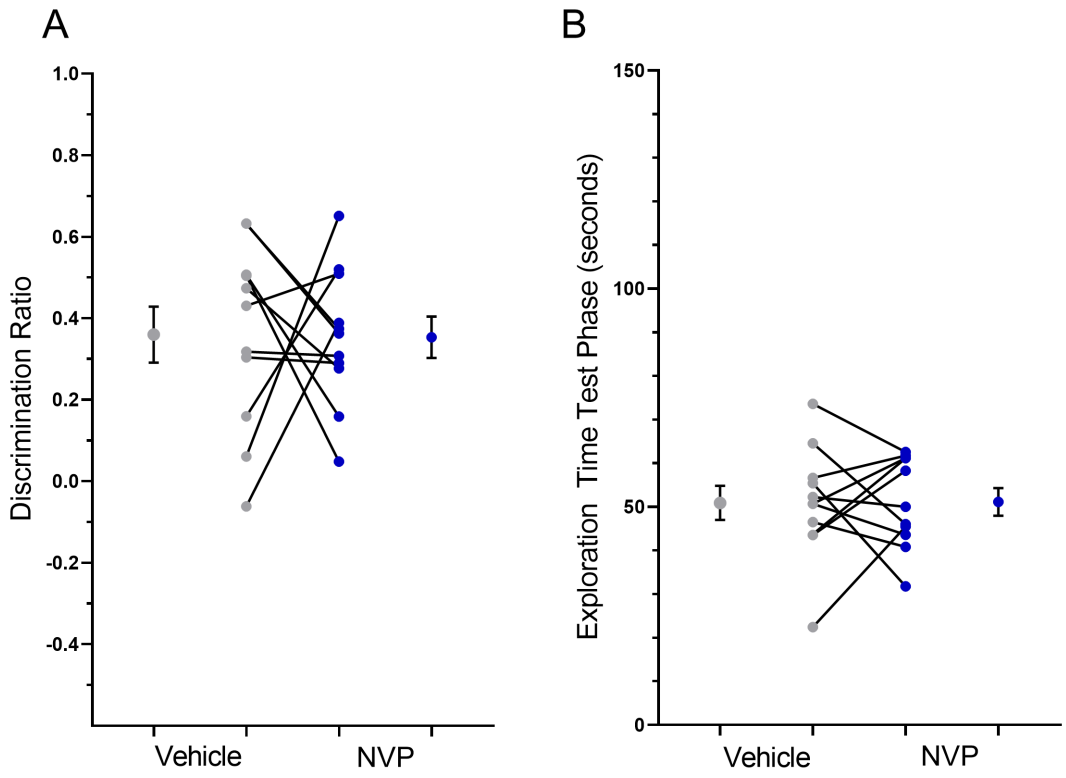

Figure 5.8: Blocking GluN2A containing NMDARs in the MD had no effect on the object location

A: Infusions of NVP AAM077 prior to the test phase had no effect on the object location task. There were no significant differences between NVP AAM077 and vehicle infusions ($p > 0.05$, $n = 11$). **B:** There were no significant differences between mean total exploration times at the test phase following infusions of NVP AAM077 or vehicle ($p > 0.05$, $n = 11$). Graphs display individual data points paired across conditions alongside the group means ± SEM.

5.3.8 Neither long term potentiation nor long term depression underlies associative memory retrieval in the MD

Infusions of ZIP and TAT-GluR2$_3\gamma$ were used to assess the putative role of long term potentiation or long term depression mechanisms in the MD during associative memory retrieval, respectively. For controls both peptides have a scrambled form which is also taken in to the cells but has no biological effect. These are scrambled ZIP (Scr-ZIP) and scrambled TAT-GluR2$_3\gamma$ (Scr-TAT-GluR2$_3\gamma$).

Firstly, infusions of ZIP into the MD prior to the test phase had no effect on OiP

performance and animals which received ZIP (DR = 0.30 ± 0.41) and scrambled ZIP (DR = 0.32 ± 0.05) could successfully discriminate between novel and familiar object configurations (scrZIP: t_{11} = 7.001, p <0.001, n = 11; ZIP: t_{11} = 7.332, p <0.001, n = 11). There were no significant differences between the mean discrimination ratios of each group (t_{11} = 0.274, p = 0.790, n = 11) (Figure5.9 A). Total exploration time during the test phase did not differ between ZIP (62.35 s ± 4.25) and scr-ZIP (53.96 s ± 5.53 s) receiving groups. There were no significant differences between mean total exploration times of each group (t_{11} = -1.251, p = 0.239, p = 11) (Figure 5.9 B).

Animals which received infusions of TAT-GluR2$_3\gamma$ (DR = 0.42 ± 0.10) and Scr-TAT-GluR2$_3\gamma$ (DR = 0.23 ± 0.09) could successfully discriminate between novel and familiar object configurations (Scr-TAT-GluR2$_3\gamma$: t_9 = -2.455, p = 0.036, n = 10; TAT-GluR2$_3\gamma$: t_9 = 4.213, p = 0.002, n = 10) (Figure 5.10 A). Comparisons between the group means showed a significant improvement in discrimination ratio when animals received TAT-GluR2$_3\gamma$ (t_9 = -2.375, p = 0.042, n = 10). Total exploration time during the test phase did not differ between TAT-GluR2$_3\gamma$ (60.74 s ± 3.28 s) and Scr-TAT-GluR2$_3\gamma$ (60.33 s ± 4.11 s) groups. There were no significant differences between mean total exploration times of each group (t_9 = -0.068, p = 0.947, n = 10) (Figure 5.10 B).

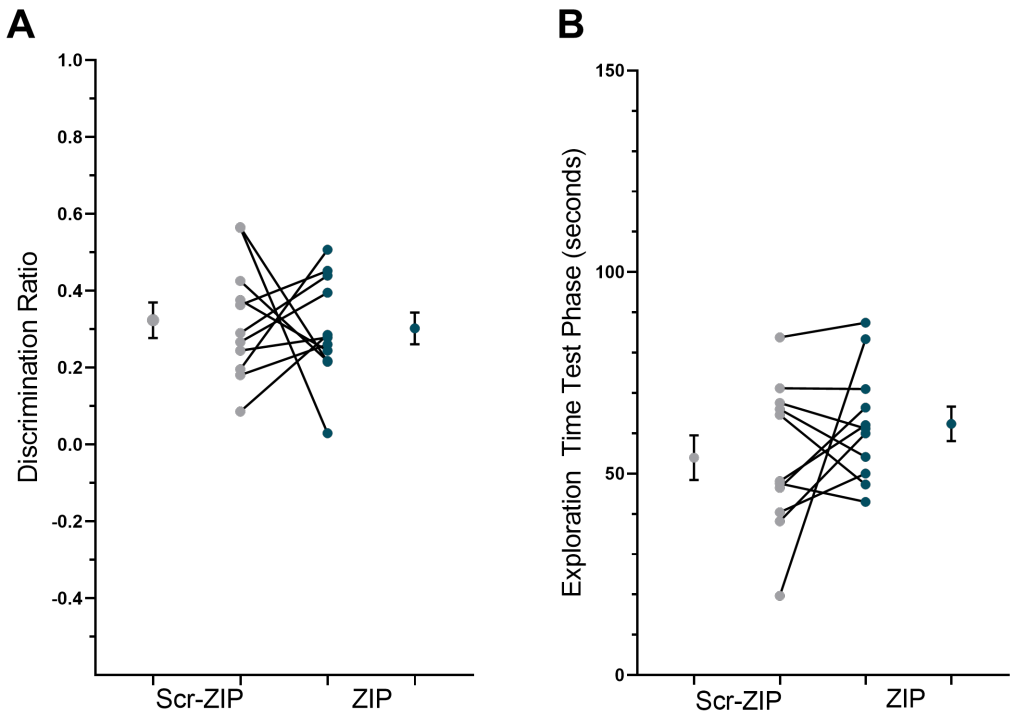

Figure 5.9: Infusions of ZIP into the MD had no effect on OiP performance

A: Infusions of ZIP prior to the test phase had no effect on animals' performance in OiP task. There were no significant differences in mean discrimination ratio between ZIP and Scr-ZIP receiving groups ($p > 0.05$, $n = 11$). **B:** There were no significant differences between mean total exploration times at the test phase following infusions of ZIP or Scr-ZIP ($p > 0.05$, $n = 11$). Graphs display individual data points paired across conditions alongside the group means ± SEM.

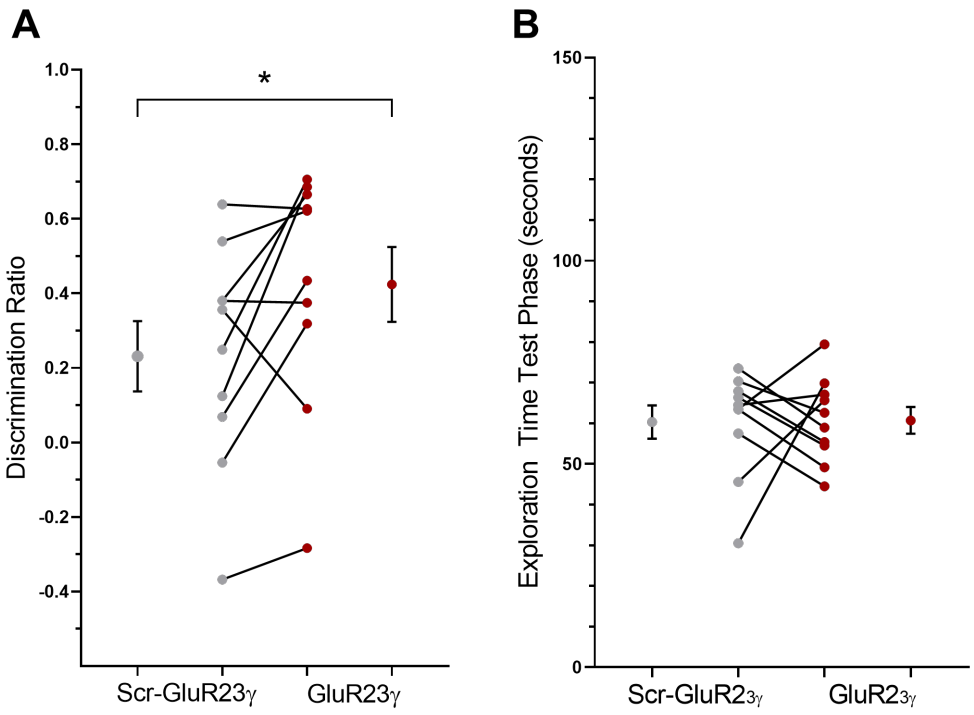

Figure 5.10: Infusions of TAT-GluR2$_3\gamma$ into the MD improved OiP performance **A:** Infusions of TAT-GluR2$_3\gamma$ prior to the test phase significantly improved animals' performance in the OiP task ($p = 0.042$, $n = 10$). **B:** There were no significant differences between mean total exploration times at the test phase following infusions of TAT-GluR2$_3\gamma$ or Scr-TAT-GluR2$_3\gamma$ ($p > 0.05$, $n = 10$). Graphs display individual data points paired across conditions alongside the group means ± SEM.

Table 5.1: Mean Exploration Times Across Experiments

Drug	**Infusion Timing**	**Mean Exploration Time at Sample Phase (s)**	**Mean Exploration Time at Test Phase (s)**	**Mean DR**
AP-5	Pre-Test OiP	102.68 ± 7.22	67.59 ± 3.19	-0.06 ± 0.04
Saline	Pre-Test OiP	104.71 ± 6.17	68.68 ± 3.33	0.15 ± 0.04
NVP AAM077	Pre-Sample OiP	81.66 ± 5.60	58.35 ± 4.17	-0.01 ± 0.07
Saline	Pre-Sample OiP	106.49 ± 7.40	58.97 ± 4.51	0.34 ± 0.07
NVP AAM077	Pre-Test OL	71.98 ± 4.00	51.15 ± 3.15	0.35 ± 0.05
Saline	Pre-Test OL	81.66 ± 4.92	50.92 ± 3.92	0.36 ± 0.07
RO 25-6981	Pre-Test OiP	81.66 ± 6.89	61.48 ± 4.28	0.19 ± 0.07
Saline	Pre-Test OiP	111.87 ± 9.07	63.10 ± 3.60	0.24 ± 0.05
Saline Control	Pre-Test OiP	150.10 ± 3.62	75.91 ± 2.13	0.20 ± 0.06
TAT-GluR2$_3\gamma$	Pre-Test OiP	115.53 ± 5.69	60.74 ± 3.28	0.42 ± 0.10
Scr-TAT-GluR2$_3\gamma$	Pre-Test OiP	81.66 ± 4.87	60.33 ± 4.11	0.23 ± 0.09
UBP-791	Pre-Test OiP	81.66 ± 6.29	51.38 ± 4.52	-0.08 ± 0.06
Saline	Pre-Test OiP	90.30 ± 7.83	54.29 ± 5.00	0.40 ± 0.07
UBP-791	Pre-Test OL	81.66 ± 6.08	49.90 ± 5.18	0.30 ± 0.08
Saline	Pre-Test OL	74.17 ± 4.11	45.44 ± 2.55	0.29 ± 0.08
ZIP	Pre-Test OiP	81.66 ± 5.86	62.35 ± 4.25	0.30 ± 0.04
Scr-ZIP	Pre-Test OiP	109.74 ± 7.30	53.96 ± 5.53	0.32 ± 0.05

5.3.9 Properties of NMDA and AMPA receptors at mPFC - MD synapse

To investigate the relative properties of AMPA and NMDA receptors at the mPFC - MD synapse, AMPA and NMDA currents were isolated and EPSCs were measured (Figure 5.11 C).

The NMDA/AMPA ratio was calculated by dividing the peak NMDA EPSC amplitude by the peak AMPA EPSC amplitude. The mean NMDA/AMPA ratio across 18 cells was 0.61 ± 0.08 with peak amplitude through AMPA receptors being higher than NMDA receptors on average (Figure 5.11 B).

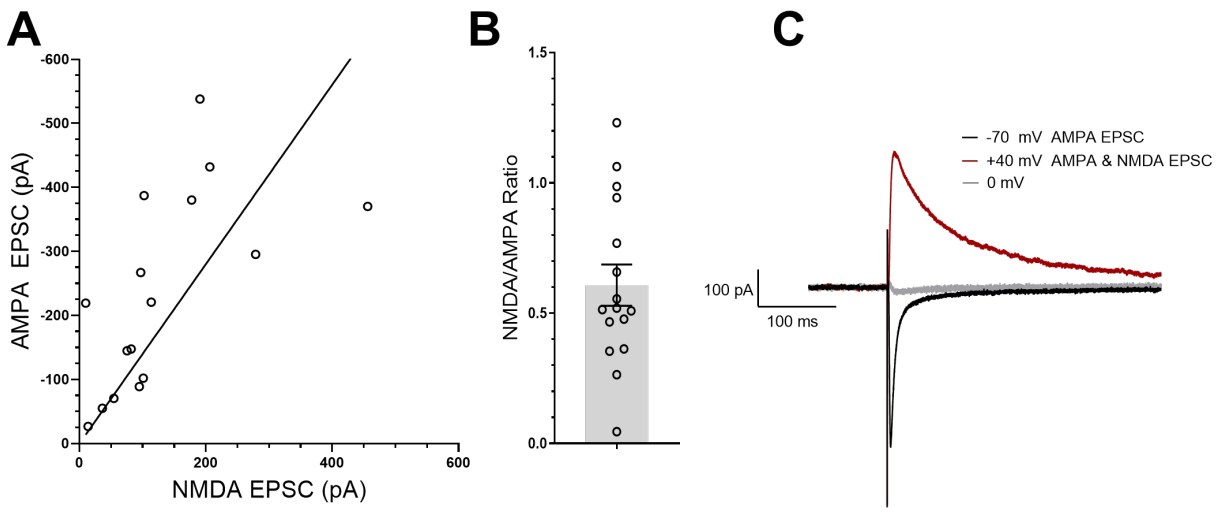

Figure 5.11: NMDA/AMPA properties at mPFC - MD synapse

A: Scatter plot of NMDA current versus AMPA current. Each circle represents an individual cell. **B:** A bar plot of the NMDA/AMPA ratio. Each circle represents the ratio from a single cell. Bar shows the mean ± the SEM. **C:** Representative trace from a single MD neuron, showing an AMPA and NMDA EPSC (red), an AMPA EPSC (black) and the reversal potential at 0 mV (grey).

5.3.10 GluN2B containing NMDARs are present at mPFC - MD synapse

In whole cell patch clamp, cells were voltage clamped and NMDA EPSCs were isolated. Ro 25-6981 was bath applied at 1 μM and the effects on the NMDA EPSC was observed over twenty minutes (Figure 5.12)

Data were normalised and expressed as a percentage. Drug conditions were compared against the baseline with a one sample t test set to a value of 100 %. There was no significant effect of applying Ro 25-6981 after ten minutes (105.15 % ± 21.10 %) (t_4 = -0.453, p = 0.674, n = 5), but there was a significant decrease in normalised peak amplitude after twenty minutes (51.64 % ± 3.50 %) (t_2 = -13.802, p = 0.005, n = 3) (Figure 5.12 A).

There were no significant effects on the normalised time taken for the NMDA EPSC to decay to 50 % of its peak amplitude after ten minutes of Ro 25-6981 (99.39 % ± 3.72 %) (t_4 = -0.784, p = 0.477, n = 5), or twenty minutes (97.51 % ± 1.61 %) (t_2 = -1.553, p = 0.261, n = 3) (Figure 5.12 B).

There were also no significant differences on the normalised input resistance after application of Ro 25-6981 after ten minutes (106.45 % ± 19.38 %) (t_4 = 0.438, p = 0.684, n = 5), or twenty minutes (87.95 % ± 19.00 %) (t_2 = -0.634, p = 0.591, n = 3) (Figure 5.12 C).

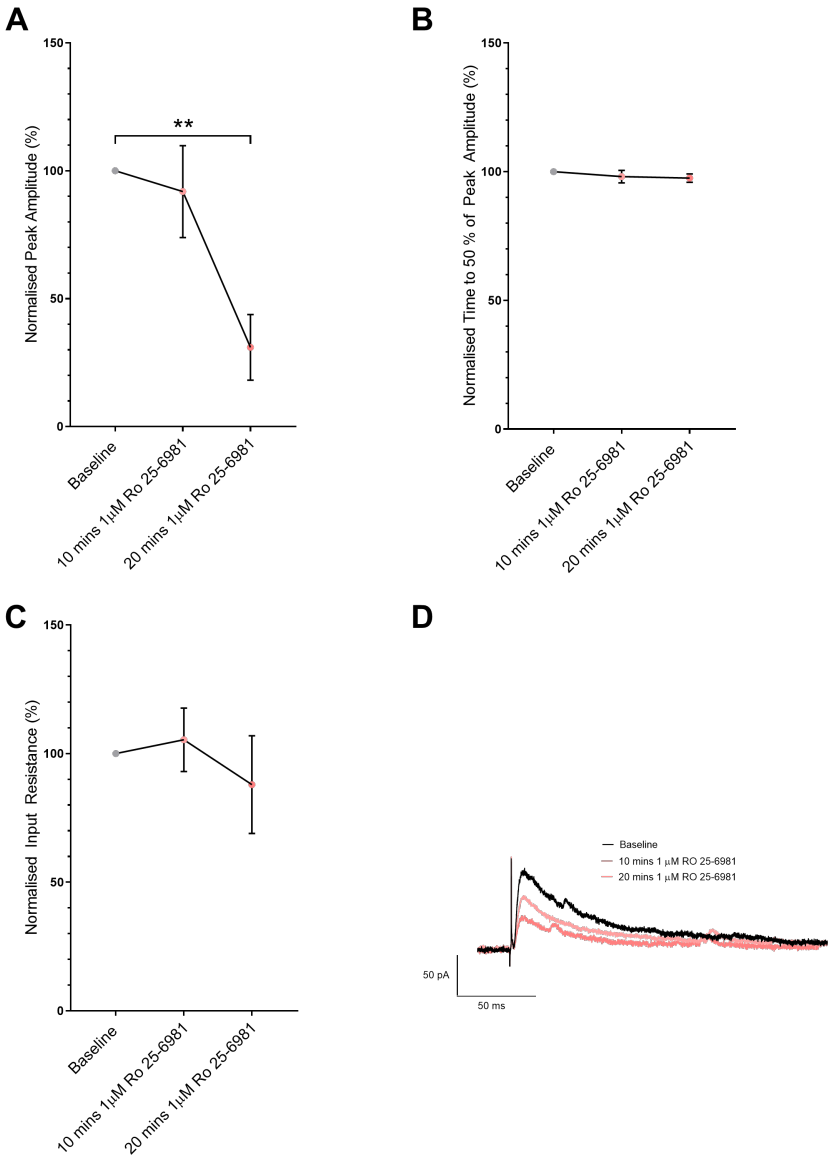

Figure 5.12: Effect of Ro 25-6981 on NMDA EPSCs

A: Ro 25-6981 significantly decreased normalised peak amplitude after twenty minutes (p = 0.005, n = 3). **B:** No significant differences on the normalised time for peak amplitude to fall to 50 % after Ro 25-6981 application (p >0.05, n = 5 (10 mins), n = 3 (20 mins)). **C:** There were no significant changes in input resistance following Ro 25-6981 application (p >0.05, n = 5 (10 mins), n = 3 (20mins)). Data in A-C display the group means ± SEM. **D:** Representative NMDA EPSCs from one cell showing baseline and in the presence of Ro 25-6981 at ten and twenty minutes.

5.3.11 GluN2C/D containing NMDARs present at mPFC - MD synapse

In whole cell patch clamp, cells were voltage clamped and NMDA EPSCs were isolated. UBP-791 was applied and effects on the EPSC was observed over twenty minutes.

Data were normalised and expressed as a percentage. Drug conditions were compared against the baseline with a one sample t test set to a value of 100 %. Applying UBP-791 significantly decreased peak amplitude after 10 minutes (65.67 % ± 11.69 %) (t_3 = -3.945, p = 0.029, n = 4). But there was no significant effect on peak amplitude following 20 minutes of UBP-791 application (53.84 % ± 15.06 %) (t_2 = -3.066, p = 0.092, n = 3) (Figure 5.13 A). It approached significance, but the sample size was too low to interpret.

The time taken for the EPSC to decay to 50 % of its peak amplitude was also measured and normalised for comparisons between cells. There was no significant effect on the normalised mean time taken to decay to 50 % after ten minutes of UBP-791 (100.71 % ± 1.38 %) (t_3 = 0.516, p = 0.641, n = 4), or after twenty minutes (92.32 % ± 4.51 %) (t_2 = -1.702, p = 0.231, n = 3) (Figure 5.13 B).

Input resistance was normalised for comparisons between cells. A one sample t test revealed a significant decrease in input resistance after ten minutes of UBP-791 application (69.66 % ± 8.43) (t_3 = -3.598, p = 0.037. n = 4). There was also a significant change in input resistance at twenty minutes (71.10 % ± 2.92) (t_2 = -9.907, p = 0.010, n = 3) (Figure 5.13 C)

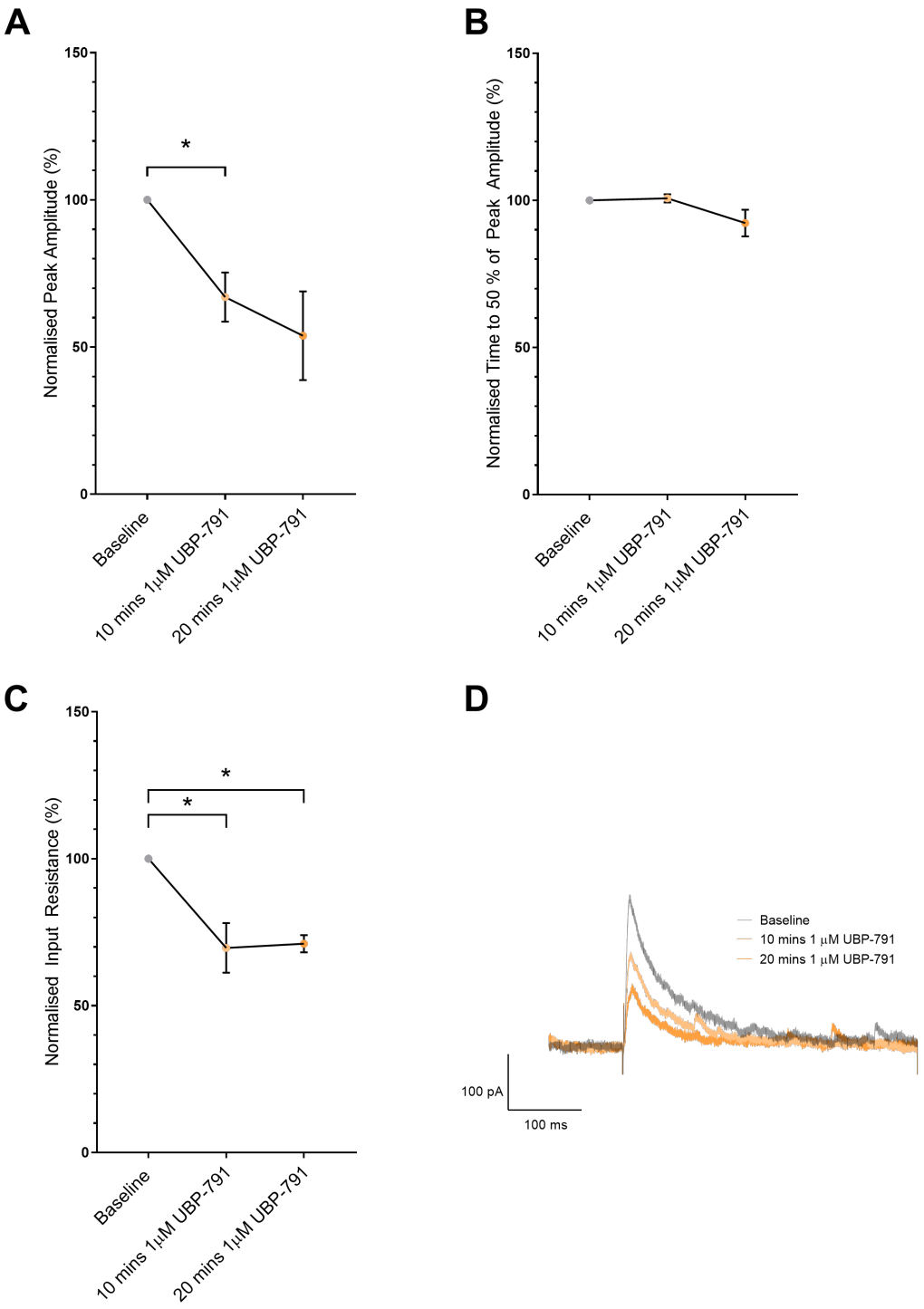

Figure 5.13: Effect of UBP-791 on NMDA EPSCs

A: UBP-791 significantly decreased normalised peak amplitude after ten minutes ($p = 0.029$, $n = 4$). **B:** No significant differences on the normalised time for peak amplitude to fall to 50 % after UBP-791 application ($p > 0.05$, $n = 4$). **C:** There was a significant decrease in input resistance at ten minutes ($p = 0.037$, $n = 4$) and twenty minutes (p

= 0.010, n = 3). Data from A-C display means ± the SEM. **D:** Representative NMDA EPSCs from one cell showing baseline and in the presence of UBP-791 at ten and twenty minutes.

5.4 Discussion and conclusions

5.4.1 Main findings

The data in this chapter show that associative memory retrieval is dependent on NMDARs in the MD, and specifically, NMDARs containing GluN2A and/or GluN2C/D subunits. Additionally, *in vitro* experiments demonstrated that GluN2B and GluN2C/D containing NMDARs are present at the mPFC-MD synapse as selective antagonists reduced EPSCs through these receptors. The data also show that blocking mechanisms involved in LTP or LTD during retrieval had no effect, suggesting these mechanisms of LTP and LTD are not occurring in the MD during associative memory retrieval.

5.4.2 NMDA receptors in memory retrieval

Infusing the NMDAR antagonist, AP-5, in to the MD impaired associative recognition memory retrieval. This finding is unique, as typically blocking NMDARs has blocked memory encoding in other brain regions involved in associative recognition memory. For example, infusions of AP-5 into the mPFC and NRe has impaired encoding but not retrieval of OiP information [93, 95], and impaired encoding of object recognition after infusions into the perirhinal cortex [94]. The role of NMDARs in encoding has also been attributed to their role in NMDA dependent LTP, a mechanism which has been argued to be underlying the learning and encoding of new memories [96, 97, 130].

There is evidence however, of NMDARs being required during memory retrieval in other forms of memory [131, 132]. AP-5 infusions in to the retrosplenial cortex reduced freezing behaviour in a fear conditioning study using mice [132]. The study also demonstrated that blocking GluN2a containing NMDARs, but not GluN2B NMDARs impaired fear conditioning [132]. Blocking NMDARs in the HPC during the same behavioural paradigm produced had no effect, but it did impair acquisition [132]. This is similar to the differences observed in the associative recognition memory literature, where previously blocking AP5

has impaired encoding in the mPFC and NRe [93]. Another study by Joelle et al showed that, in the amygdala, memory retrieval requires ongoing protein synthesis and NMDA-dependent AMPAR trafficking [131]. The results in this thesis show for the first time that NMDARs support associative memory retrieval in the MD. whilst potential mechanisms have been identified in other brain regions during other types of memory, there is still much to be understood about the specific mechanisms underlying NMDAR involvement in associative recognition memory.

As incoming information from the mPFC to the MD is crucial during retrieval, but not encoding in the MD (unpublished work L. Cross, G. Barker), it could be that activity at NMDARs is crucial for the transmission of such information. Whilst the infusions into the MD do not specifically block incoming signals from the mPFC, the *in vitro* experiments in chapter 4 have demonstrated short term plasticity between the mPFC and MD is dependent on NMDARs. Also, the *in vitro* experiments in this chapter showed that blocking specific subtypes of NMDARs (GluN2B and GluN2C/D) has decreased evoked EPSCs through NMDARs at this corticothalamic synapse. Together these results show that NMDARs are crucial in the MD during memory retrieval, and to support successful transmission between mPFC and the MD, and this could suggest that NMDARs at the mPFC - MD synapse are crucial for supporting associative recognition memory retrieval.

Several experiments investigating the role of MD in working memory hypothesise that the MD is recruited by the mPFC to guide task relevant behaviour. Whilst these tasks can not be directly compared to the associative memory tasks due to them being different forms of memory, used in this chapter, it is useful to speculate how the role of the MD may differ or be the same in this context. Thus, it could be hypothesised that the mPFC recruits the MD and the MD amplifies signals back to the mPFC to guide retrieval. This would favour relevant signals for the task at hand and suppress task irrelevant signals, or 'interference'. If transmission is reduced by blocking the NMDARs it could dampen the signals sent back to the mPFC from the MD, and thus increasing interference and disrupting appropriate recognition memory retrieval.

5.4.3 NMDAR properties in the MD

Further *in vitro* experiments tested the contribution of NMDARs at the mPFC - MD synapse and applied subunit specific antagonists to isolated NMDA currents. The data

showed that blocking GluN2B and GluN2C/D containing NMDARs resulted in a decrease in NMDA EPSCs, suggesting the NMDA component at this synapse is from GluN2B and GluN2C/D containing NMDARs. However, as the input resistance varied significantly during the GluN2C/D experiments, it is not clear whether the reduction in amplitude is caused by a real effect of the drug, or by the series resistance increasing. This experiment also requires repeating to test if there is a contribution of GluN2A subunits at the mPFC - MD synapse also.

5.4.4 Antagonist selectivity

Only recently have subunit selective antagonists been produced for NMDARs, and most of these antagonists will interact at other subunits, hence careful selection of concentrations was important. There are no specific antagonists for the GluN2C or GluN2D subunits, however there are compounds that selectively target both. UBP-791 is a recently developed antagonist for both GluN2C and GluN2D containing NMDARs [91]. However, UBP-791 interacts with GluN2B subunits at around a concentration of 1 μM but its EC_{50} for GluN2B is around 10 μM, therefore a concentration of 1 μM was chosen to ensure GluN2C/D containing NMDARs were targeted whilst limiting the effect on GluN2B subunits. As blocking GluN2B NMDARs had no effect on associative memory retrieval, any off target effects at the GluN2B receptors during the GluN2C/D experiments can be ruled out.

5.4.5 No effect on object location

Previous work has shown that the MD is not required for object location as lesions to the MD have no impact on animals' performance in this task [4]. However, the task is dependent on the HPC [107], a region that could sustain damage due to the position of the cannulae. As all animals in this cohort could successfully discriminate in the object location task, it is unlikely that any damage to the HPC was not sufficient to impair OL. Therefore, any deficits in the OiP cannot be explained by hippocampal damage.

These control experiments also aimed to rule out whether drugs were having an effect in the HPC. Drug infusate can flow dorsal from the cannula tip and potentially affect the HPC. The experiments conducted in chapter 3 using fluorescent muscimol also indicated that there was no spread of the infusate to the HPC.

5.4.6 LTP mechanisms dependent on PKM elevation do not underlie associative memory retrieval

Infusions of ZIP into the MD had no effect on associative recognition memory retrieval. This peptide blocks the atypical protein kinase C isoform, protein kinase M (PKM). During LTP PKM levels are elevated. PKM prevents GluR2 dependent endocytosis of postsynaptic AMPARs [133]. It is thought to maintain long term memory by maintaining elevated levels of postsynaptic AMPARs by preventing their removal [133]. Thus, these experiments show that LTP, dependent on PKM mechanisms, is not required for associative recognition memory retrieval in the MD.

Whilst evidence of LTP and elevated levels of PKM has been demonstrated in the HPC and the cortex during learning [134], it is unknown if similar levels are present in the thalamus and, specifically, during associative recognition memory. It is also unknown whether incoming projections to the MD undergo synaptic plasticity, and what mechanism would underlie LTP if they did. Whilst infusions of ZIP have specifically interfered with PKM dependent LTP, there are other ways LTP can be induced. For example, other kinases can increase AMPAR conductance or number at the synapse and these processes are independent to PKM and not affected by ZIP [134, 135].

Further experiments are required to investigate whether the mPFC - MD synapse undergoes LTP *in vitro*, and if applying ZIP to the intracellular solution affects the induction and/or maintenance of LTP. This would clarify whether this form of LTP occurs at this specific synapse and would confirm or deny whether this is being blocked within the infusion experiments presented in this chapter.

5.4.7 Blocking AMPA receptor endocytosis in the MD improves associative recognition memory retrieval

Infusions of TAT-GluR2$_3\gamma$ peptide into the MD prior to the test phase significantly improved animals' performance in the OiP task. This peptide acts intracellularly and has been shown to block LTD *in vitro* [136–138]. Its mechanism of action involves interfering with protein interactions between the GluR2 subunit of AMPARs and Brag2 which is a clathrin adaptor protein that activates Arf6 to begin AMPAR endocytosis [136]. By blocking AMPA receptor endocytosis via this signalling pathway,

TAT-GluR2$_3\gamma$ improved rodents' performance in the OiP task.

This result was unexpected, as previously infusions of TAT-GluR2$_3\gamma$ into the mPFC impaired retrieval [73]. It was also shown to block an $\alpha4\beta2$ nAChR receptor dependent form of LTD at the HPC-mPFC pathway *in vitro* [73]. It could be that by blocking AMPA receptor endocytosis occurring naturally, and not necessarily due to LTD, enhanced glutamatergic signalling within the MD. This may have amplified incoming or outgoing information and as a result improved memory retrieval.

It is unknown whether the mPFC - MD synapse undergoes LTD via this mechanism specifically. It would be useful to explore whether LTD can be induced at the mPFC - MD synapse *in vitro*, and if this is blocked by applying TAT-GluR2$_3\gamma$ to the internal solution.

5.4.8 Study caveats

Series resistance

Whilst series resistance was not allowed to increase higher than 20 MΩ, any increases during recordings would result in a decrease in peak amplitude which could be mistaken for an effect caused by drug application.

The series resistance significantly changed during the UBP-791 experiments, making it unclear whether the effect on peak amplitude is real or not. To demonstrate that reductions in peak amplitude were an effect of drug, a control experiment measuring NMDAR EPSCs over thirty minutes, with no drug application, should be carried out. This will show whether peak amplitude changes due to fluctuations in series resistance, and also any rundown in current through these receptors may be observed.

5.4.9 Future experiments

Role of metabotropic glutamate receptors in the MD

This study focused on ionotropic NMDA receptors, however the role of mGluRs in the MD is also unknown. As transmission from mPFC to MD is glutamatergic, it would be interesting to investigate whether mGluRs are involved in this transmission, and whether

they are required for associative recognition memory retrieval in the MD.

A study by Copeland et al conducted *in vivo* recordings in the MD whilst evoking responses by electrically stimulating the mPFC, they then explored the effects of manipulating mGluRs on the firing of MD neurons [58]. Infusions of a group II mGluR agonist into the MD reduced burst firing of MD neurons [58]. As a reduction in burst firing results from MD neurons becoming more depolarised, they hypothesised that these receptors are present on inhibitory projections to the MD, thus causing a reduction in inhibitory drive to MD neurons [58]. They speculated that these receptors are likely present on inhibitory projections coming from the TRN [58].

Role of GABAergic transmission in the MD

The experiments in this chapter focused on glutamatergic transmission, however there is an important GABAergic supply to the MD from the TRN [50, 139, 140]. What is also interesting is that the mPFC sends projections to the TRN, so anatomically the mPFC is capable of indirectly inhibiting the MD via the TRN [48, 141, 142]. Due to these anatomical connections, it was hypothesised that the TRN may be involved in learning and memory. However, a lesion study found no effect of damage to the TRN on spatial learning and memory [139]. There was a minor impairment during the start of a forced choice alternation in a T maze which quickly dissipated leaving performance unaffected overall [139], which is similar to the effects on this task following MD lesions [31]. This study however focused on tasks that are sensitive to damage of the anterior thalamic nuclei, and not the MD. A more recent study found that early lesions to the TRN (at postnatal day four) resulted in impairments in the novel object recognition task [142]. Animals which had received lesions were also found to have reduced cell density in the mPFC and the MD when compared to the sham group [142].

A study in mice recently demonstrated that the TRN is required in fear extinction memory [140]. The projections from the rostroventral TRN (rvTRN) to the medial dorsomedial thalamus (mDMT) which consists of the MDM and PVT, and projections from the rostro dorsal TRN (rdTRN) to the lateral DMT (lDMT) which consists of the MDL and CMT, were manipulated using optogenetics [140]. They found that the rvTRN projection to the mDMT suppresses spiking activity in mDMT neurons, and that blocking this by silencing the projection from rvTRN - mDMT resulted in impaired fear extinction memory [140].

Together, the studies discussed in this section demonstrate that the TRN could be more involved in memory processing than previously thought, and it would be worth exploring whether it supports the reciprocal connections between the mPFC and MD during associative recognition memory.

5.4.10 Conclusion

NMDARs containing the GlUN2A and/or the GluN2C/D subunit are required in the MD during associative recognition memory retrieval. GlUN2C/D NMDARs appear to be present at the mPFC - MD synapse. There does not appear to be a role of LTP or LTD mechanisms, but other mechanisms could be involved instead.

Chapter 6

Discussion and Conclusions

This thesis aimed to investigate the role of acetylcholine in the MD during associative memory retrieval. It also aimed to characterise the properties of MD neurons and the properties of the mPFC - MD synapse. This chapter will summarise the main findings presented within this thesis and place the work in context with existing literature.

6.1 Main findings

The data presented in this thesis demonstrate crucial roles for $\alpha4\beta2$ nAChRs and NMDARs in the MD during associative recognition memory retrieval. Additionally, they show that NMDARs containing GluN2A and or GluN2C/D subunits are required in the MD for associative recognition memory retrieval, but not NMDARs containing GluN2B.

Further *in vitro* experiments were used to explore the specific input from the mPFC to the MD. These experiments showed that this corticothalamic synapse undergoes short term plasticity whereby trains of stimuli at 5, 10 and 20 Hz, cause a facilitation in EPSP size that is frequency dependent. These data showed that this short term plasticity is dependent also on NMDARs, but not $\alpha4\beta2$ nAChRs.

6.2 Role of $\alpha4\beta2$ nAChRs in the MD during associative recognition memory retrieval

The experiments in Chapter 3 aimed to characterise the role of acetylcholine in the MD during associative recognition memory retrieval. This study showed that only $\alpha4\beta2$ nAChRs are required and that there was no requirement for $\alpha7$ nAChRs or mAChRs.

Further *in vitro* experiments in Chapter 4 aimed to investigate the role of $\alpha4\beta2$ nAChRs at the mPFC-MD synapse. These experiments demonstrated that there was no effect of manipulating these receptors on short term plasticity at the mPFC - MD synapse nor were there any effects on EPSP properties. This suggests that the $\alpha4\beta2$ nAChRs are not modulating incoming transmission from the mPFC to the MD, and are modulating transmission from other regions coming into the MD. Or they are affecting signals leaving the MD. These experiments highlight the need for further experiments to identify where $\alpha4\beta2$ nAChRs are located in the MD and understand how they are modulating neuronal transmission during associative recognition memory retrieval.

Previous literature on the expression profiles of $\alpha4\beta2$ nAChRs have shown that these receptors are expressed abundantly throughout the rodent thalamus, including the MD [71]. In comparison, there is very little evidence showing $\alpha7$ nAChRS in the MD. A study measured nAChR subunit mRNA expression using *in situ* hybridisation histochemistry and found that there was mRNA for $\alpha4$ and $\beta2$ subunits in the MD, but they do not report observations of $\alpha7$ subunits [112]. This data would suggest that only $\alpha4\beta2$ nAChRs are present in the MD. However, other studies have found effects of infusing MLA, a specific $\alpha7$ nAChR antagonist, into the MD on behavioural experiments, suggesting contrasting evidence regarding their presence in the MD [86, 143]. One of these studies found manipulating $\alpha7$ nAChRs with PNU, a positive allosteric modulator, blocked the impairments caused by ethanol [143]. The authors suggest that $\alpha7$ nAChRs are expressed on presynaptic terminals supplying the MD and that their activation results in increased glutamate release in the MD [143].

Sabec et al 2015 speculated that $\alpha4\beta2$ nAChRs are expressed on interneurons within the mPFC. There are also other studies from the HPC suggesting that these receptors are expressed on inhibitory neurons [144, 145]. Kuroda et al found that there were no interneurons present in the MD, thus ruling out the possibility of $\alpha4\beta2$ nAChRs being

expressed on these in the MD [46]. However, the MD does receive extensive inhibitory input from the TRN, and some inhibitory input from the basal forebrain [53]. Considering this information, it could be that $\alpha4\beta2$ nAChRs are expressed presynaptically on inhibitory terminals into the MD. This would mean incoming cholinergic transmission would enhance the release of GABA from these inhibitory terminals and hyperpolarise MD neurons. However, this would result in MD neurons switching to burst firing, and it is currently unknown whether signals are transmitted via tonic or burst firing, or a mix of the two, during associative recognition memory retrieval.

Overall, where $\alpha4\beta2$ nAChRs are located in the MD needs further clarification to understand how blocking this receptor is disrupting signals in the MD.

6.3 Role of NMDARs in the MD during associative recognition memory retrieval

The results presented in chapters 4 and 5 of this thesis demonstrated that there is a crucial role of NMDARs in the MD during associative recognition memory retrieval. Specifically, NMDARs that contain the GluN2A subunit and/or the GluN2C/D subunit are required for retrieval. Further experiments investigated which NMDAR subunits are present at the mPFC - MD synapse and suggested that both GluN2C/D and GluN2B containing NMDARs are present, however these experiments require a larger sample size, and whether GluN2A NMDARs are present here also remains to be tested. The data also showed that the NMDARs are crucial for short term plasticity at the mPFC - MD synapse, and blocking NMDARs reduced the amplitude of facilitation evoked by trains of stimuli.

The impairment in memory following the block of NMDARs during associative recognition memory retrieval is an unusual result as typically impairments have been observed after AP-5 infusions during encoding, such as in the NRe and the mPFC [93, 95, 146]. Previous experiments have demonstrated however, that incoming information from the mPFC to the MD is crucial for supporting associative recognition memory. Optogenetic silencing of mPFC projections to the MD impaired OiP performance when they were silenced during the test phase, but not the sample phase, further consolidating the hypothesis that the MD supports retrieval, and demonstrating that incoming information from the mPFC to the MD during retrieval is essential (unpublished work,

G. Barker). As blocking NMDARs impairs transmission between the mPFC and MD, and also infusions of NMDAR *in vivo* impair memory retrieval, it could be speculated that the effects observed are due to incoming information from the mPFC being interrupted. The projection is unable to undergo short term plasticity and therefore signals from the mPFC are unable to be processed correctly by the MD and sent back to the cortex. For example, if incoming signals from the mPFC are typically amplified and relayed back to the mPFC in order to sustain task relevant cortical representations to aid retrieval, blocking NMDARs could be weakening the task relevant information coming from the mPFC, resulting in a reduced signal to noise ratio and the mPFC unable to mediate top down control over memory retrieval.

With these considerations in mind, it may be hypothesised that information from the mPFC to the MD is amplified via a NMDA dependent short term facilitation that ensures task relevant information is sent to the MD and relayed to the mPFC to aid successful memory retrieval. It is likely NMDARs are present postsynaptically on MD neurons and are composed of GluN2A and or GluN2C/D containing NMDARs. Further experiments are required to clarify the NMDA receptor subtype present at the mPFC - MD synapse.

6.4 Overall role of the MD in associative recognition memory

In summary, the data collated in this thesis solidify the evidence that the MD is required during associative recognition memory retrieval. The data show for the first time that this retrieval is dependent on the activation of both $\alpha4\beta2$ nAChRs and GluN2A and/or GluN2C/D containing NMDARs. Evidence suggests that the mPFC to MD projection supports this memory retrieval, and *in vitro* experiments demonstrated that this pathway undergoes short term plasticity, dependent on NMDARS.

The MD is not required for the encoding of associative recognition memory, suggesting that spatial and contextual information during the OiP task is not collated within the MD [18]. Whilst this information may be sent to the MD during the sample phase (encoding), it is not a requirement for supporting memory encoding. Previously it was speculated that the impairment in OiP as a result of inactivating the MD with muscimol was a result of disrupting the mPFC due to their reciprocal connection - rather than a

loss of incoming data to the MD itself [18]. However, the data in this thesis show evidence against this by showing that memory was impaired without inactivating the MD, and that it is dependent on the activation of NMDARs and $\alpha4\beta2$ nAChRs. Additionally, optogenetic disconnection of mPFC to MD impaired OiP performance when the pathway was disconnected during retrieval but not encoding (unpublished work G Barker). Combined these data demonstrate the MD has its own role within OiP memory and that impairments are not a result of disruption in the mPFC due to MD inactivation. It is possible that the MD is required to receive information from the mPFC and relay this information back to the mPFC, and perhaps other cortical regions, and aid in guiding memory retrieval. Whilst the evidence to date suggests that the memory engram for the OiP task is not stored in the MD, it can be hypothesised that the MD is required to aid the mPFC in supporting top down retrieval.

Previous ideas in the literature have speculated that the MD relays information from the mPFC back to the mPFC and other cortical regions [18, 28]. More recently, there are increasing hypotheses in the literature that debate the MD and the thalamus's role as more than simply relaying information. Whilst the MD is likely relaying incoming signals from the mPFC back to the mPFC, it could be amplifying task relevant signals and filtering incoming information from the mPFC in order to aid the mPFC during top-down retrieval, however more study is required to understand the relationship between the mPFC and MD. Evidence within the literature suggests that the MD is relaying cortical information back to the mPFC and could be amplifying relevant signals back to the mPFC to support memory retrieval. Short term facilitation of signal transmission from the mPFC to the MD could be a way that this occurs. The relevance of short term plasticity has been linked to learning and memory suggesting that is involved in signal filtering and information processing [147].

With all of this information in mind, I propose that the MD is required for associative recognition memory retrieval to receive and amplify/diminish signals from the mPFC in order to sustain task appropriate representations in the cortex and allow for successful recognition. When tasks involve associative aspects, they are more complex and the animal must engage the MD in order to aid with cortical signals and ensure signal to noise ratio is correct.

6.5 Future studies

This thesis has provided more information regarding the MDs role in associative recognition memory retrieval, and how input from the mPFC may be supporting this on a synaptic level. However, there are still many unknowns regarding both the mPFC and MD in associative recognition memory, and several studies could be proposed following on from the research presented here.

6.5.1 *in vivo* experiments

Evidence suggests that the MD has a role in associative recognition memory retrieval and is not required for initial encoding. It is unknown whether the MD is required during memory consolidation, between the initial encoding event and subsequent retrieval, or whether incoming information from the mPFC to the MD is required during this time. To test this, infusions of muscimol into the MD could be administered after the sample phase but long enough prior to the test phase that effects on retrieval are minimised.

Whilst this thesis has focused on the projection from the mPFC to the MD, there is little understood about the MD to mPFC projection. The current hypothesis is that MD projections to the mPFC are also required for associative recognition memory retrieval, but this has not been tested. Optogenetic experiments could be conducted in order to silence the MD projection to mPFC during the test phase to investigate the involvement of this projection.

6.5.2 *in vitro* experiments

This thesis provided a broad overview of the synaptic properties of MD neurons. Cells were mostly patched from the medial and sometimes central regions of the MD. As the MD is broken up into three different subdivisions, it would be interesting to further characterise the properties of neurons and compare across these divisions to investigate whether they share similar properties and respond to mPFC input in the same way.

6.6 Implications for pathological conditions

Whilst this thesis sought to understand the contribution of the MD and the communication it may receive from the mPFC during associative recognition memory in healthy rodents, it is important to consider how these findings will aid in furthering our understanding of these mechanisms in humans. Advancing our understanding of the physiological mechanisms is crucial in order to understand how these mechanisms are altered in pathological conditions.

6.6.1 Alzheimer's Disease

Alzheimer's disease (AD) is the most prevalent form of dementia [148]. It is a neurodegenerative disease that presents with impairments in memory and cognition [148, 149]. Patients with AD commonly struggle with recollecting memories [148]. There is evidence to suggest that both the dlPFC and the MD in humans are affected during AD [149, 150]. There has been evidence demonstrating that the MD shrinks in patients with AD [150]. This will likely impact on its reciprocal functionality with the dlPFC and subsequently impair memory. Understanding how these regions and their communication occurs normally will aid in understanding how communication is disrupted by AD and other dementias.

6.6.2 Schizophrenia

Schizophrenia is a psychiatric disorder that is prevalent within approximately one percent of the population [151, 152]. Patients can suffer from a range of symptoms, but of relevant interest is the effect the condition has on cognitive processes such as episodic and working memory, executive function, and attention [58, 151–153]. A functional interaction between the mPFC and MD is essential for cognition, and abhorrent communication between the two can result in deficits in a range of cognitive tasks [4, 154]. There is evidence from brain imaging studies that the MD in schizophrenic patients is functioning abnormally [123]. Additionally, there is emerging evidence that the functional connection between the mPFC and MD is also abnormal in schizophrenic patients [123]. Understanding how the mPFC and MD are functioning together normally is essential for untangling how they are dysfunctional during schizophrenia.

Within the literature there is a model of schizophrenia stating that some of the symptoms are a result of NMDAR hypofunction [155]. This is supported by evidence that NMDAR antagonists can cause psychosis amongst other behavioural and cognitive impairments in humans and rodents [155]. However, it is not fully understood how NMDAR hypofunction is resulting in symptoms associated with schizophrenia. The data in this thesis has highlighted a role for NMDARs in the MD during associative recognition memory retrieval and supporting information transfer between the mPFC and MD. Whilst not directly comparable this finding could be useful for understanding how these two regions are functionally connected and how NMDARs support information flow between the two.

There is also evidence that there are abnormalities in $\alpha4\beta2$ nAChRs in schizophrenia [156]. These $\alpha4\beta2$ nAChRs are crucial in the MD for supporting associative recognition memory retrieval, and are likely required in other cognitive tasks utilising the MD. Although this thesis did not demonstrate a role of $\alpha4\beta2$ nAChRs underlying communication between the mPFC and MD during associative recognition memory, there still could be a role for $\alpha4\beta2$ nAChRs during working memory which also relies on the reciprocal connections between the mPFC and MD and is disrupted in schizophrenia.

6.7 Conclusion

Overall, this thesis has presented evidence for the first time that associative recognition memory retrieval in the MD requires activation of both $\alpha4\beta2$ nAChRs and NMDARs, specifically NMDARs containing GluN2A and GluN2C/D subunits. Evidence within this thesis also shows that the mPFC - MD synapse undergoes short term plasticity, whereby signals facilitate in a frequency dependent manner and this is dependent on NMDAR activation.

After considering the data within this thesis and existing literature, it can be hypothesised that NMDARs are required at the mPFC - MD synapse for amplifying signals from the mPFC - MD to guide task relevant memory retrieval. Whilst the mPFC-MD pathway may not be modulated by acetylcholine during memory retrieval, it could also be hypothesised that acetylcholine modulates the TRN input to the MD via presynaptic $\alpha4\beta2$ nAChRs.

Chapter 7

References

1. John P. Aggleton, Julie R. Dumont, and Elizabeth Clea Warburton. *"Unraveling the contributions of the diencephalon to recognition memory: A review"*. Learning and Memory 8 (2011), pp. 384-400. doi: 10.1101/lm.1884611.

2. Francesco Scalici, Carlo Caltagirone, and Giovanni Augusto Carlesimo. *"The contribution of different prefrontal cortex regions to recollection and familiarity. A review of fMRI data"*. In: Neuroscience and Biobehavioral Reviews 83 (2017), pp. 240–251. doi: 10.1016/j.neubiorev.2017.10.017.

3. Endel Tulving. *"Episodic Memory: From Mind to Brain"*. In: Annual Review Pyschology 53 (2002), pp. 1–25.

4. Laura Cross et al. *"The medial dorsal thalamic nucleus and the medial prefrontal cortex of the rat function together to support associative recognition and recency but not item recognition"*. In: Learning and Memory 20.1 (2013), pp. 41–50. doi: 10.1101/lm.028266.112.

5. Rebecca D. Burwell and Sharon C. Furtak. *"Recognition Memory: Can You Teach an Old Dogma New Tricks?"* In: Neuron 59.4 (2008), pp. 523–525. doi: 10.1016/j.neuron.2008.08.004.

6. Christoph T. Weidemann and Michael J. Kahana. *"Dynamics of brain activity reveal a unitary recognition signal"*. In: Journal of Experimental Psychology: Learning Memory and Cognition 45.3 (2018), pp. 440–451. doi: 10.1037/xlm0000593.

7. Rachel A. Diana et al. *"Models of recognition: A review of arguments in favor of a*

dual-process account". In: Psychonomic Bulletin and Review 13.1 (2006), pp. 1-21. doi: 10.3758/BF03193807.

8. Howard Eichenbaum. *"Memory systems"*. In: Wiley Interdisciplinary Reviews: Cognitive Science 1.4 (2010), pp. 478–490. doi: 10.1002/wcs.49.

9. George Mandler. *"Recognizing: The judgment of previous occurrence"*. In: Psychological Review 87.3 (1980), pp. 252–271. doi: 10.1037/0033-295X.87.3.252.

10. Andrew P. Yonelinas et al. *"Recollection and Familiarity: Examining Controversial Assumptions and New Directions"*. In: Hippocampus 20.11 (2010), pp. 1178–1194. doi:10.1002/hipo.20864.

11. John P. Aggleton and Malcolm W. Brown. *"Interleaving brain systems for episodic and recognition memory"*. In: Trends in Cognitive Sciences 10.10 (2006), pp. 455-463. doi: 10.1016/j.tics.2006.08.003.

12. Giulio Pergola et al. *"The role of the thalamic nuclei in recognition memory accompanied by recall during encoding and retrieval: An fMRI study"*. In: NeuroImage 74 (2013), pp. 195–208. doi: 10.1016/j.neuroimage.2013.02.017

13. Gareth RI Barker and Elizabeth Clea Warburton. *"Multi-level analyses of associative recognition memory: the whole is greater than the sum of its parts"*. In: Current Opinion in Behavioral Sciences 32 (2020), pp. 80–87. doi: 10 . 1016 / j . cobeha . 2020 . 02 . 004.

14. Lola Danet et al. *"Medial thalamic stroke and its impact on familiarity and recollection"*. In: eLife 6 (2017). doi: 10.7554/eLife.28141.

15. Ysbrand D. Van Der Werf et al. *"Contributions of thalamic nuclei to declarative memory functioning"*. In: Cortex 39.4-5 (2003), pp. 1047–1062. doi: 10.1016/S0010-9452(08)70877-3.

16. A. Ennaceur and J. Delacour. *"A new one-trial test for neurobiological studies of memory in rats. 1: Behavioral data"*. In: Behavioural Brain Research 31.1 (1988), pp. 47–59. doi: 10.1016/0166-4328(88)90157-X.

17. Abdelkader Ennaceur, Nick Neave, and John P. Aggleton. *"Spontaneous object recognition and object location memory in rats: The effects of lesions in the cingulate cortices, the medial prefrontal cortex, the cingulum bundle and the*

fornix". In: Experimental Brain Research 113.3 (1997), pp. 509–519. doi: 10.1007/PL00005603.

18. E.C. Warburton and M.W. Brown. *"Neural circuitry for rat recognition memory"*. In: Behavioural Brain Research 285 (May 2015), pp. 131–139 doi: 10.1016/j.bbr.2014.09.050.

19. G. R. I. Barker et al. *"Recognition Memory for Objects, Place, and Temporal Order: A Disconnection Analysis of the Role of the Medial Prefrontal Cortex and Perirhinal Cortex"*. In: Journal of Neuroscience 27.11 (2007), pp. 2948–2957. doi: 10.1523/JNEUROSCI.5289-06.2007.

20. Robert P. Vertes. *"Differential Projections of the Infralimbic and Prelimbic Cortex in the Rat"*. In: Synapse 51.1 (2004), pp. 32–58. doi: 10.1002/ syn.10279.

21. Harry B.M. Uylings, Henk J. Groenewegen, and Bryan Kolb. *"Do rats have a prefrontal cortex?"* In: Behavioural Brain Research 146.1-2 (2003), pp. 3–17. doi: 10.1016/j.bbr.2003.09.028.

22. Howard Eichenbaum. *"Prefrontal–hippocampal interactions in episodic memory"*. In: Nature Reviews Neuroscience 18.9 (2017), pp. 547–558.. doi: 10.1038/nrn.2017.74.

23. Howard Eichenbaum et al. "*The Hippocampus, Memory, Review and Place Cells: Is It Spatial Memory or a Memory Space? might occur at different locations. Olton and colleagues Neuron 210 Figure 1. Schematic Overhead Views of Four Different Types of Apparatus and Examples of Location-S"*. In: Neuron 23 (1999), pp. 209–226.

24. Anna S. Mitchell. *"The mediodorsal thalamus as a higher order thalamic relay nucleus important for learning and decision-making"*. In: Neuroscience and Biobehavioral Reviews 54 (2015), pp. 76–88. doi: 10 . 1016 / j . neubiorev . 2015 . 03 . 001.

25. S. M. Sherman and R. W. Guillery. *"On the actions that one nerve cell can have on another: Distinguishing "drivers" from "modulators"*. In: Proceedings of the National Academy of Sciences (1998) pp. 7121-7126. doi: 10.1073/pnas.95. 12.7121.

26. Carmen Varela. *"Thalamic neuromodulation and its implications for executive networks"*. In: Frontiers in Neural Circuits 8.June (2014), pp. 1–22. doi: 10.3389/fnci.2014.00069.

27. Anna S. Mitchell and Subhojit Chakraborty. *"What does the mediodorsal thalamus do?"* In: Frontiers in Systems Neuroscience 7 (2013). doi: 10. 3389/fnsys.

28. Rajeev V. Rikhye, Aditya Gilra, and Michael M. Halassa. *"Thalamic regulation of switching between cortical representations enables cognitive flexibility"*. In: Nature Neuroscience 21.12 (2018), pp. 1753–1763. doi: 10.1038/s41593018-0269-z.

29. Robert P. Vertes. *"Analysis of projections from the medial prefrontal cortex to the thalamus in the rat, with emphasis on nucleus reuniens"*. In: Journal of Comparative Neurology 442.2 (2002), pp. 163–187. doi: 10.1002/cne.10083.

30. Peter R. Hunt and John P. Aggleton. *"Medial dorsal thalamic lesions and working memory in the rat"*. In: Behavioral and Neural Biology 55.2 (1991), pp. 227–246. doi: 10.1016/0163-1047(91)80141-Z.

31. Peter R. Hunt and John P. Aggleton. "*An examination of the spatial working memory deficit following neurotoxic medial dorsal thalamic lesions in rats"*. In: Behavioural Brain Research 97.1-2 (1998), pp. 129–141. doi: 10. 1016/S0166-4328(98)00033-3.

32. Peter R Hunt and John P Aggleton. *"Neurotoxic lesions of the dorsomedial thalamus impair the acquisition but not the performance of delayed matching to place by rats: a deficit in shifting response rules."* In: The Journal of neuroscience: the official journal of the Society for Neuroscience 18.23 (1998), pp. 10045–52. doi: 10 . 1002 / 2015GL067056.

33. H. J. Groenewegen. "*Organization of the afferent connections of the mediodorsal thalamic nucleus in the rat, related to the mediodorsal-prefrontal topography"*. In: Neuroscience 24.2 (1988), pp. 379–431. doi: 10.1016/03064522(88)90339-9.

34. David R Euston, Aaron J Gruber, and Bruce L Mcnaughton. "The Role of Medial Prefrontal Cortex in Memory and Decision Making". In: Neuron 76.6 (2013), pp. 1057–1070. doi: 10.1016/j.neuron.2012.12.002.

35. S R Sesack et al. *"Topographical organization of the efferent projections of the medial prefronatl cortex in the rat: An anterograde tract tracing study with phaseolus vulgaris Leucoagglutinin"*. In: The Journal of Comparative Neurology 290 (1989), pp. 213–242. doi: 10.1002/cne.v290.

36. H. Barbas. *"Prefrontal Cortex: Structure and Anatomy"*. In: Encyclopedia of Neuroscience 2010, pp. 909–918. doi:10.1016/B978-008045046-9.00427-7.

37. Danai Riga et al. *"Optogenetic dissection of medial prefrontal cortex circuitry*". In: 8.December (2014), pp. 1–19. doi: 10.3389/fnsys.2014.00230.

38. Karlijn I. Van Aerde and Dirk Feldmeyer. *"Morphological and physiological characterization of pyramidal neuron subtypes in rat medial prefrontal cortex"*. In: Cerebral Cortex 25.3 (2015), pp. 788–805. doi: 10.1093/cercor/bht278.

39. Kathleen K.A. Cho et al. *"Cross-hemispheric gamma synchrony between prefrontal parvalbumin interneurons supports behavioral adaptation during rule shift learning"*. In: Nature Neuroscience (2020). doi:10.1038/s41593-020- 0647-1.

40. Eriko Kuramoto et al. *"Individual mediodorsal thalamic neurons project to multiple areas of the rat prefrontal cortex: A single neuron-tracing study using virus vectors"*. In: Journal of Comparative Neurology 525.1 (2017),pp. 166–185. doi: 10.1002/cne.24054.

41. Walter B. Hoover and Robert P. Vertes. *"Anatomical analysis of afferent projections to the medial prefrontal cortex in the rat"*. In: Brain Structure and Function 212.2 (2007), pp. 149–179. doi: 10.1007/s00429-007-0150-4.

42. James P. Ray et al. *"Sources of presumptive glutamatergic/aspartatergic afferents to the mediodorsal nucleus of the thalamus in the rat"*. In: Journal of Comparative Neurology 320.4 (1992), pp. 435–456. doi: 10.1002/cne.903200403.

43. Fabien Alcaraz et al. *"Parallel inputs from the mediodorsal thalamus to the prefrontal cortex in the rat"*. In: European Journal of Neuroscience 44.3 (2016), pp. 1972–1986. doi: 10.1111/ejn.13316.

44. David P. Collins et al. *"Reciprocal Circuits Linking the Prefrontal Cortex with Dorsal and Ventral Thalamic Nuclei"*. In: Neuron 98.2 (2018), pp. 366–379. doi: 10.1016/j.neuron.2018.03.024.

45. Masaru Kuroda, Laura L´opez-Mascaraque, and Joseph L. Price. *"Neuronal and synaptic composition of the mediodorsal thalamic nucleus in the rat: A light and electron microscopic golgi study"*. In: Journal of Comparative Neurology 326.1 (1992), pp. 61–81. doi: 10.1002/cne.903260106.

46. J. M. Minderhoud. *"An anatomical study of the efferent connections of the thalamic reticular nucleus"*. In: Experimental Brain Research 12.4 (1971), pp. 435–446. doi: 10.1007/BF00234497.

47. John W. Crabtree. *"Functional Diversity of Thalamic Reticular Subnetworks"*. In: Frontiers in Systems Neuroscience 12 (2018). doi:10. 3389/fnsys .2018.00041.

48. J. Cornwall and O. T. Phillipson. *"Afferent projections to the dorsal thalamus of the rat as shown by retrograde lectin transport. II. The midline nuclei"*. In: Brain Research Bulletin 21.2 (1988), pp. 147–161. doi: 10.1016/03619230(88)90227-4.

49. Mathieu Wolff and Seralynne D. Vann. *"The cognitive thalamus as a gateway to mental representations"*. In: Journal of Neuroscience 39.1 (2019), pp. 3–14. doi: 10.1523/JNEUROSCI.0479-18.2018.

50. Byoung Kyong Min. *"A thalamic reticular networking model of consciousness"*. In: Theoretical Biology and Medical Modelling 7.1 (2010), pp. 1–13. doi: 10.1186/1742-4682-7-10.

51. K. McAlonan, V. J. Brown, and E. M. Bowman. *"Thalamic reticular nucleus activation reflects attentional gating during classical conditioning"*. In: Journal of Neuroscience 20.23 (2000), pp. 8897–8901. doi: 10.1523/jneurosci.20-23-08897.2000.

52. C. Varela et al. *"Anatomical substrates for direct interactions between hippocampus, medial prefrontal cortex, and the thalamic nucleus reuniens"*. In: Brain Structure and Function 219.3 (2014), pp. 911–929. doi: 10.1007/s00429-013-0543-5.

53. Adam Kepecs and Gordon Fishell. *"Interneuron cell types are fit to function"*. In: Nature 505.7843 (2014), pp. 318-326. doi: 10.1038/nature12983.

54. Robin Tremblay, Soohyun Lee, and Bernardo Rudy. "GABAergic Interneurons in the Neocortex: From Cellular Properties to Circuits". In: Neuron 91.2 (2016), pp. 260-292. doi: 10.1016/j.neuron.2016.06.033.

55. Chao Ding et al. *"Layer-Specific Inhibitory Microcircuits of Layer 6 Interneurons in Rat Prefrontal Cortex"*. In: Cerebral Cortex 31.1 (2021), pp. 32–47. doi: 10.1093/cercor/bhaa201.

56. Fleur Zeldenrust, Pascal Chameau, and Wytse J. Wadman. *"Spike and burst coding in thalamocortical relay cells"*. In: PLoS Computational Biology 14.2 (2018). doi: 10.1371/journal.pcbi.1005960.

57. C. S. Copeland, S. A. Neale, and T. E. Salt. *"Neuronal activity patterns in the mediodorsal thalamus and related cognitive circuits are modulated by metabotropic glutamate receptors"*. In: Neuropharmacology 92 (2015), pp. 16–24. doi: 10.1016/j.neuropharm.2014.12.031.

58. Sybren F. de Kloet et al. *"Bi-directional regulation of cognitive control by distinct prefrontal cortical output neurons to thalamus and striatum"*. In: Nature Communications 12.1 (2021). doi:10.1038/s41467-021-22260-7.

59. David A. McCormick. "*Neurotransmitter actions in the thalamus and cerebral cortex and their role in neuromodulation of thalamocortical activity"*. In: Progress in Neurobiology 39.4 (1992), pp. 337-388. doi: 10.1016/0301-0082(92)90012-4.

60. John Koester and Steven A. Sigelbaum *"Local Signaling : Passive Electrical Properties of the Neuron"*

61. John M. Bekkers. *"Changes in dendritic axial resistance alter synaptic integration in cerebellar Purkinje cells"*. In: Biophysical Journal 100.5 (2011), pp. 1198–1206. doi: 10.1016/j.bpj.2011.01.042.

62. Rebecca A. Mease et al. *"Multiplexed Spike Coding and Adaptation in the Thalamus"*. In: Cell Reports 19.6 (2017),pp. 1130–1140. doi:10.1016/j.celrep.2017.04.050.

63. S M Sherman. *"Tonic and burst firing: dual modes of thalamocortical relay."* In: Trends in neurosciences 24.2 (2001), pp. 122–6.

64. Erika E. Fanselow et al. *"Thalamic bursting in rats during different awake behavioral states"*. In: Proceedings of the National Academy of Sciences of the United States of America 98.26 (2001), pp. 15330–15335. doi: 10.1073/pnas.261273898.

65. Michael E. Hasselmo. *"The role of acetylcholine in learning and memory"*. In: Current Opinion in Neurobiology 16.6 (2006), pp. 710-715. doi: 10.1016/j.conb.2006.09.002.

66. Eliane Proulx et al. *"Nicotinic acetylcholine receptors in attention circuitry: The role of layer VI neurons of prefrontal cortex"*. In: Cellular and Molecular Life Sciences 71.7 (2014), pp. 1225–1244. doi:10.1007/s00018-013-1481-3.

67. Bernard Bloem, Rogier B. Poorthuis, and Huibert D. Mansvelder. *"Cholinergic modulation of the medial prefrontal cortex: the role of nicotinic receptors in attention and regulation of neuronal activity"*. In: Frontiers in Neural Circuits 8.March (2014). doi: 10.3389/fncir.2014.00017.

68. Jie Wu. *"Understanding of nicotinic acetylcholine receptors"*. 2009. doi: 10.1038/ aps.2009.89.

69. Edson X. Albuquerque et al. *"Mammalian nicotinic acetylcholine receptors: From structure to function"*. In: Physiological Reviews 2009. doi: 10.1152/physrev.00015.2008.

70. Martin Sarter, Vinay Parikh, and W. Matthew Howe. *"Phasic acetylcholine release and the volume transmission hypothesis: Time to move on"*. In: Nature Reviews Neuroscience 10.5 (2009). doi: 10.1038/ nrn2635.

71. Marie H. Sabec et al. *"Nicotinic Acetylcholine Receptors Control Encoding and Retrieval of Associative Recognition Memory through Plasticity in the Medial Prefrontal Cortex"*. In: Cell Reports (2018). doi: 10.1016/j.celrep.2018.03.016.

72. Jan Svoboda, Anna Popelikova, and Ales Stuchlik. "*Drugs interfering with muscarinic acetylcholine receptors and their effects on place navigation"*. In: Frontiers in Psychiatry 8.November (2017). doi: 10.3389/fpsyt.2017.00215.

73. A. I. Levey et al. *"Identification and localization of muscarinic acetylcholine receptor proteins in brain with subtype-specific antibodies"*. In: Journal of Neuroscience 11.10 (1991), pp. 3218–3226. doi: 10.1523/jneurosci.11-10-03218.1991.

74. K. A. Frey and M. M. Howland. *"Quantitative autoradiography of muscarinic cholinergic receptor binding in the rat brain: Distinction of receptor subtypes in antagonist competition assays"*. In: Journal of Pharmacology and Experimental Therapeutics 263.3 (1992), pp. 1391–1400.

75. Zi Wei Zhang et al. "*Confocal analysis of cholinergic and dopaminergic inputs onto pyramidal cells in the prefrontal cortex of rodents"*. In: Frontiers in Neuroanatomy (2010). doi: 10.3389/fnana.2010.00021.

76. Michael E. Ragozzino. *"The contribution of cholinergic and dopaminergic afferents in the rat prefrontal cortex to learning, memory, and attention"*. In: Psychobiology (2000). doi: 10.3758/BF03331982.

77. Satoh and H. C. Fibiger. *"Cholinergic neurons of the laterodorsal tegmental nucleus: Efferent and afferent connections"*. In: Journal of Comparative Neurology 253.3 (1986), pp. 277–302. doi: 10.1002/cne.902530302.

78. Icnelia Huerta-Ocampo et al. *"Distribution of midbrain cholinergic axons in the thalamus"*. In: eNeuro 7.1 (2020). doi: 10.1523/ENEURO.0454- 19.2019.

79. G. R I Barker and Elizabeth C. Warburton. *"Critical role of the cholinergic system for object-in-place associative recognition memory"*. In: Learning and Memory (2009). doi: 10.1101/lm.1121309.

80. Michael E. Hasselmo and Jill McGaughy. "*High acetylcholine levels set circuit dynamics for attention and encoding and low acetylcholine levels set dynamics for consolidation"*. In: Progress in Brain Research. 2004. doi: 10.1016/S00796123(03)45015-2.

81. Michael E. Hasselmo. *"Calcuating LD50/LC50 using Probit Analysis"*. In: Current Opinion in Neurobiology 16.6 (2009), pp. 710–715. doi: 10.1016/ j.conb.2006.09.002.

82. Ann E. Hallanger et al. *"The origins of cholinergic and other subcortical afferents to the thalamus in the rat"*. In: Journal of Comparative Neurology 262.1 (1987), pp. 105–124. doi: 10.1002/cne.902620109.

83. Renee F. Bolton, James Cornwall, and Oliver T. Phillipson. *"Collateral axons of cholinergic pontine neurones projecting to midline, mediodorsal and parafascicular thalamic nuclei in the rat"*. In: Journal of Chemical Neuroanatomy 6.2 (1993), pp. 101–114. doi: 10.1016/0891-0618(93)90031-X.

84. Reginald Cannady et al. *"Nicotinic antagonist effects in the mediodorsal thalamic nucleus: Regional heterogeneity of nicotinic receptor involvement in cognitive function"*. In: Biochemical Pharmacology 78.7 (2009), pp. 788–794. doi: 10.1016/j.bcp.2009.05.021.

85. Craig P. Mantanona et al. *"Dissociable contributions of mediodorsal and anterior thalamic nuclei in visual attentional performance: A comparison using nicotinic and*

muscarinic cholinergic receptor antagonists". In: Journal of Psychopharmacology 34.12 (2020), pp. 1371–1381. doi: 10.1177/0269881120965880.

86. Julie A. Williams et al. *"State-dependent release of acetylcholine in rat thalamus measured by in vivo microdialysis"*. In: Journal of Neuroscience 14.9 (1994), pp. 5236–5242. doi: 10.1523/jneurosci.14-09-05236.1994.

87. David A. McCormick and Thierry Bal. *"Sleep and arousal: Thalamocortical mechanisms"*. In: Annual Review of Neuroscience (1997). doi: 10.1146/annurev.neuro.20.1.185.

88. Heather Chaffey and Paul L. Chazot. "*NMDA receptor subtypes: Structure, function and therapeutics"*. In: Current Anaesthesia and Critical Care 19.4 (2008), pp. 183–201. doi: 10.1016/j.cacc.2008.05.004.

89. Jue Xiang Wang et al. *"Structural basis of subtype-selective competitive antagonism for GluN2C/2D-containing NMDA receptors"*. In: Nature Communications 11.1 (2020). doi: 10.1038/s41467-020-14321-0.

90. G.R.I. Barker and E.C. Warburton. "*A critical role for the nucleus reuniens in long-term, but not short-term associative recognition memory formation"*. In: The Journal of Neuroscience (2018), pp. 1802–17. doi: 10.1523/ JNEUROSCI.1802-17.2017.

91. G. R. I. Barker and E. C. Warburton. *"NMDA Receptor Plasticity in the Perirhinal and Prefrontal Cortices Is Crucial for the Acquisition of Long-Term Object-in-Place Associative Memory"*. In: Journal of Neuroscience 28.11 (2008), pp. 2837–2844. doi: 10.1523/JNEUROSCI.4447-07.2008.

92. E. Clea Warburton, Gareth R.I. Barker, and Malcom W. Brown. *"Investigations into the involvement of NMDA mechanisms in recognition memory"*. In: Neuropharmacology 74 (2013), pp. 41-47. doi: 10. 1016/j.neuropharm.2013.04.013.

93. P. J. Banks, Z. I. Bashir, and M. W. Brown. *"Recognition memory and synaptic plasticity in the perirhinal and prefrontal cortices"*. In: Hippocampus 22.10 (2012), pp. 2012–2031. doi: 10.1002/hipo.22067.

94. P. J. Banks et al. *"Mechanisms of synaptic plasticity and recognition memory in the perirhinal cortex"*. In: Progress in Molecular Biology and Translational Science 122 (2014), pp. 193–209. doi: 10.1016/B978-0-12-420170- 5.00007-6.

95. Graham Collingridge. *"The role of NMDA receptors in learning and memory"*. In: Nature 330.6149 (1987), pp. 604–605. doi: 10.1038/330604a0.

96. Gernot Riedel, Bettina Platt, and Jacques Micheau. "*Glutamate receptor function in learning and memory"*. In: Behavioural Brain Research 140.1-2 (2003), pp. 1-47. doi: 10.1016/S0166-4328(02)00272-3.

97. Amir H. Rezvani. *"Involvement of the NMDA system in learning and memory"*. In: Animal Models of Cognitive Impairment. 2006, pp. 37–48. doi: 10.1201/9781420004335.ch4.

98. Aparna Ravikrishnan et al. "*Region-specific Expression of NMDA Receptor GluN2C Subunit in Parvalbumin-Positive Neurons and Astrocytes: Analysis of GluN2C Expression using a Novel Reporter Model"*. In: Neuroscience 380 (2018), pp. 49–62. doi: 10.1016/j.neuroscience.2018.03.011.

99. Subhrajit Bhattacharya et al. *"Triheteromeric GluN1/GluN2A/GluN2C NMDARs with Unique Single-Channel Properties Are the Dominant Receptor Population in Cerebellar Granule Cells"*. In: Neuron 99.2 (2018), pp. 315–328. doi: 10.1016/j.neuron.2018.06.010.

100. Antoine Koehl et al. "*Structural insights into the activation of metabotropic glutamate receptors"*. In: Nature 566.7742 (2019), pp. 79–84. doi: 10.1038/s41586-019-0881-4.

101. Colleen M. Niswender and P. Jeffrey Conn. *"Metabotropic glutamate receptors: Physiology, pharmacology, and disease"*. In: Annual Review of Pharmacology and Toxicology 50 (2010), pp. 295-322. doi: 10.1146/annurev.pharmtox.011008.145533.

102. Fani Lourenc¸o Neto et al. *"Differential distribution of metabotropic glutamate receptor subtype mRNAs in the thalamus of the rat"*. In: Brain Research 854.1-2 (2000), pp. 93–105. doi: 10.1016/S0006-8993(99)02326-4.

103. Paul J Banks, E Clea Warburton, and Zafar I Bashir. *"Plasticity in Prefrontal Cortex Induced by Coordinated Synaptic Transmission Arising from Reuniens/Rhomboid Nuclei and Hippocampus"*. In: Cerebral Cortex Communications 2.2 (2021), pp. 1–16. doi: 10.1093/texcom/tgab029.

104. G. R. I. Barker and E. C. Warburton. *"When Is the Hippocampus Involved in Recognition Memory?"* In: Journal of Neuroscience 31.29 (2011), pp. 10721–10731..

doi: 10.1523/JNEUROSCI.6413-10.2011.

105. George Paxinos and Charles Watson. "*The rat brain in stereotaxic coordinates*". (2005)

106. Michael E. Hasselmo and Martin Sarter. *"Modes and models of forebrain cholinergic neuromodulation of cognition"*. In: Neuropyschopharmacology 36.1 (2011), pp. 52-73. doi: 10.1038/npp.2010.104.

107. Marie H. Sabec et al. *"Nicotinic Acetylcholine Receptors Control Encoding and Retrieval of Associative Recognition Memory through Plasticity in the Medial Prefrontal Cortex"*. In: Cell Reports 22.13 (2018), pp. 3409–3415. doi: 10.1016/j.celrep.2018.03.016

108. Trisha A. Jenkins et al. "*Determination of acetylcholine and dopamine content in thalamus and striatum after excitotoxic lesions of the pedunculopontine tegmental nucleus in rats*". In: Neuroscience Letters 322.1 (2002), pp. 45–48. doi: 10.1016/S0304-3940(02)00084-8.

109. R. E. Ryan and R. E. Loiacono. "*Nicotinic receptor subunit mRNA in the thalamus of the rat: Relevance to schizophrenia?*" In: NeuroReport 11.17 (2000), pp. 3693–3698. doi: 10.1097/00001756-200011270-00021.

110. R. S. Broide et al. *"Developmental expression of7 neuronal nicotinic receptor messenger RNA in rat sensory cortex and thalamus"*. In: Neuroscience 67.1 (1995), pp. 83–94. doi: 10.1016/0306-4522(94)00623-D.

111. J. A. Tonnaer et al. *"Cholinergic innervation and topographical organization of muscarinic binding sites in rat brain: a comparative autoradiographic study."* In: Journal of chemical neuroanatomy 1.2 (1988), pp. 95–110.

112. Roser Cort´es and Jos´eM M. Palacios. *"Muscarinic cholinergic receptor subtypes in the rat brain. I. Quantitative autoradiographic studies"*. In: Brain Research 362.2 (1986), pp. 227–238. doi: 10.1016/0006-8993(86)90448-8.

113. E. Clea Warburton et al. *"Cholinergic neurotransmission is essential for perirhinal cortical plasticity and recognition memory*". In: Neuron 38.6 (2003), pp. 987–996. doi: 10.1016/S0896-6273(03)00358-1.

114. Jianli Li, Martha E. Bickford, and William Guido. *"Distinct Firing Properties of Higher Order Thalamic Relay Neurons"*. In: Journal of Neurophysiology 90.1 (2006), pp. 291–299. doi: 10.1152/jn.01163.2002.

115. E. J. Ramcharan, J. W. Gnadt, and S. M. Sherman. *"Higher-order thalamic relays burst more than first-order relays"*. In: Proceedings of the National Academy of Sciences of the United States of America 102.34 (2005), pp. 12236–12241. doi: 10.1073/pnas.0502843102.

116. Lisa Kinnavane, Mathieu M. Albasser, and John P. Aggleton. *"Advances in the behavioural testing and network imaging of rodent recognition memory"*. In: Behavioural Brain Research 285 (2015), pp.67–78. doi:10.1016/j.bbr.2014.07.049.

117. Iman T. Jhangiani-Jashanmal et al. *"Electroresponsive properties of rat central medial thalamic neurons"*. In: Journal of Neurophysiology 115.3 (2016), pp. 1533–1541. doi: 10.1152/jn.00982.2015.

118. Yumiko Watanabe and Shintaro Funahashi. *"Thalamic mediodorsal nucleus and working memory"*. In: Neuroscience and Biobehavioral Reviews 36.1 (2012), pp. 134–142. doi:10.1016/j.neubiorev.2011.05.003.

119. Robert P. Vertes, Stephanie B. Linley, and Walter B. Hoover. *"Limbic circuitry of the midline thalamus"*. In: Neuroscience and Biobehavioural Reviews 54 (2015), pp. 89-107. doi: 10.1016/j.neubiorev.2015.01.014.

120. Stuart M. Cain and Terrance P. Snutch. *"T-type calcium channels in burst-firing, network synchrony, and epilepsy"*. In: Biochimica et Biophysica Acta – Biomembranes 1828.7 (2013), pp. 1572-1578. doi: 10.1016/j.bbamem.2012.07.028.

121. Jeongjin Kim et al. "*Thalamic T-type Ca2+ channels mediate frontal lobe dysfunctions caused by a hypoxia-like damage in the prefrontal cortex"*. In: Journal of Neuroscience 31.11 (2011), pp. 4063–4073. doi: 10.1523/JNEUROSCI.4493-10.2011.

122. Jonathan J. Couey et al. "*Distributed Network Actions by Nicotine Increase the Threshold for Spike-Timing-Dependent Plasticity in Prefrontal Cortex"*. In: Neuron 54.1 (2007), pp. 73–87. doi: 10.1016/j.neuron.2007.03.006.

123. A. S. Mitchell, M. G. Baxter, and D. Gaffan. *"Dissociable Performance on Scene Learning and Strategy Implementation after Lesions to Magnocellular Mediodorsal*

Thalamic Nucleus". In: Journal of Neuroscience 27.44 (2007), pp. 11888–11895. doi: 10.1523/JNEUROSCI.1835-07.2007.

124. Gareth R.I. Barker et al. "*The different effects on recognition memory of perirhinal kainate and NMDA glutamate receptor antagonism: Implications for underlying plasticity mechanisms"*. In: Journal of Neuroscience 26.13 (2006), pp. 3561–3566. doi: 10.1523/JNEUROSCI.3154-05.2006.

125. Paul James Banks et al. *"Disruption of hippocampal–prefrontal cortex activity by dopamine D2R-dependent LTD of NMDAR transmission"*. In: Proceedings of the National Academy of Sciences 112.35 (2015), pp. 11096–11101. doi: 10.1073/pnas.1512064112.

126. Jo¨elle Lopez et al. *"Memory Retrieval Requires Ongoing Protein Synthesis and NMDA Receptor Activity-Mediated AMPA Receptor Trafficking"*. In: The Journal of Neuroscience 35.6 (2015), p. 2465. doi: 10 .1523/ JNEUROSCI.0735-14.2015.

127. Kevin A. Corcoran et al. *"NMDA Receptors in Retrosplenial Cortex Are Necessary for Retrieval of Recent and Remote Context Fear Memory"*. In: The Journal of Neuroscience 31.32 (Aug. 2011), p. 11655. doi: 10.1523/JNEUROSCI.2107-11.2011.

128. Paola Virginia Migues et al. "*PKM maintains memories by regulating GluR2-dependent AMPA receptor trafficking"*. In: Nature Neuroscience 13.5 (2010), pp. 630–634. doi: 10.1038/nn.2531.

129. John Lisman, Ryohei Yasuda, and Sridhar Raghavachari. "*Mechanisms of CaMKII action in long-term potentiation"*. (2012), pp. 169-182. doi: 10.1038/nrn3192.

130. Fiona Y. Choi et al. *"Interference with AMPA receptor endocytosis: Effects on behavioural and neurochemical correlates of amphetamine sensitization in male rats"*. In: Journal of Psychiatry and Neuroscience 39.3 (2014), pp. 189–199. doi: 10.1503/jpn.120257.

131. Kaiyun Yang et al. *"The regulatory role of long-term depression in juvenile and adult mouse ocular dominance plasticity"*. In: Scientific Reports 1 (2011), pp. 1–11. doi: 10.1038/srep00203.

132. Pan Wong Tak et al. *"Hippocampal long-term depression mediates acute stress-induced spatial memory retrieval impairment"*. In: Proceedings of the

National Academy of Sciences of the United States of America 104.27 (2007), pp. 11471–11476. doi: 10.1073/pnas.0702308104.

133. L. A.K. Wilton et al. "*Excitotoxic lesions of the rostral thalamic reticular nucleus do not affect the performance of spatial learning and memory tasks in the rat*". In: Behavioural Brain Research (2001). doi: 10.1016/S01664328(00)00369-7.

134. Joon Hyuk Lee et al. "*The rostroventral part of the thalamic reticular nucleus modulates fear extinction*". In: Nature communications 10.1 (2019), p. 4637. doi: 10.1038/s41467-019-12496-9.

135. Basilis Zikopoulos and Helen Barbas. *"Circuits for multisensory integration and attentional modulation through the prefrontal cortex and the thalamic reticular nucleus in primates"*. In: Reviews in the Neurosciences 18.6 (2007), pp. 417–438. doi: 10.1515/REVNEURO.2007.18.6.417.

136. Hasna El Boukhari et al. "*Early lesion of the reticular thalamic nucleus disrupts the structure and function of the mediodorsal thalamus and prefrontal cortex*". In: Developmental Neurobiology 79.11-12 (2019), pp. 913–933. doi: 10.1002/dneu.22733.

137. John McDaid et al. *"Ethanol-induced motor impairment mediated by inhibition of 7 nicotinic receptors"*. In: Journal of Neuroscience 36.29 (2016), pp. 7768–7778 doi: 10.1523/JNEUROSCI.0154-16.2016.

138. Jong Hyun Son and Ursula H. Winzer-Serhan. *"Expression of neuronal nicotinic acetylcholine receptor subunit mRNAs in rat hippocampal GABAergic interneurons"*. In: Journal of Comparative Neurology 511.2 (2008), pp. 286–299. doi: 10.1002/cne.21828.

139. Sterling N. Sudweeks and Jerrel L. Yakel. "*Functional and molecular characterization of neuronal nicotinic ACh receptors in rat CA1 hippocampal neurons*". In: Journal of Physiology 527.3 (2000), pp. 515–528. doi: 10.1111/j.1469-7793.2000.00515.x.

140. G R Barker et al. *"A temporally distinct role for group I and group II metabotropic glutamate receptors in object recognition memory"*. In: Learn Mem 13.2 (2006), pp. 178–186. doi: 10.1101/lm.77806.

141. Bai Chuang Shyu and Brent A. Vogt. *"Short-term synaptic plasticity in the nociceptive thalamic-anterior cingulate pathway"*. In: Molecular Pain 5 (2009). doi: 10.1186/1744-8069-5-51.

Qiao Chen and William C. Mobley. *"Exploring the pathogenesis of Alzheimer disease in basal forebrain cholinergic neurons: Converging insights from alternative hypotheses"*. In: Frontiers in Neuroscience 13.May (2019). doi: 10.3389/fnins.2019.00446.

142. John P. Aggleton et al. "*Thalamic pathology and memory loss in early Alzheimer's disease: Moving the focus from the medial temporal lobe to Papez circuit"*. In: Brain 139.7 (2016), pp. 1877-1860. doi: 10.1093/brain/aww083.

143. Zakaria Ouhaz, Hugo Fleming, and Anna S. Mitchell. *"Cognitive functions and neurodevelopmental disorders involving the prefrontal cortex and mediodorsal thalamus"*. In: Frontiers in Neuroscience 12.Feb (2018). doi: 10.3389/fnins.2018.00033.

144. Nina V. Kraguljac, Annusha Srivastava, and Adrienne C. Lahti. *"Memory deficits in Schizophrenia: A selective review of functional magnetic resonance imaging (fMRI) studies"*. In: Behavioural Sciences 3.3 (2013), pp. 330-347. doi: 10.3390/bs3030330.

145. Mar´ıa D. Rubio, Jana B. Drummond, and James H. Meador-Woodruff. *"Glutamate receptor abnormalities in schizophrenia: Implications for innovative treatments"*. In: Biomolecules and Therapeutics 20.1 (2012) pp, 1-18. doi: 10.4062/biomolther.2012.20.1.001.

146. Camille Jantzi et al. "Retrieval practice improves memory in patients with schizophrenia: *New perspectives for cognitive remediation"*. In: BMC Psychiatry 19.1 (2019). doi: 10.1186/s12888-019-2341-y.

147. Mathieu Wolff et al. *"Mediodorsal but not anterior thalamic nuclei lesions impair acquisition of a conditional discrimination task"*. In: Neurobiology of Learning and Memory 125 (2015), pp. 80–84. doi: 10.1016/j.nlm.2015.07.018.

148. Zoran Vukadinovic. *"NMDA receptor hypofunction and the thalamus in schizophrenia"*. In: Physiology and Behaviour 131 (2014), pp. 156-159. doi: 10.1016/j.physbeh.2014.04.038.

149. Evelyn K. Lambe, Marina R. Picciotto, and George K. Aghajanian. *"Nicotine induces glutamate release from thalamocortical terminals in prefrontal cortex"*. In: Neuropsychopharmacology 28.2 (2003), pp. 216–225. doi: 10.1038/sj.npp.1300032.